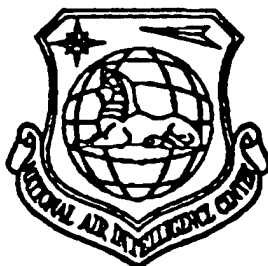


NAIC-ID(RS)T-0062-96

NATIONAL AIR INTELLIGENCE CENTER



SELECTED ARTICLES



19970414 133

Approved for public release:
distribution unlimited

[DTIC QUALITY INSPECTED 5]

HUMAN TRANSLATION

NAIC-ID(RS)T-0062-96 30 January 1997

MICROFICHE NR:

SELECTED ARTICLES

English pages: 188

Source: Daodan Yu Hangtian Yunzai Jishu (Missiles and Space Vehicles), Nr. 213, February 1995, IIR
Enclosure 1 68140043-96; pp. I-II; 1-80.

Country of origin: China

Translated by: SCITRAN

F33657-84-D-0165

Requester: NAIC/TASS/Scott D. Fairheller

Approved for public release: distribution unlimited.

THIS TRANSLATION IS A RENDITION OF THE ORIGINAL FOREIGN TEXT WITHOUT ANY ANALYTICAL OR EDITORIAL COMMENT STATEMENTS OR THEORIES ADVOCATED OR IMPLIED ARE THOSE OF THE SOURCE AND DO NOT NECESSARILY REFLECT THE POSITION OR OPINION OF THE NATIONAL AIR INTELLIGENCE CENTER.

PREPARED BY:

TRANSLATION SERVICES
NATIONAL AIR INTELLIGENCE CENTER
WPAFB, OHIO

TABLE OF CONTENTS

Graphics Disclaimer	iii
MISSILES AND SPACE VEHICLES	
CHINA CARRIER ROCKET TECHNOLOGY RESEARCH INSTITUTE	1
REVIEW OF CALT'S LAUNCH SERVICE IN 1994 AND 1995, by Chen Bingfang, Wang Qingsyang	3
SPACECRAFT FLEXIBLE MULTI-BODY DYNAMICS AND ITS DEVELOPMENT, by Wang Yi, Wu Delong	16
RECOGNIZING THE FAULT PATTERNS OF LIQUID ROCKET ENGINES BY NEURAL NETWORKS, by Yang Erfu, Zhang Zhenpeng, Cui Dingjun, Liu Groqiu	44
A THERMODYNAMIC VENT SYSTEM APPLIED TO CRYOGENIC PROPELLANTS TANK UNDER MICROGRAVITY ENVIRONMENTS, by Liu Chunhui, Cai Ze	62
GPS ONBOARD TRANSLATOR TRACKING SYSTEM FOR RANGE TESTS, by Yao Yu, Zhang Liyu	77
THE REAL-TIME WEIGHTED RECURSIVE ALGORITHM OF LEAST SQUARES ESTIMATION AND ITS INITIAL APPLICATIONS, by Luo Xucheng	88
TWO U.S. COMPANIES PUT FORWARD NEW CARRIER ROCKET DESIGN PLANS	107
FERRITE MAGNETIC HEAD OF EXPANDING RECORDING BANDWIDTH, by Zhang Peixing	108
CONNECTION DEVICES USED IN SATELLITE ROCKET SEPARATION, by Feng Zhenxing	127
SIMILARITY CRITERIA OF INTERIOR BALLISTICS IN LAUNCH CANISTER, by Shao Yang	129
LECTURE BULLETIN, by Chun Hui	150
NEW USES ASSOCIATED WITH COMBINED ENVIRONMENTAL TEST MODULE, by Feng Zhenxing	152
ENGINE MALFUNCTIONS EXPOSED BY SPACE FLIGHT LAUNCHES, by Sun Guoqing	153
APCATS '94 CONVENED IN HANGZHOU, by Chun Hui	166
CHINESE SPACE FLIGHT SCHOLARS WITHIN CHINA AND ABROAD GET TOGETHER IN BEIJING, by Chun Hui	168
NEWS IN BRIEF	
CZ-3A RISES SMOOTHLY ALOFT ARIAN FALLS IN THE OCEAN, by Yu Tian	170
INDIA'S POLAR ORBIT SATELLITE CARRIER ROCKET LAUNCH SUCCESSFUL, by Yu Tian	172

A U.S. COMPANY PUTS FORWARD DESIGN PLANS FOR REUSABLE SINGLE STAGE ORBITAL ENTRY ROCKETS, by Yu Tian	175
EUROPEAN SPACE AGENCY SELECTS REUSABLE ROCKET DEMONSTRATOR DESIGN	177
U.S. AIR FORCE LAUNCHES MINUTEMAN 3 MISSILE	178
UKRAINIAN ASTRONAVIGATIONAL ACTIVITIES	179
SIMPLE RULES FOR THE SOLICITATION OF CONTRIBUTIONS TO "MISSILES AND SPACE VEHICLES"	185

GRAPHICS DISCLAIMER

All figures, graphics, tables, equations, etc. merged into this
translation were extracted from the best quality copy available.

NAIC 62

MISSILES AND SPACE VEHICLES

China Carrier Rocket Technology Research Institute

Translation of "Dao Dan Yu Hang Tian Yun Zai Ji Shu";
Missiles and Space Vehicles, 1, 1995, pp I-II

NEW YEARS MESSAGE

China Carrier Rocket Technology Research Institute Chief Li Jianzhong

1995 happens to be the conclusion of "85". "95" will begin a crucial year. In the new year, successes and difficulties will go hand in hand. Challenges and opportunities will coexist. Looking back at history, accomplishments have been brilliant. Our minimum expenditures and fastest speeds have achieved accomplishments that have drawn the attention of the world. The successful launch of the CZ-2E rocket has already caused carrying capabilities associated with near earth orbit to reach 9200kg. Two successive successful launches of the CZ-3A rocket in 1994 has also caused carrying capabilities associated

with distant earth orbit to reach 2600kg. Launch technologies associated with Long March series carrier rockets have already reached advanced world levels. Looking forward to the future, prospects are broad. Our institute not only has real capabilities to catch up with and surpass advanced world levels in technology. It also has a staff contingent of high quality, working hard to move upward, and able to fight the good fight. A fine astrovavigational tradition, in the persons of the older generation of space flight personnel, has clearly shown its mighty power, and, in the persons of a new generation of astronavigational people, is also in the midst of moving forward--laying foundations, seeking development, and climbing ever higher. At the present time, we are in the midst of a series of steps to realize scientific research for the year 2000, managing to high levels, and living vigorously--projects are blueprinted, measures are drawn up, and deployments are carried out.

Facing the formidable tasks of 1995, we have already made ideological preparations to accomplish arduous missions. With full confidence in the inevitable victory, we are on the verge of carrying out the "95" plan which indicates that our institute will enter into a period associated with a new high tide in development--a period producing results in various areas. We will welcome the 21st century with even greater accomplishments and aspirations!

CONGRATULATIONS TO "MISSILES AND SPACE VEHICLES". YOU ARE GETTING BETTER AS YOU GO. CONGRATULATIONS TO THE EDITORS OF THIS PUBLICATION AND HAPPY NEW YEAR TO THE ENTIRE STAFF OF THE INSTITUTE!

Li Jianzhong

31 December 1994

REVIEW OF CALT'S LAUNCH SERVICE IN 1994 AND 1995

Chen Bingfang Wang Qingyang

Translation of "Zhong Guo Yun Zai Huo Jian Ji Shu Yan Jiu Yuan 1994 Nian Yu 1995 Nian De Guo Ji Shang Wu Fa She Huo Dong"; Missiles and Space Vehicles, No.1, 1995, Overall No. 213, pp 1-6

ABSTRACT In 1994, 5 satellite launch contracts were obtained. In accordance with contract specifications, 11 foreign satellites will be launched. The launch activities will continue until the beginning of the next century. In 1994, the CZ-3 and CZ-2E were respectively used to launch the Asia Pacific company's APSTAR-1 and two OPTUS-B3 satellites of the Optus Communications company. This demonstrated again that Long March rockets possess consummate design, superb technology, and high reliability. 1995 will be a year when our institute's launch service operations will be very busy. According to plans, 5 foreign satellites will be launched.

KEY WORDS Commercial launch vehicle Launching Review

1994 was a year when our institute's launch service operations achieved important accomplishments. This can be elaborated from two perspectives.

a. As far as the five contracts which were obtained for the launch of foreign satellites are concerned, they add up to a total of four foreign users launching six satellites. In a situation where deals are made for follow on ECHOSTAR projects, it is possible to launch another five satellites. Launch times will last until the beginning of the next century. /2

b. The initial test flight of the CZ-3A was successful. In conjunction with that, on 30 November it will carry out its first commercial flight--launching China's autonomously developed high capacity communications satellite, the Dongfanghong-3. Besides this, CZ-2E and CZ-3 have also successfully launched two foreign satellites.

These successful launch vehicle flights have demonstrated again that the Long March rocket series which our institute developed possesses fine design technology and superb manufacturing techniques--guaranteeing reliable quality. This will very, very greatly strengthen the confidence of domestic and foreign users in our Long March rockets.

1995 will be a particularly busy year for our institute's launch services. In accordance with the stipulations of foreign contracts, five foreign satellites will be launched. This is unprecedented in the history of China's space delivery activities.

1 1994 LAUNCH ACTIVITIES

1.1 Survey of Contracts Signed in 1994

Table 1 Survey of Contracts Our Institute Signed in 1994

① 序号	用户 ②	卫星名称 ③	卫星制造商 ④	火箭型号 ⑤ 及轨道	签订合同 ⑥ 时间	预计发射 ⑦ 时间	备注 ⑧
1	亚太卫星公司 ⑨	APSTAR-2 亚太二号 ⑩ (HS-601)	休斯公司 ⑪	CZ-2E LEO	1994.1.18	1994.12	因卫星制造商的原因, 发射时间推迟到 1995.1 ⑫
2	澳普图斯通信公司 ⑬	OPTUS B3 (HS-601)	休斯公司 ⑭	CZ-2E LEO	1994.2.28	1994.7	于 1994.8.28 顺利发射成功 ⑮
3	回声公司 ⑯	ECHOSTAR (E 7000)	马丁-玛丽埃塔公司 ⑰	CZ-2E LEO	1994.2.22	ECHOSTAR -1 1995.8~10	★回声星合同共包括七颗星。现已签订了两颗星的合同, 其余几颗星的合同待签, 基本上每年一发, 发射可能延续至 2001 年 ⑯
4	国际通信卫星组织 ⑲	INTELSAT 805	马丁-玛丽埃塔公司 ⑳	CZ-3B GTO	1994.5.12	1997.3~5	★回声公司同时采购河西公司制造的 EPKM (固体火箭发动机), 与卫星一起作为 CZ-2E 的有效载荷。EPKM 在与 CZ-2E 分离后将卫星送入地球同步转移轨道 ⑱
5	国际通信卫星组织 ⑲	INTELSAT 801	马丁-玛丽埃塔公司 ㉑	CZ-3B GTO	1994.7.22	1995.12 ~ 1996.1	

Key: (1) Serial No. (2) User (3) Satellite Nomenclature (4) Satellite Manufacturing Firm (5) Rocket Models and Orbits (6) Time Contract Signed (7) Projected Launch Times (8) Remarks (9) Asia Pacific Satellite Company (10) APSTAR-2 (11) Hughes Company (12) Because of causes associated with satellite manufacturing firm, launch time postponed to 1995.1. (13) Optus Communications Company (14) Hughes Company (15) Smooth Launch Successful 1994.8.28 (16) Echo Company (17) Martin Marietta Company (18) * ECHOSTAR contract includes a total of seven satellites. Currently, contracts have already been signed for two satellites. Contracts for the other few satellites still wait to be signed. Basically, there is one launch a year. Launches are capable of lasting until the year 2001. * Echo Company

simultaneously opted for the purchase of the EPKM (solid rocket motor) manufactured by the Hexi Company, which acted as the CZ-2E useful load together with the satellite. After separation from the CZ-2E, the EPKM will take the satellite and send it into a geosynchronous transfer orbit. (19) International Communications Satellite Organization (20) Martin Marietta Company

Here, what requires supplemental explanation is the following.

a. What the Echo company and the Great Wall company signed is a contract to use CZ-2E launch vehicles to take Echo satellites and send them into LEO orbits. On the basis of the contract in question, our institute is only responsible for using CZ-2E's to take useful loads and send them into low earth orbits. Moreover, the Echo company simultaneously purchases for us the EPKM solid rocket motor produced by the Hexi Company (Inner Mongolia). In this way, it acts as a part of the CZ-2E useful load which is sent into LEO together with the satellite. After that, the EPKM takes the Echo satellite and sends it into GTO. This then means that carrier rockets not only must coordinate on the satellite side. They must also coordinate with the Hexi company the carrying out of EPKM technology. Of course, this is already not the first example. The AsiaSat-2, which was originally set for launch in the first quarter of 1995 had the same contract modality as the Echo satellites--even to the point of the satellite manufacturing firm being the same one, that is, the Martin Marietta company. Because of this, it should be said that this type of coordination will not present any difficulties.

b. As far as AUSSAT B3 is concerned, there was nearly just six months of time from contract signing to carrying out the launch. This is a type of special case. Due to the fact that during the CZ-2E AUSSAT B2 launch on 21 December 1992, after the rocket had gone aloft for 47.8s, the satellite gave rise to an explosion, it was, because of this, not able to complete its predetermined missions. The next launch was imperative under the circumstances. Therefore, the Chinese and the U.S. sides both have adequate preparation in terms of technology and in terms of

materiel. However, both sides have disputes in areas of commercial affairs and in terms of technological problems. After going through a long period of hard negotiations, both sides finally reached a consensus. In conjunction with this, on 28 February 1994, the B3 launch contract was formally signed. Of course, this certainly does not mean, under any circumstances, that we both possess capabilities to carry out satellite launches six months after the signing of the contract.

c. The APSTAR-2 satellite launch date was stipulated as the end of 1994 when the contract was signed. Later, because of causes associated with the satellite manufacturing firm, it was projected that it would be delayed until January of 1995. In the case of this particular contract, it was less than a year from signing to the carrying out of the launch. This is unprecedented. The reason was the special nature of the user. The Asia Pacific Satellite company is registered in Hong Kong. It is composed by joint investments of seven domestic and foreign companies. The Hong Kong Weitaisi (phonetic) Systems Ltd. company is one of the four sponsoring companies subordinate to the main aviation industry corporation. The former deputy chief of our institute, He Kerang, is the director general of the Asia Pacific company. Based on this background and with the vigorous support of the main corporation and our institute--under the meticulous planning and organization of the institute's project control department--a plan was arranged to carry out launch at the end of 1994--satisfying urgent user requirements. Because of this, the implementation period for this contract was also unusual.

1.2 Two Satellites Launched in 1994 (See Table 2)

Table 2 Two Satellites Launched in 1994

① 卫星名称	② 用 户	③ 卫星制造商	④ 火箭型号	⑤ 发射日期
APSTAR-1	⑥ 亚太卫星公司	⑧ 休斯公司	CZ-3	94.7.21
OPTUS B3	⑦ 澳普图斯通信公司	⑨ 休斯公司	CZ-2E	94.8.28

Key: (1) Satellite Nomenclature (2) User (3) Satellite Manufacturing Firm (4) Rocket Model (5) Launch Date (6) Asia Pacific Satellite Company (7) OPTUS Communications Company (8) Hughes Company (9) Hughes Company

The two successful launches have extremely important significance with regard to the two CZ-3 and CZ-2E types of rockets. In actuality, they also demonstrate to the people of the world that the analysis and malfunction resolution capabilities of the personnel who developed our Long March series launch vehicles are outstanding--thus being capable of guaranteeing very high reliabilities for Long March rockets.

a. As is common knowledge, after the CZ-3 rocket had successfully carried out seven launch iterations, on 28 December 1991, at the time of the eighth flight, it was not capable of taking a useful load and sending it into predesignated orbit, leading to failure of the launch. Going through conscientious and detailed analysis, technological personnel believe that the malfunction was due to the development of leaks in the third stage power system engine control gas bottle and piping systems. This led to the creation of premature engine shut down due to inadequate control gas pressure when the rocket flight reached approximately 897s. /4

Commercial launches are a high risk activity, "long tested" rockets like the French Arian also still frequently give rise to

malfunctions. On 24 January 1994, the Arian 4 failed during the 63d Arian launch iteration. The fact that malfunctions occur is certainly not important. What is important is to find out the causes of the malfunction, and, in conjunction with that, adopt effective measures. After analysis by technicians, and, in conjunction, confirming the causes of the CZ-3 malfunction, a series of targeted measures was adopted, increasing launch reliability. For example, numbers of third stage motor control gas bottles and pressurization gas bottles were increased. Piping seal designs were improved, and so on. Besides this, in order to make full use of the carrying capabilities associated with the CZ-3 and increase satellite life in orbit, in this launch iteration, the CZ-3 will also adopt the several measures below. (1) Jet tube expansion ratios associated with second stage main motors are enlarged. (2) Course deviation yaw program systems are added to the third stage to lower orbital angles of inclination. (3) Apogee offsets are raised. Flights demonstrate that these measures are all effective.

b. Development of the CZ-2E rocket was completed using 18 months. Moreover, on 16 July 1990, the first test flight was a success. This was the working of a miracle in the history of Chinese astronavigation. In international space flight circles also, it made the rounds as a story on everyone's lips. On 22 March 1992, in the case of the first AUSSAT B1 launch, due to the appearance of malfunctions in ignition systems, the launch was suspended. However, the malfunctions were very quickly checked out. In conjunction with this, effective measures were adopted. Going through a period of time under 5 months, the B1 satellite was successfully sent into predetermined orbit on 14 August 1992. However, on 21 December 1992, when the second AUSSAT satellite--that is, B2--was launched, the satellite gave rise to an explosion during the rocket flight. When we and the Hughes company were in the midst of striving to find the cause of this malfunction, some people still purposely confused right and wrong--imputing the blame for the satellite explosion to the carrier rocket. Initially, it was said that the rocket vibration environment exceeded

specifications. It was also said that the rocket cowling was first destroyed, creating damage in the satellite. For a short time, in international space flight circles and insurance circles, various types of misunderstandings and conjectures were given rise to--producing doubts with regard to the reliability of the CZ-2E rocket. Insurance firms believed that underwriting satellite launches using CZ-2E rockets was too risky. They wanted to greatly increase insurance premiums. Some even went as far as to deny coverage.

In October 1993, the Great Wall company and our institute jointly organized a delegation under the leadership of deputy institute chief Wang Dechen which went to London to make explanations and publicity directed toward international insurance circles. The several leading space risk assurance firms at the present time all took part in this conference. The delegation made use of such materials as telemetry data, photographs of cowling remains, and so on, to adequately demonstrate that the cause of the satellite explosion was certainly not the launch vehicle (including cowlings). This explanation and publicity achieved justification, benefits, and savings, speaking just in terms of ourselves to say nothing of others--obtaining very good results. The doubts and misunderstandings of the insurance circles were cleared up. U.S. insurance firms said, "CALT's explanations and publicity are credible and reliable." However, these were, in the final analysis, only proofs and explanations. The real test is the actual flight of the rockets. The successful flight of 28 August 1994 really demonstrated that our analyses and proofs were correct, once again proving to the people of the world that the Long March series of launch vehicles is reliable.

It should also be pointed out that, as far as several CZ-2E launch iterations are concerned, their precisions were all far, far higher than the specified nominal values (nominal orbit data: perigee 185-200km; apogee 1040-1045km; angle of inclination 28°). Even in the type of instance like the B2 launch--with respect to the occurrence of explosions associated with useful loads and in

situations where the configurations gave rise to very great changes--CZ-2E rockets having very strong capabilities to respond to emergencies still took the remaining useful load and sent it into an orbit which was more accurate than the predetermined one. Table 3 gives the precisions associated with CZ-2E mooring orbits.

Table 3 CZ-2E Mooring Orbit Precision Parameters

(1) 轨道参数	(2) 名义值 3σ	(3) 试飞	(4) 澳星 B1	(5) 澳星 B2	(6) 澳星 B3
(7) 近地点 (km)	6	- 0.762	- 0.686	+ 3.804	- 0.513
(8) 远地点 (km)	12.4	+ 3.042	+ 1.790	- 6.246	- 3.707
(9) 倾角 ($^{\circ}$)	0.15	- 0.006	- 0.076	+ 0.064	0.017
(10) 升交点 ($^{\circ}$)	0.5	+ 0.058	+ 0.363	- 0.040	
(11) 近地点幅角 ($^{\circ}$)	2.25	+ 0.534	+ 0.176	- 2.011	- 0.319

Key: (1) Orbital Parameters (2) Nominal Value (3) Test Flight
 (4) AUSSAT B1 (5) AUSSAT B2 (6) AUSSAT B3 (7) Perigee (8)
 Apogee (9) Angle of Inclination (10) Ascending Node (11)
 Perigee Angle of Amplitude

/5

Besides that--responding to user requirements--with regard to cowlings of the CZ-2E rockets which launched B3, adoption was made of a number of strengthening measures (see Fig.1).

(a) The number of bolts connecting the terminal head cap and the forward cone was increased from 42 to 82 (see 1 in the Fig.).

(b) The number of mating bolts associated with the two halves of the terminal head cap was increased from 12 to 23 (see 2 in the Fig.).

(c) Between the terminal head cap and the forward cone, there were added two semicircular partitions in order to strengthen the overall solidity of the cowling (see 3 in the Fig.).

(d) Diameters of 20 rivets at 6 sites were increased from $\Phi 3$ to $\Phi 4$ (see 4 in the Fig.).

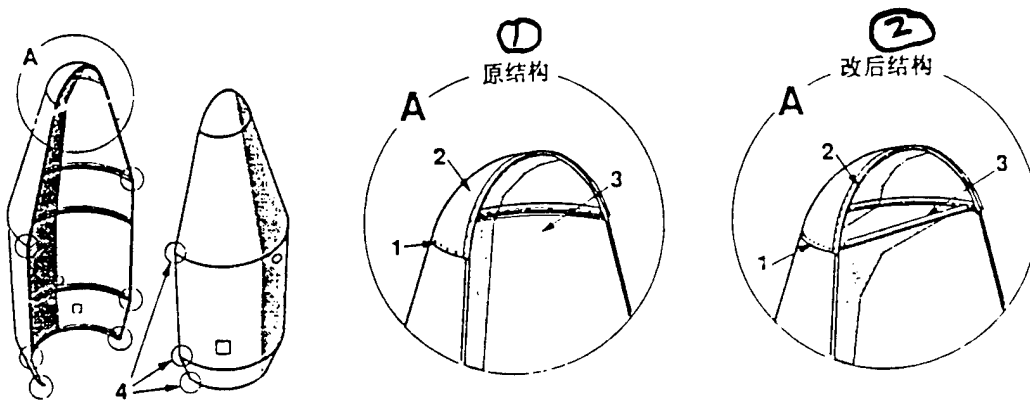


Fig.1 Schematic of CZ-2E Rocket Strengthening Measures

Key: (1) Original Structure (2) Structure After Changes

1.3 Two Launches that Possess Far Reaching Influences

1994 also had two carrier rocket launches which possessed far reaching influences. These were none other than the first test flight of the CZ-3A on 8 February 1994 and the carrying out of the first commercial flight of the CZ-3A at the end of November in the same year--launching the domestically produced Dongfanghong-3 communications satellite. On the foundation of the CZ-3, the CZ-3A takes the third stage and switches it for a newly developed third stage possessing greater thrust and forming a new type of launch vehicle. Using the somewhat improved CZ-3A as the

core stage, option is made for the use of the strapdown technology which China has already mastered to strap on four liquid boosters (the structure and performance is completely the same as CZ-2E boosters) then creating a launch vehicle which possesses maximum carrying capabilities among China's Long March series of carrier rockets--the CZ-3B. Its GTO capability can reach 5000kg.

Up to the present time, the CZ-3B launch vehicle has already obtained three contracts. Besides items 4 and 5 in Table 1, there are also 7A satellites. The user is the international communications satellite organization in all cases. The first 7A satellite contract was signed on 24 April 1992. At that time, not only was the CZ-3B simply an idle paper theory, the CZ-3A was also still in development. Because of this, the user reasonably made the CZ-3A development process act as the milestones for the carrying out of the contract. That is, whether or not the CZ-3A's first test flight as well as the first commercial flight were successes was, in both cases, closely related to whether or not a CZ-3B contract could be carried out. Once the user discovered that the CZ-3A development pace did not meet requirements, influencing CZ-3B progress, it then had the right to suspend the contract.

At the present time, we can proudly announce that the first test flight of the CZ-3A on 8 February 1994 was completely successful. Looking at flight telemetry data, CZ-3A performance also had very great latent capabilities. Because of this, the general designer of the CZ-3A and CZ-3B, deputy institute chief Long Lehao, has already formally announced that CZ-3A launch capabilities are already not the 2300kg announced in the past but are 2500kg. The corresponding CZ-3B carrying capability was also increased from 4800kg to 5000kg. At the time the authors were completing this manuscript, the CZ-3A's first commercial flight had not yet been carried out. However, we have reason to believe that it will indeed achieve complete success (Ed. Note: The rocket in question was already launched successfully on 30 November 1994.)

/6

2 LAUNCH OPERATIONS THAT WILL BE CARRIED OUT IN 1995

Foreign satellites that will be launched in 1995 are seen in Table 4.

Table 4 Table of Satellites that Will Be Launched in 1995

① 序号	预计发射时间 ②	火箭型号 轨道 ③	用户 ④	卫星名称 ⑤	卫星制造商 ⑥	⑦ 备注
1	1995.1	CZ-2E / LEO	亚太卫星公司 ⑧	APSTAR-2 (HS-601)	休斯公司 ⑨	
2	1995.5	CZ-2E / LEO	亚洲卫星公司 ⑩	ASIASAT-2 (7000 系列) ⑪	MMOS ⑫ 马丁-玛丽 ⑬ 埃塔公司 ⑭	用户采购河西公司的 EPKM 将卫星从 LEO 送入 GTO ⑮
3	1995.8	CZ-2E	回声公司 ⑯	ECHOSTAR-1 (7000 系列) ⑰	MMOS ⑯ 马丁-玛丽 ⑯ 埃塔公司 ⑯	
4	1995.10	CZ-3B	国际通信 卫星组织 ⑲	INTELSAT 7A	SS / L 洛拉公司 ⑳ 空间系统部 ㉑	
5	1995 年底 ~ 1996 年初 ㉒	CZ-3B	国际通信 卫星组织 ㉓	INTELSAT 801 (7000 系列) ㉔	SS / L ㉕ 马丁-玛丽 ㉖ 埃塔公司 ㉗	

Key: (1) Sequence No. (2) Projected Launch Time (3) Rocket Model/Orbit (4) User (5) Satellite Nomenclature (6) Satellite Manufacturing Firm (7) Remarks (8) Asia Pacific Satellite Company (9) Hughes Company (10) Asia Satellite Company (11) Series (12) Martin-Marietta (13) User Procured Hexi Company EPKM to Take Satellite and Send It into GTO (14) Echo Company (15) International Communications Satellite Organization (16) Luola Company Space Systems Division (17) End of 1995 - Beginning of 1996

Foreign satellite launch missions which are to be completed in 1995 involve certain difficulties. First of all, operations associated with the Xichang launch base will be very busy. Because these five launch iterations will all be carried out from the No.2 pad at the Xichang launch center, these five launch iterations in one year create a record in and of themselves. In addition, launching CZ-2E's and CZ-3B's involves a number of changes with regard to the requirements associated with launch towers. Because of this, configuration transformations also require time. This presents higher requirements with regard to our institute's coordinating Xichang base operations as well.

Next, from Table 4, it is possible to see that the launch periods for the APSTAR-2 and the ECHOSTAR-1 are very close to each other. The two international communications satellites are also launched very close to one another. Speaking in terms of our institute's design and manufacturing contingents as well as the rear service support departments, they will face a situation of continuous operations.

After achieving success in 1994, we have full confidence in the prospects for 1995. We have faith that the entire staff of CALT will certainly achieve glory for the Chinese space flight enterprise.

SPACECRAFT FLEXIBLE MULTI-BODY DYNAMICS
AND ITS DEVELOPMENT

Wang Yi Wu Delong

Translation of "Hang Tian Rou Xing Duo Ti Dong Li Xue Ji Qi Fa Zhan"; Missiles and Space Vehicles, Overall No. 213, No.1, 1995, pp 7-18

ABSTRACT Introduction is made of the history of the development of spacecraft flexible multi-body dynamics as well as the main academic schools of thought in international academic circles at the present time along with the current state of research. Through discussions of two types of representative methods--Kane and Lagrange--set up processes associated with spacecraft flexible multi-body dynamic mathematical models are introduced. In conjunction with this, comprehensive analyses and conclusions are carried out with regard to such things as kinematic descriptions, discrete methods, as well as numerical value calculations and simulations of the theory associated with the setting up of models for flexible multi-body dynamics. Finally, discussions are carried out with respect to the characteristics of spacecraft flexible multi-body dynamics and questions related to it.

KEY WORDS Astrodynamics Structural dynamics Flexible body Mathematical model

[This article was received on 10 January 1994. The topic in question was a subject aided by the He Hongsang Space Flight Science and Technology Personnel Training Fund.]

1 INTRODUCTION

Multi-body systems are systems composed of multiple rigid bodies or flexible bodies connected to each other. Spacecraft being engineered, weapons systems, vehicles, operating mechanical arms, robots, complex mechanical systems, as well as organisms used in motion studies, and so on, are all actual multi-body systems. In systems, the various unit bodies use such different types of diverse methods as hinges, slides, springs, dampers, connecting cables, and so on, to connect themselves together. Between the various unit bodies, there exist relative motions. Unit bodies themselves also give rise to elastic deformations--thereby, forming extremely complex multi-body kinematic systems. /8

As far as the development of multi-body dynamics is concerned, it is closely related to the development of space flight technology. In the design of modern spacecraft, a good number of new problems are met with. Many are also related to multi-body dynamics. In the realm of international space flight, research with regard to multi-body dynamics is looked on very seriously. In particular, in the 1970's-1980's, the U.S. Freedom space station project as well as the permanently manned vehicle project were carried out, causing large model flexible spacecraft as well as multi-body system dynamics and control problems to become one of the hot spots associated with astronavigational dynamics research at the present time. Kane, Linkins, Hughes, Meirovitch, Modi, Shabana, Haug, and others, carried out large amounts of ground breaking work in this regard. In conjunction with this, they put out, one after the other, multi-body system dynamics analysis software which can be used in the analysis of spacecraft--for example, DISCOS, MULTIBODY, TREETOPS, ALLFLEX, ADAMS, DADS, RASNA, and so on. Among these, the largest portion are multiple rigid body system analysis software. The minority are capable of

carrying out flexible multiple body system dynamics analysis. Following along with the development of Chinese astronavigational high technology, ever more numerous multi-body dynamics problems have already been met with--beginning an understanding of the importance of developing space flight flexible multi-body systems dynamics research.

2 DEVELOPMENT HISTORY OF FLEXIBLE MULTI-BODY DYNAMICS

Multi-body dynamics research has gone through 30 years of development. It has already achieved a good number of results. As far as work in the early period is concerned, it was mostly concentrated in research associated with multiple rigid body systems [1]. From the 1960's to the present time, multiple rigid body dynamics has already formed a good number of methods each possessing special characteristics--for example, Newton-Euler methods, Lagrange methods, Roberson-Wittenburg methods, Kane methods, Huston methods, and so on. In conjunction with this, quite superb results have been achieved--already resolving a good number of actual applied problems in engineering.

Following along with the development of astronavigational high technology--in particular, the implementation of large model space stations and permanently manned facilities in the 1980's--in engineering, one had the appearance of large numbers of load bearing mechanical hands and arms which moved at fast speeds and were light weight. They were capable of deploying satellite antennas and solar panels with large areas and were basic space structures which were able to combine large dimensions, small mass, and structural complexity, etc. As a result, as far as consideration of more generalized flexible multi-body dynamics problems having flexible components or ones filled with fluids is concerned, it has already become a new development direction.

With respect to flexible multi-body dynamics research, Ho [9] put forward a direct path method of studying flexible multi-body dynamics. Use of this concept was also opted for in other later

flexible multi-body dynamics methods. Singh et al [10] made use of Kane equations obtained in studies of multiple rigid body dynamics. Component mode functions used discretely represent elastic deformations of objects, deriving a general equation associated with flexible multi-body dynamics. In conjunction with this, the TREETOPS simulation software system was formed. Meirovitch and Quinn [11] made use of perturbation methods, taking high order, nonlinear equation sets and separating them into zero order, low dimension rigid body motions and first orders corresponding to rigid body motions, as well as elastic motions associated with relationships between high dimension numbers and times. Modi [12] made use of concepts associated with Lagrange equations, deriving a general use flexible multi-body dynamics equation suitable for use in spacecraft. In conjunction with this, use was made of REDUCE symbol operating software to complete derivation of motion equations. Shabana [13] used consistent mass finite unit methods to carry out discrete dispersion with regard to deformable bodies. Haug [14] used concentrated mass finite unit methods to carry out discrete dispersion of deformable bodies. They both used the first type of Lagrange method to set up formulated mathematical dynamics models for flexible multi-body systems. The former developed DADS software. The latter added a flexible analysis module into ADAMS software. Besides this, Vu-Quock and Simo [15] put forward rotating and floating frame methods. Spanos and Tsuha [16] opted for the use of component mode methods. There are also other scholars who opted for the use of other methods.

Following along with in depth research on flexible multi-body systems, people have paid attention to dynamic stiffening phenomena associated with rotating components in multi-body systems. Due to the fact that inertial forces exist during rotation--particularly, when rotation speeds are very large--when use is made of linear stress-strain relationships to describe flexible multi-body system component elastic deformations, it is not possible to predict system dynamic behavior very well. Simo [17], Wallrap [18], Shabana [13] and others have, respectively, made use of nonlinear

stiffness matrices and mass formulae to study dynamic stiffening phenomena. With regard to large model multi-body systems, after consideration of geometric stiffening matrices, calculation amounts increase very greatly. With a view to this phenomenon, Banerjee [19] and others also put forward "motion induced stiffening matrices". Reductions are carried out in the degrees of freedom associated with geometric stiffness matrices--thereby lowering system dimension numbers.

/9

3 MATHEMATICAL MODELS ASSOCIATED WITH ASTRONAVIGATIONAL FLEXIBLE MULTI-BODY DYNAMICS

As was discussed above, there are already a good number of scholars who have carried out research with regard to astronavigational multi-body dynamics problems. In conjunction with this, different academic characteristics and schools of thought have been formed. Among these many astronavigational flexible multi-body dynamics mathematical models, Kane methods and Lagrange methods possess representative natures. Kane methods possess the advantages associated with the two Newton-Euler and Lagrange methods. Opting for the use of Kane equations, it is possible in analyses to automatically eliminate constraining internal forces which do not act and to do away with the need for introducing differential scalar energy functions. This is even more advantageous with regard to large multi-body system problems [10]. Lagrange methods opt for the use of absolute coordinate methods to describe large displacement system motions. Use is made of finite element methods or mode methods to carry out discrete dispersion with regard to deformation bodies. As far as various unit bodies are concerned, Lagrange equations respectively operate to set up the dynamics equations. In conjunction with this, they are formed into system dynamics equations. Use is made of motion constraint equations to express connection relationships. The advantage of the methods in question is convenience for formalized computer processing. Below, Kane methods and Lagrange methods are

respectively introduced.

3.1 Kane Methods

Giving consideration to NB mutually connected flexible multi-body space systems--not to lose universality--assume that they possess a tree shaped topological structure. See Fig.1.

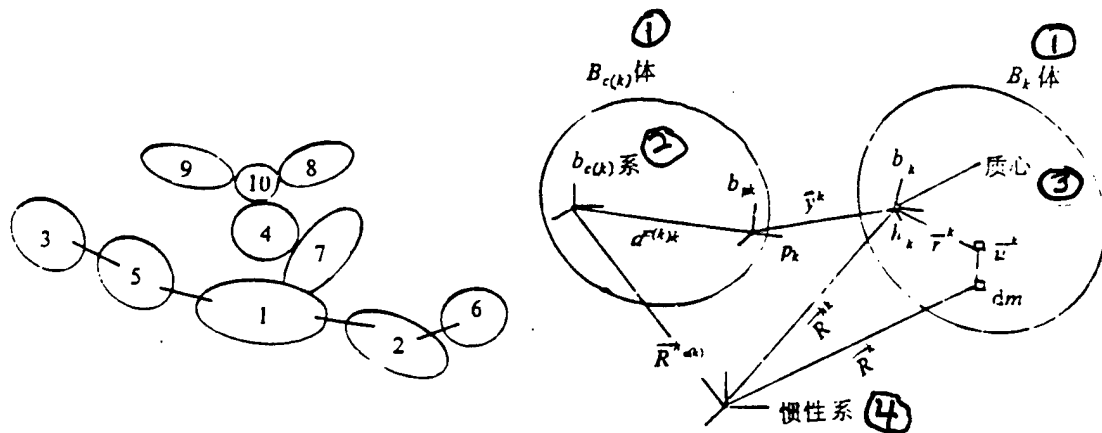


Fig.1 Coordinate System Associated with Tree Shaped Flexible Multi-Body Systems

Key: (1) Body (2) System (3) Center of Mass (4) Inertial System

First of all, in accordance with direct path concepts, grade separation is done on systems. In conjunction with this, selected body 1 is the center body of the system. With regard to an arbitrary object k , $c(k)$ represents the internally connected bodies. The center of the earth is selected as the inertial coordinate system. A hinge in Fig.1 is defined as two material points on two adjacent objects. As far as a point p_k on body $c(k)$

and a point h_k on body k are concerned, coordinate systems b_{pk} and b_k are set up on point p_k and point h_k respectively. Thus, the degrees of freedom associated with object k can be discretely dispersed as horizontal movements and rotations of b_k relative to the coordinate system b_{pk} .

With respect to multi-body dynamics expressions, selecting the mass unit dm on the k th object, it is not difficult to give the dm expression corresponding to inertial coordinate systems after object b_k deformation:

$$R^k = R^{hk} + r^k + u^k \quad (1)$$

In this, r^k is the dm radius vector associated with h_k when deformation has not yet taken place. u^k is elastic deformation:

/10

$$u^k = \sum_{i=1}^{NM} \Phi_i^k (r^k) \dot{\eta}_i^k \quad (2)$$

In this, $\Phi_i^k (r^k)$ is mode vector. $\dot{\eta}_i^k$ is mode coordinate.

The time derivative in inertial space associated with R^k is

$$\dot{R}^k = \dot{R}^{hk} + \omega^k (r^k + u^k) + \dot{u}^k \quad (3)$$

In this, (\circ) expresses time derivatives in local coordinate systems (here, it is the b_k system). ω^k is the inertial angular velocity vector associated with the reference system b_k . The mode vector Φ_i^k r^k which draws attention in formula (2) is fixed in the reference system b_k . Thus, the relative deformation speed is

$$\dot{u}^k = \sum_{i=1}^{NM} \Phi_i^k (r^k) \ddot{\eta}_i^k \quad (4)$$

On the basis of Kane methods, using a set of generalized

speeds w_1, w_2, \dots, w_{NS} to represent degrees of freedom associated with systems, \dot{R}^k is then always capable of expressing a combination of generalized speeds.

$$\dot{R}^k = \sum_{p=1}^{NS} V_p^k w_p + V_i^k \quad (5)$$

In the same way, \dot{R}^{hk} , ω^k , and \dot{u}^k are all capable of expressing combinations of generalized speeds.

$$\dot{R}^{hk} = \sum_{p=1}^{NS} V_p^{hk} w_p + V_i^{hk} \quad (6)$$

$$\omega^k = \sum_{p=1}^{NS} \omega_p^k w_p + \omega_i^k \quad (7)$$

$$\dot{u}^k = \sum_{p=1}^{NS} V_p^{nk} w_p \quad (8)$$

Taking equations (6) - (8) and substituting into equation (3), and, in conjunction with that, carrying out comparisons with equation (5), one obtains:

$$V_p^k = V_p^{hk} + \omega_p^k [r^k + \sum_{i=1}^{NM} \Phi_i^k (r^k) \eta_i^k] + V_p^{nk} \quad (9)$$

$$V_i^k = V_i^{hk} + \omega_i^k [r^k + \sum_{i=1}^{NM} \Phi_i^k (r^k) \eta_i^k] \quad (10)$$

From equations (9) and (10), it is possible to know that in \dot{R}^k , deviation velocities V_p^k and V_i^k are dependent on the selection of deviation velocities V_p^{hk} , V_i^{hk} , and V_i^{nk} , as well as angular deviation velocities ω_p^k and ω_i^k .

From Fig.1, it is possible to know that multi-body system dynamics have the recurrence relationships below:

$$\dot{R}^{hk} = R^{hc(k)} + d^{c(k)} k + y^k \quad (11)$$

$$d^{c(k)k} = D^{c(k)k} + \sum_{i=1}^{NB} \Phi_i^{c(k)}(p_k) \dot{\eta}_i^{c(k)} \quad (12)$$

In equations, $D^{c(k)k}$ is the radius vector before $B_{c(k)}$ body transformation from h_{ck} to p_k . $\Phi_i^{c(k)}(p_k)$ is fixed on mode displacements at p_k point values in $B_{c(k)}$ reference systems.

$$\omega^k = \omega^{c(k)} + \sum_{i=1}^{NB} \Phi_i^{c(k)}(p_k) \dot{\eta}_i^{c(k)} + \omega^{kc(k)} \quad (13)$$

/11

Through the relationships above, it is possible to take \ddot{R}^{hk} , and ω^k (including \ddot{R}^{hk} , and $\dot{\omega}^k$) in the same way) and express them in the form of recurrence relationships.

As far as the setting up of dynamics equations is concerned, it is possible to use Newton's second law, considering dm mass micro element equilibrium relationships, to obtain it. For example,

$$\sum_{k=1}^{NB} \int_{B_k} V_p^k df - \sum_{k=1}^{NB} \int_{B_k} V_p^k \ddot{R}^k dm = 0 \quad (p=1, 2, \dots, NS) \quad (14)$$

Equation (14) can be expressed as a series of NS equations

$$f_p + f_p^* = 0 \quad (p=1, 2, \dots, NS) \quad (15)$$

In this, f_p and f_p^* are, respectively, generalized drive forces and inertial forces.

Taking equation (9) and substituting it into equation (14), it is possible to obtain the pth generalized drive force

$$f_p = \sum_{k=1}^{NB} \int_{B_k} V_p^k df = \sum_{k=1}^{NB} (M^{hk} \omega_p^k + F^k V_p^{hk} + \int_{B_k} V_p^k d\bar{f}) \quad (16)$$

In this, M^{hk} is acting forces which are equivalent to hinge point moments (constraining forces which do not act are eliminated). The final term expresses the contributions of internal elastic forces associated with the body B_k and other effects on bodies from external forces. Each p corresponds to one of the mode speeds associated with the body B_k . Integrals represent the first row of

generalized stiffness matrices (and damping matrices) multiplied by the first column negative values associated with mode coordinates (and mode speeds).

In the same way, the pth generalized inertial force is

$$\begin{aligned}
 -\dot{f}_p &= \sum_{k=1}^{NB} \int_{B_k} V'_k \tilde{R}^k dm \\
 &= \sum_{k=1}^{NB} [m_k (\tilde{R}^{hk} + \ddot{l}^k) V^{hk}{}_p + (\dot{H}^{hk} + m_k l^k \times \tilde{R}^{hk}) \omega_p^k + \tilde{R}^{hk} \int V'^k dm \\
 &\quad + \dot{\omega}^k \int_{B_k} (r^k + u^k) \times V'^k dm + 2\omega^k \int_{B_k} \dot{u}^k V'^k dm + \int \ddot{u}^k V'^k dm - \omega^k D_p^k \omega^k] \quad (17)
 \end{aligned}$$

In this equation, m_k is the mass of B_k . l^k is the radius vector h_k corresponding to the center of mass of body B_k after deformation. The symbols (*) and (**) stand for first order and second order derivatives in inertial coordinate systems. The symbols (^o) and (^{oo}) stand for first order and second order derivatives in reference systems B_k . u^k is defined by equation (2). Thus, one then gets dynamic equations (15) associated with NB flexible multi-body systems.

3.2 Lagrange Methods

With regard to any flexible unit body B_1 (Fig.2), reference coordinate systems are set up, and, in conjunction with that, finite element network divisions are carried out--taking flexible body distribution masses and condensing them at N nodal points. Assuming that the position of any nodal point i ($i=1, 2, \dots, N$) is \bar{r}_i^0 in the floating coordinate system $O_1x_1y_1z_1$ when deformation has not yet occurred, and flexible deformation is \bar{u}_i , then, m_i mass elements after deformation correspond to the coordinate system $O_1x_1y_1z_1$. Position vectors associated with the inertial system $O_0x_0y_0z_0$ are

$$\bar{R}_i = \bar{R}_i + \bar{r}_i^0 + \bar{u}_i \quad (18)$$

$$u_i = P_i \Phi_i a_i = \Phi_i' a_i \quad (19)$$

In equations, P_i is a projection matrix. Φ_j ($j=1, 2, \dots, MM$) is mode vectors associated with unit mass nodal point deformations. a_j is mode coordinate. Thus, equation (18) is written into vector form as

/12

$$\dot{R} = R + A_r r' + A_\rho \Phi a \quad (20)$$

In this, A_1 is the transformation matrix for the floating coordinate system $O_1x_1y_1z_1$ relative to the inertial system coordinates $O_0x_0y_0z_0$.

$$\dot{R} = R + A_r r' + A_\rho \Phi a \quad (21)$$

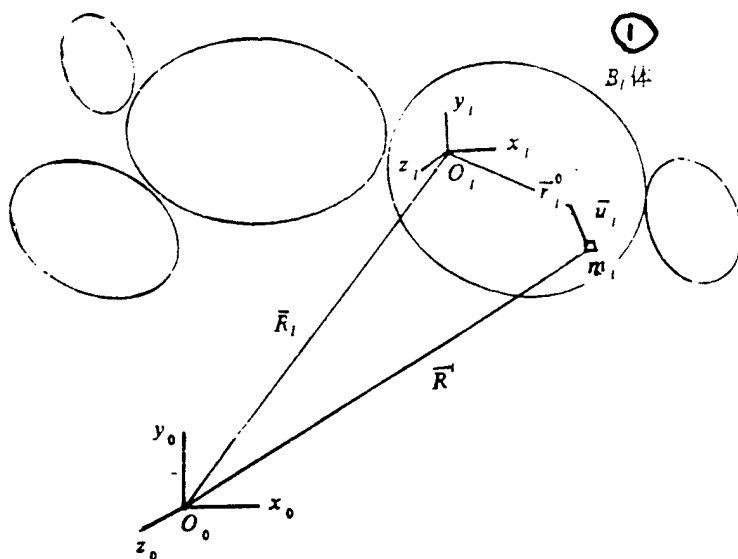


Fig. 2 Flexible Body Reference Coordinate System

Key: (1) Body

If use is made of rotations between Euler quaternion description coordinate systems, that is, making use of expressions associated with $q = [q_0, q_1, q_2, q_3]^T$. Then, on the basis of Poisson equations [2], one has

$$\dot{A}_r \rho_i = -2A_r \bar{\rho}_i G_i \dot{q} \quad (22)$$

In this,

$$\bar{\rho}_i = \begin{bmatrix} 0 & -\rho_{iz} & \rho_{iy} \\ \rho_{iz} & 0 & -\rho_{ix} \\ -\rho_{iy} & \rho_{ix} & 0 \end{bmatrix} \quad G_i = \begin{bmatrix} -q_1 & q_0 & q_3 & -q_2 \\ -q_2 & -q_3 & q_0 & q_1 \\ -q_3 & q_2 & -q_1 & q_0 \end{bmatrix} \quad (23)$$

Thus, from equation (21)

$$\dot{R}' = \dot{R}_i - 2A_i \bar{\rho}_i G_i \dot{q} + A_i \Phi_{ij}' \dot{a}_j = [I - 2A_i \bar{\rho}_i G_i \quad A_i \Phi_{ij}'] \begin{bmatrix} \dot{R}_i \\ \dot{q} \\ \dot{a}_j \end{bmatrix} \quad (24)$$

The kinetic energy associated with a single flexible body is the sum of kinetic energies associated with masses condensed at N nodal points.

$$T = \frac{1}{2} \sum_{i=1}^N m_i \dot{R}'^T \dot{R}' = \frac{1}{2} \begin{bmatrix} \dot{R}_i \\ \dot{q} \\ \dot{a}_j \end{bmatrix}^T M \begin{bmatrix} \dot{R}_i \\ \dot{q} \\ \dot{a}_j \end{bmatrix} \quad (25)$$

$$M = \begin{bmatrix} \sum_{i=1}^N m_i & -2A_i \sum_{i=1}^N m_i \bar{\rho}_i G_i & A_i \sum_{i=1}^N m_i \Phi_{ij}' \\ 4G_i^T \sum_{i=1}^N m_i \bar{\rho}_i^T \bar{\rho}_i G_i & -2G_i^T \sum_{i=1}^N m_i \bar{\rho}_i^T \Phi_{ij}' \\ \text{对称} & \sum_{i=1}^N m_i \Phi_{ij}^T \Phi_{ij}' \end{bmatrix} \quad /13 \quad (26)$$

Elastic strain energies associated with B_1

$$U = \frac{1}{2} u^T K_T u = \frac{1}{2} a_j^T \Phi_{ij}^T K_T \Phi_{ij} a_j = \frac{1}{2} a_j^T K_{aa} a_j \quad (27)$$

In this, K_T is stiffness matrices associated with flexible unit bodies. Generalized variable forms written in terms of flexible bodies include

$$U = \frac{1}{2} \begin{bmatrix} R_i \\ q \\ a_j \end{bmatrix}^T \begin{bmatrix} 0 & 0 & 0 \\ 0 & 0 & 0 \\ 0 & 0 & K_{aa} \end{bmatrix} \begin{bmatrix} R_i \\ q \\ a_j \end{bmatrix} = \frac{1}{2} q^T K_{aaT} q, \quad (28)$$

Potential energy dissipation associated with elastic damping and flexible unit bodies is

$$V = \frac{1}{2} \dot{u}^T N \dot{u} = \frac{1}{2} \dot{a}_j^T \Phi_{ij}^T N \Phi_{ij} \dot{a}_j = \frac{1}{2} \dot{a}_j^T N_{aa} \dot{a}_j \quad (29)$$

In equations, N is a unit body damping coefficient matrix. Writing this into generalized variable form associated with flexible

$$V = \frac{1}{2} \begin{bmatrix} \dot{R}_i \\ \dot{q} \\ \dot{a}_j \end{bmatrix}^T \begin{bmatrix} 0 & 0 & 0 \\ 0 & 0 & 0 \\ 0 & 0 & N_{aa} \end{bmatrix} \begin{bmatrix} \dot{R}_i \\ \dot{q} \\ \dot{a}_j \end{bmatrix} = \frac{1}{2} \dot{q}^T N_{aaT} \dot{q}, \quad (30)$$

Substituting into Lagrange equations [2], one has

$$\frac{d}{dt} \left(\frac{\partial T}{\partial \dot{q}} \right)^T - \left(\frac{\partial T}{\partial q} \right)^T + \left(\frac{\partial U}{\partial q} \right)^T + \left(\frac{\partial V}{\partial \dot{q}} \right)^T = F \quad (31)$$

Thus, dynamics equations associated with flexible body B_1 are

$$M \ddot{q}_s = Q \quad (32)$$

$$Q = F - M \dot{q}_s - K_{aaT} q_s - N_{aaT} \dot{q}_s + \frac{1}{2} \dot{q}_s^T \left(\frac{\partial M}{\partial q_s} \right) \dot{q}_s \quad (33)$$

With regard to multi-body systems composed of M flexible bodies, the dynamics equations can be combined from single flexible body equations (32) to obtain:

$$\bar{M} \ddot{\bar{q}}_s = \bar{Q} \quad (34)$$

In the equation, \bar{M} and \bar{Q} respectively stand for mass matrices and generalized force vectors associated with systems after combination. \bar{q}_s is the overall degree of freedom of the system.

After going through combination, the various unit bodies in systems are no longer free bodies. Between unit body and unit

body, they are subject to constraints associated with such things as hinge links. As a result, the equations above must be set up simultaneously with constraint equations. Only then is it possible to solve them.

The spacecraft flexible multi-body dynamics equations which are finally obtained are /14

$$\begin{cases} \bar{M}\ddot{\bar{q}} + \Phi^T \lambda = \bar{Q} \\ \Phi = 0 \end{cases} \quad (35)$$

In the equations, Φ is the Jacobi matrix associated with all the constraint equations above. λ is the Lagrange factor. Equation set (35) is a set of differential-algebraic equations.

4 TECHNOLOGICAL PATH OF RESEARCH ASSOCIATED WITH ASTRONAVIGATIONAL FLEXIBLE MULTI-BODY DYNAMICS

4.1 Dynamics Descriptions

Dynamics descriptions primarily involve how to select parameter coordinate systems, effectively describe large displacements of objects within systems, large rotational movements, as well as elastic movements associated with objects. At the present time, coordinates describing large displacements and large rotational motions in systems can be roughly divided into three types--that is, minimum number coordinate methods, hinged relative coordinate methods, and absolute coordinate methods. The forms associated with flexible multi-body system dynamics equations and the coordinate systems selected for use are closely related. However, it goes without saying that whatever type of coordinate system is selected for use, equations will, in the end, all fall into one of the two forms below.

(36)

$$A\ddot{q} = B$$

or
$$\begin{cases} A\ddot{q} + \Phi^T \lambda = B \\ \Phi = 0 \end{cases} \quad (37)$$

The system dynamics equation form obtained from minimum number

coordinate methods is equation (36). The equation number is equal to the number of degrees of freedom associated with the system. The method in question is very convenient with regard to numerical value integrals. However, with respect to large model, complicated multi-body systems, the forms of matrices A and B are very complex. Moreover, the arbitrary nature of the selection of generalized coordinates is very great. Different selection methods will obtain different forms of matrices A and B. This is not conducive to the setting up of formulated models.

Hinged relative coordinate systems originate in spacecraft dynamics. Because the majority of early spacecraft present tree shaped topological structures, with regard to this type of system, the dynamics equation forms are the same as equation (36). However, with regard to systems including closed loop motion constraints, the dynamics equation forms are as in equation (37). Opting for the use of hinged relative coordinate methods, it is possible to set up pure coupling dynamics equations associated with comparatively small numbers. The efficiency of numerical value operations is comparatively high. Moreover, it is easy to realize symbolic algorithms.

Absolute coordinate systems are widely used in multi-body mechanical systems containing closed loops. Large displacement motions associated with each body require using six (or seven) individual coordinates for description. The system dynamics equations obtained in association with the methods in question are of the form of equation (37). The forms of matrices A and B are not subject to the influences of topological structures, and the forms are simple. Φ and Φ_q are capable of being produced through standard constraint processing methods. At the present time, this is a comparatively good selection for the setting up of formulated models. However, the methods in question usually lead to a set of enormous combined differential-algebraic equations. The equation dimension number is relatively high. There is a need to opt for the use of rare matrix methods for solutions. Efficiencies are not as good as for relative coordinate solutions.

After making selections of coordinate methods--when concretely describing characteristic quantities associated with large displacements and large rotational motions in systems (such physical quantities as position or azimuth for each object, speed or angular velocity, acceleration or angular acceleration, and so on)--various methods of mathematical representation are also involved. The most basic are vectors and matrices. Next, are azimuth angles (commonly used ones are Euler angles and Bryant angles), pseudo coordinates (pseudo velocities), quaternions, homogeneous coordinates, spinors, rotational vectors, and so on, and so forth. Various types of mathematical representations have different types of characteristics. As far as their good and bad aspects are concerned, selections and evaluations can only be made by combining the conveniences associated with specific applications or theoretical discussions.

4.2 Selection of Floating Coordinate Systems

With regard to multiple rigid body models--during processes associated with system motions--motions associated with the use of connected body coordinate systems firmly connected to bodies are capable of completely representing the movement status of the bodies in question. With respect to flexible bodies, as far as the generation of changes as a function of time in distances between any two points inside objects is concerned, coordinates connected to objects no longer have precisely specified meanings. At this time, we are only able to select one type of moving coordinate system which has been studied in association with floating bodies--floating coordinate systems. Through floating coordinate systems, descriptions are made of elastic deformation movements associated with objects. At the same time, motions associated with floating coordinate systems reflect large displacements and large rotational movements in association with objects. /15

A good number of scholars have carried out theoretical research with regard to problems associated with the selection of floating coordinate systems. The principle of selection is to make

the dynamics equations which are finally obtained eliminate as much as possible coupling terms associated with large displacements, large rotational movements, and movements associated with small elastic deformations. At the present time, commonly used floating coordinate systems include five types. One is local adhesion coordinate systems. These directly adopt rigidly connected body coordinate systems to describe elastic motions associated with objects. Second is floating center of mass main axis systems. The origin is selected on the instantaneous center of mass of deformation bodies. Basic vector directions are chosen in the direction of each instantaneous main axis associated with deformation bodies. Third is Brucken mean axis systems. The selection of direction causes the square of elastic corresponding displacement modes to take extremely small values (Brucken condition). Fourth is Tisserand mean axis systems. The selection of direction causes the kinetic energy associated with floating coordinate systems corresponding to elastic bodies to take extremely small values (Tisserand conditon). Fifth is rigid body mode systems.

4.3 Discrete Dispersion Methods

In the setting up of models associated with flexible multi-body system theory, flexible body discrete dispersion is another important problem. Looked at in general terms, discrete dispersion methods can be divided into two types--that is, discrete dispersion associated with object models and discrete dispersion associated with mathematical models. Moreover, accurately reflecting actual physical models of multi-body systems and simple and effective mathematical models will be the special features of the formation of flexible multi-body dynamics.

The primary resolution of discrete dispersion in object models uses discrete dispersion in actual flexible multi-body system engineering in order to be able to carry out object models which have been researched theoretically, taking the external forces to which various components of systems are subject, connection

stiffness, surface friction, gaps between surfaces, and so on, and idealizing them. In conjunction with this, use is made of appropriate model simulations. There are the several problems below which require detailed consideration. One is the simplification of objects or components in systems. Normally, system simplifications become systems composed of rods, beams, plates, shells, and so on, as well as their combined component assemblies. This is primarily convenient for finding modality bases associated with elastic deformation objects. Even if option is made for the use of finite element modality coordinates, it is still advantageous for numerical value analysis. Second is simplification associated with connection methods. Connections associated with actual multi-body system engineering are idealized as a number of basic connections or as combinations of several basic types of connections. Third is flexible, damped simulation simplifications appearing in actual system connections. Option is made for the use of the addition of springs and damper devices at connector head locations. Parameters associated with these springs and damping devices are normally selected by test collection methods or certain types of regressive analysis methods. Four is liquid shaking inside systems filled with liquid. Fifth is boundary surface discrete dispersion problems associated with actual flight craft multi-body systems. In modern spacecraft, there exist a good number of separation surfaces and connection docking surfaces. At the present time, they are all considered to be rigid connections. If it is desired to precisely analyze the influences associated with connection surfaces on the overall dynamic characteristics of space craft, it is necessary to take the entire system and discretely disperse it into a multi-body system. As far as connection boundary surfaces are concerned, it is possible to use such ideal component combinations as springs, damping devices, friction elements, and so on, for simulations.

Discrete dispersions associated with mathematical models are primarily how to select appropriate mathematical expressions in order to describe flexible deformations of bodies in flexible

multi-body systems. At the present time, with regard to the description of small elastic deformations, in appropriate floating coordinate systems, elastic displacements are represented as $u = \sum \Phi_i \eta$. In this, what is important is doing a good job of selecting the function Φ . Selection methods that are often used are primary function methods, modal function methods, and finite element methods.

Primary function methods are to take entire flexible body displacement fields as approximating a linear combination of a set of primary functions. The success or failure of this type of method depends entirely on whether or not the selection of primary functions is appropriate. Moreover, if it is desired to select a set of appropriate functions, it is usually necessary to have understanding of an a priori nature with regard to displacement fields associated with flexible bodies. Modal function methods partially overcome the weak points of primary function methods. They are to use flexible body vibration mode functions to act as primary functions. Mathematically, their superiority has already been proved. However, unless flexible body modalities already use test measurements or analytical methods for their acquisition, vibration mode functions themselves will, otherwise, also use numerical value methods to obtain them.

Finite element methods take flexible bodies and divide them into a good number of single elements. Applying finite element methods--through characteristic value equations--solutions are made for free vibration mode modalities. The advantage of making use of free vibration mode modalities is broad adaptability. The disadvantage is that convergence ratios are relatively fast. There is a need for multiple order modalities. Only then is it possible to describe deformation motions relatively well.

As far as the three types of discrete dispersion methods above are concerned--with regard to describing the geometrical nonlinearities given rise to by large deformations of flexible bodies--they do not, then, seem adequate. Some scholars still opt for the use of floating coordinate systems. During strain

calculations, geometrical nonlinearity terms increase. Some scholars put forward corrective Lagelangri (phonetic) methods of description with regard to the use of finite elements. However, none of them are mature. They are still in the theoretical research stage.

/16

4.4 Dynamics Principles

With respect to the setting up dynamics equations, there are a good number of types of methods. However, carrying out induction from dynamics principles, one primarily has the three large categories below.

One starts out from Newton-Euler equations (that is, center of mass momentum principles and principles of moments of inertia). As far as characteristics are concerned, during the process of setting up models, there is a need to make isolated body analyses with regard to each object, setting out dynamics equations associated with single bodies. After that, eliminating ideal constraining forces and constraining moments of force, equation sets associated with systems are finally obtained. In the handling of constraining forces, a good number of scholars go through analytical methods associated with topological structures to eliminate constraining forces, thereby forming different methods for setting up models, which bear the names of the scholars--for example, Margulies/Hooker methods based on graphical theory, Roberson/Wittenburg methods, and so on.

A second starts out from analytical dynamics methods derived from Dalangbeier (phonetic) principles (or Ruodang principles). Its characteristics are that ideal constraining forces (or moments of force) do not appear naturally in equations--the set up of equations is even more formulated. This type of method has a good number of deformation forms. The most successful are Lagrange methods and Kane methods. Soon afterwards, there were scholars who used generalized movement activity methods, Haimo methods, Apeiier (phonetic) equations, Lagelangri (phonetic) operators, and so on, to make dynamic analyses in applications to multi-body dynamics

equations. At the present time, these methods have already become the theoretical foundation for a good number of large scale softwares abroad--for example, TREETOPS, RASNA, ADAMS, DADS, and so forth.

A third sets out from Gaussian minimal value principles. Its characteristics are to use systems to act as integral considerations. During the setting up of models, constraining counter forces do not appear. At the same time, this type of method provides a new path where there is no need to set up differential motion equations and it is possible to directly apply optimization calculation methods. There are Lilov methods and Popov methods based on Gaussian principles.

4.5 Numerical Value Calculation Methods

As far as solutions of space craft flexible multi-body dynamics equations are concerned, they are summarized in solutions for a set of differential equations or differential-algebraic equations. With regard to solutions for differential equations, it is possible to make use of comparatively mature numerical value integration methods associated with differential equations. There are such relatively familiar numerical value integration methods as fourth order Runge-Kutta methods, Trenor methods, Adams methods, Newmark methods, Gear methods, and so on. Among these, Gear methods are ones worthy of praise in flexible multi-body dynamics calculations. Among several types of methods, they have the best convergence characteristics and stability. With regard to solutions of differential-algebraic equation sets, there are primarily expansion methods and shrinking and combining methods. Analyses are carried out of system matrices with respect to constraint equations. After that, numerical value integration is then carried out on differential equations. The primary contradiction associated with multi-body dynamics numerical value calculations is a morbid state problem. The causes creating the morbid states are the several points below. One is that multi-body system dynamics equations are very complicated. System matrices

present severe nonlinearities or are enormous differential-algebraic equation sets. Amounts of calculation work are great. Error accumulation is severe. Second is that, in regard to flexible multi-body systems, large ranges of motion parameters associated with very large differences between orders of magnitude and mutual coupling of elastic deformation variables bring with them error accumulations. Third is the simultaneous appearance of low frequency large range motion variables and high frequency elastic deformation variables. There is a requirement to take integration increment lengths and shrink them very small. In regard to the solution of space craft multi-body dynamics equations, morbid states associated with equations must necessarily be given consideration. During the setting up of mathematical models, necessary measures are adopted. In conjunction with this, selection is made of numerical value integration algorithms which are comparatively stable.

4.6 Simulation Software

As far as the setting up of theoretical models associated with multi-body systems and calculation algorithms are concerned, in the end, in all cases, practical realization is achieved in computer programs. With regard to the development of an excellent multi-body dynamics simulation software, the several areas below are worthy of attention.

(1) During the carrying out of dynamics descriptions in the phase for the setting up of theoretical models and the selection of dynamics principles, consideration should then be given to the design of simulation software, causing expressions associated with dynamics relationships and dynamics equations to correspond even more with the realization of computer programs. Generally speaking, with regard to space craft multi-body systems, option should be made for the use of hinged relative coordinate systems. Moreover, with respect to industrial mechanical hands, they are primarily simple motion hinges. Most opt for the use of full vector and speed variational principles, thereby obtaining

recurrence forms of dynamics equations and causing calculation efficiencies to improve.

(2) Software systems should possess full functions--for example, capabilities associated with automatic analysis of system degrees of freedom, precise specification of independent generalized coordinates, and automatic deletion of superfluous constraint equations--be able to adapt to any closed loop or open loop topological structure, handle multiple types of constraints, and, in conjunction with that, reduce artificial intervention. As far as stable high efficiency numerical value integration algorithms and matrix analysis algorithms are concerned, they are capable of handling possible morbid state differential-algebraic equation sets associated with multiple flexible body dynamics. They possess comparatively large problem solution ranges and are thus capable of solving actual complex multi-body system problems.

(3) As far as the possession of good operating boundary surfaces and consummate processing functions from beginning to end are concerned, software as a whole should carry out operations in an integrated environment and option be made for the use of mutual forms of carrying out data input and preprocessing. With regard to providing complete after processing functions, realization is made of forms associated with dynamics calculation results and curve outputs. Three dimensional motion graphic displays are realized for systems. Open data bases are set up, managing multi-body system geometrical parameters, materials parameters, topological relationships, constraint information, flexible modalities, as well as such physical constants as spring, damping, and liquid shaking characteristics, and so on. In conjunction with this, there is a capability to provide data transmission and sharing with such modules as finite element analysis, linear control analysis, preprocessing and afterprocessing, three dimensional motion graphics, and so forth.

5 DISCUSSION AND CONCLUDING REMARKS

In the last ten years, flexible multi-body system dynamics research has received very great attention. Huston [20] holds that multi-body dynamics is one of the most lively realms in the area of applied dynamics at the present time. Despite the fact that there has been a good deal of obvious progress in the area of multi-body dynamic analysis, among those doing the analyzing, however, controversy still exists. With regard to multi-body systems associated with astronavigational space craft--due to the special characteristics of the operating environment--as a result, astronavigational flexible multi-body dynamics includes the characteristics and new problems below.

(1) Inseparable from the Overall Design of Space Craft. The task of overall space craft design is the precise specifying of space craft orbit and attitude on the basis of space craft orbit dynamics and attitude dynamics equations. In conjunction with this, control system design is determined on this basis--precisely determining space craft structural design on the basis of structural dynamics analysis. The flexible attachments which modern space craft carry with them are increasing. Structural forms are more and more complicated. Typical multi-body systems have already been formed. Such dynamics characteristics as orbit, attitude, structural vibrations, and so on, are no longer independent, but are mutually coupled. As a result, in overall design, flexible multi-body dynamics models should be set up with regard to space craft in order to facilitate consideration of various types of coupled terms associated with such factors as horizontal movements, rotations, vibrations, and so forth.

(2) Closely Related to Dynamics Control Problems. In regard to space craft multi-body dynamics analysis, in the end, everything comes down to the carrying out of dynamic control on systems--for example, control on the positioning of the ends of flexible mechanical space arms and control of orbits, control of

displacements associated with flexible components, control of stability characteristics of space craft as a whole during flight processes, and so on. As a result, astronavigational flexible multi-body dynamics research should, from the time of setting up theoretical models, then consider the carrying out of connections appropriate to controlling systems.

(3) Astronavigational Multi-Body Systems Are Systems Associated with Changing Structures and Changing Parameters. Space craft must complete such processes as strap down and separation, cowling jettison, deployment, and so on. During dynamic processes, system degrees of freedom will give rise to changes--even to the point of topological forms also giving rise to changes. As a result, they are systems with changing structures and changing parameters. When carrying out multi-body dynamics analysis, it is necessary to apply special considerations to constraint equations. During processes with changing structures and changing parameters, certain constraints must be activated. Certain constraints must be canceled--as a result, increasing the difficulties in handling.

(4) In Astronavigational Multi-Body Systems, Widespread Multiple Body Collision Problems Exist. As far as such things as launches and landings of space shuttles and manned spaceships, rendezvous and dockings in orbit, solar array deployments and lock downs, etc., are concerned, they all require undergoing a collision process. When structures give rise to collisions, they usually produce sudden changes in speed. This will not only produce perturbations in motions. It will, moreover, also give rise to very great collision loads. It is possible to make structures in certain sections produce yielding, cracking, and the expansion of cracks, leading to the destruction of entire structures. The carrying out of multi-body collision analysis associated with space craft is an important part of space craft design.

(5) There Is a Need to Pay Particular Attention to Astronavigational Multi-Body Dynamics Test Research. These test include three areas. One is the carrying out of a number of typical empirical verification experiments in order to test,

verify, and revise multi-body dynamics theoretical models and software to carry out astronavigational analysis. Second is to carry out physical constant tests to provide reliable experimental data for initial parameters needed in association with space craft dynamics analysis--for example, stiffness data for various unit bodies associated with different types of flexible attachments, rigidity data for complex connectors, friction data associated with separation surfaces, connection surfaces, and deployment structures, as well as stiffness data, and so on. Third is tests associated with the development of actual flights and orbital dynamics. In actual situations, analyses are carried out of dynamics parameters. In conjunction with that, final checks are done with regard to theory and the results associated with various analytical items.

/18

(THIS PAGE INTENTIONALLY LEFT BLANK)

REFERENCES

- 1 刘廷柱, 洪嘉振, 杨海兴. 多刚体系统动力学. 北京: 高等教育出版社, 1989.
- 2 袁士杰, 吕哲勤. 多刚体系统动力学. 北京: 北京理工大学出版社, 1992.
- 3 J. 维藤伯格. 多刚体系统动力学. 谢传峰译. 北京: 北京航空学院出版社, 1986.
- 4 洪嘉振主编. 多体系统动力学——理论、计算方法和应用. 上海: 上海交大出版社, 1992.
- 5 王照林. 充液系统动力学与航天高技术. 力学进展, 1988(3).
- 6 周起钊. 柔性系统力学中的主要课题. 力学进展, 1989(4).
- 7 林宝玖, 谢传峰. 挠性多体系统动力学. 力学学报, 1989(4).
- 8 曲广吉. 关于卫星动力学研究及其工程应用. 航天器工程, 1992(2).
- 9 Ho J Y L. Direct path method for flexible multibody spacecraft dynamics. *Journal of Spacecraft and Rockets*, 1977, 14(2): 102~110
- 10 Singh R P, Vander Voort R J, Likins P W. Dynamics of flexible bodies in tree topology — a computer oriented approach. *Journal of Guidance, Control, and Dynamics*, 1985, 10(5): 584~590
- 11 Meirovitch L, Quinn R D. Equation of motion for maneuvering flexible spacecraft. *Journal of Guidance, Control and Dynamics*, 1987, 10(5): 453~465
- 12 Modi V J, Ng A, Suleiman A, Morita Y. Dynamics of orbiting multibody system: a formulation with application. AIAA-91-0998-CP.
- 13 Shabana A A. Constrained motion of deformable bodies. *Int. J. numerical Methods in Engineering*, 1991, 32: 1813~1831
- 14 Wu S C., Haug E J, Kim S S. A variational approach to dynamics of flexible multibody systems. *Mechanical Structure and Machinery*, 1989, 17(1): 3~32
- 15 Vu-Quock L, Simo J C. Dynamics of earth-orbiting flexible satellite with multibody component. *Journal of Guidance, Control and Dynamics*, 1987, 10(6): 549~558
- 16 Spanos J T, Tsuha W S. Selection of component modes for the simulation of flexible multibody spacecraft. *AAS / AIAA Astrodynamics Specialist Conference*, Stowe, Vermont, No. AAS 89-438, 1989.8.
- 17 Simo J C, Vu-Quock L. On dynamics of flexible bodies under large overall motions —The plane case: Parts I and II. *ASME Journal of Applied Mechanics*, 1986, 53: 849~863
- 18 Wallrapp O, Schwertassek R. Representation of geometric stiffening in multibody system simulation. *Int. J. Numerical Methods in Engineering*, 1991, 32: 1833~1850
- 19 Banerjee A K, Lemak M E. Multi-flexible body dynamics capturing motion-induced stiffness. *J. of Applied Mechanics*, 1991, 58: 766~775
- 20 Huston R. 多体动力学——模拟和分析方法. 力学进展, 1992, 22(3).

RECOGNIZING THE FAULT PATTERNS OF LIQUID ROCKET
ENGINES BY NEURAL NETWORKS

Yang Erfu Zhang Zhenpeng Cui Dingjun Liu Guoqiu

Translation of "Ying Yong Shen Jing Wang Luo Shi Bie Ye Ti Huo Jian Fa Dong Ji De Gu Zhang Mo Shi"; Missiles and Space Vehicles, Overall No. 213, No.1, 1995, pp 19-22

ABSTRACT A brief introduction is made of the basic theory of neural networks and back propogated error algorithms (BP algorithms). A liquid rocket engine (LRE) fault diagnostic system schematic applying neural networks is given. Analyses are done of liquid rocket motor fault models, putting forward the use of model data to train neural networks. For network training, new paths are presented. Finally, based on model data, applied neural networks recognize several fault patterns.

KEY WORDS Liquid propellant rocket engine, [†]Neural network,
[†]BP algorithm, Fault diagnosis, Pattern recognition

1 INTRODUCTION

Liquid rocket motors are a type of extremely complicated propulsion system composed of propellant storage tanks, combustion gas generators, turbine pumps, various types of control valves, thrust chambers, as well as large amounts of piping. In the systems, there is a high degree of correlation between various components and various parameters. Any malfunctioning link will

influence the normal operation of the system as a whole in all cases. As a result, if it is desired to improve the reliability of liquid rocket motors, it is then necessary to carry out monitoring and control with regard to the status of motors in order to diagnose motor faults and adopt appropriate remedial measures [1].

Classifications and recognition of fault patterns are an important aspect associated with liquid rocket motor status monitoring and control as well as fault diagnosis. As far as traditional pattern recognition methods are concerned--due to the involvement of such things as characteristic adoption and classification, etc.--it is necessary to carry out effective real time recognition of these types of large amounts of fault patterns with regard to liquid rocket motors. In reality, this is very difficult. With respect to neural networks--because they possess a series of advantages--for example, large scale parallel processing and distributed type information storage, good autoadaptive characteristics, self-organizing characteristics, as well as very strong learning functions, association functions, and error tolerance functions, as a result, they are particularly suited to recognition of liquid fuel rocket motor fault patterns.

In applying neural networks to recognizing fault patterns associated with liquid rocket motors, one important problem is how to obtain fault data for training use. This problem is primarily resolved through two paths. One is fault data recorded in ground tests in the past as well as during flight tests. A second is to set up fault models associated with liquid rocket motors, acquiring, through models, fault data approaching real processes. Due to the fact that numbers of test iterations where there were faults are inadequate, and malfunction reports which already exist will also not include all possible fault patterns associated with motors, as a result, the use of only test data to set up full patterns for all faults associated with liquid rocket motors is not possible. However, the setting up of accurate and reliable fault models, able to recognize fault patterns associated with liquid rocket motors, provides extremely great conveniences. Through

analysis and processing of model data, there is a possibility of finding various types of fault patterns which can be given rise to by liquid rocket motors in tests and during flights. This article is just in the process of making use of fault data obtained from motor fault models. Going through unitization and coding processing neural network training samples are formed. Finally, use is then made of a set of verification samples to carry out calibrations.

2 BASIC PRINCIPLES OF NEURAL NETWORKS

Neural networks are a burgeoning discipline which was given rise to by and is the newest product of research based on neurology. It strives--in accordance with the same types of forms as bioneurological systems--to handle real objective objects that exist in the world. Speaking in terms of their essence, they are a type of calculation model which is suitable to the processing of large amounts of parallel information. Due to the fact that grade separated forms of forward directed network structures are simple and easy to realize, this article opts for the use of this type of network structure. In conjunction with this, it makes use of BP algorithms based on gradient methods for realization. This is one type of supervisory training. Below, a brief introduction is made of grade separated forms of forward directed networks and BP algorithms.

2.1 Mathematical Models Associated with Neural Node Points

At the present time, the neural node point models that are put forward by people are all multiple input, single output components as shown in Fig.1.

(1)

$$U_j = \sum_{i=1}^n w_{ij} V_i + \theta_j$$
$$V_j = f(U_j) \quad (2)$$

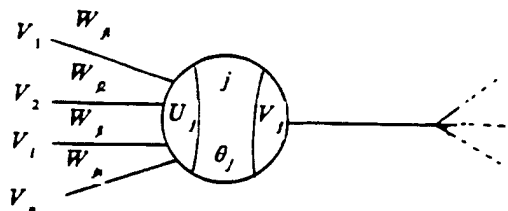


Fig.1 Neural Node Model

In the Fig., w_{ji} stands for the connection weighting value associated with the i nodal point and the j node. U_j stands for the total input sum associated with the j nodal point. V_j stands for the j node output. θ_j is the threshold value associated with the j node. V_i is the output associated with the i node immediately above. In that case, one has (1) and (2). /21

Here, $f(U_j)$ is nonlinear excitation functions associated with nodal point j . They are normally a Sigmoid function $y = \frac{1}{1 + e^{-x}}$

and arctangent function $y = \arctan x$ as respectively shown in Fig.2(a) and 2(b).

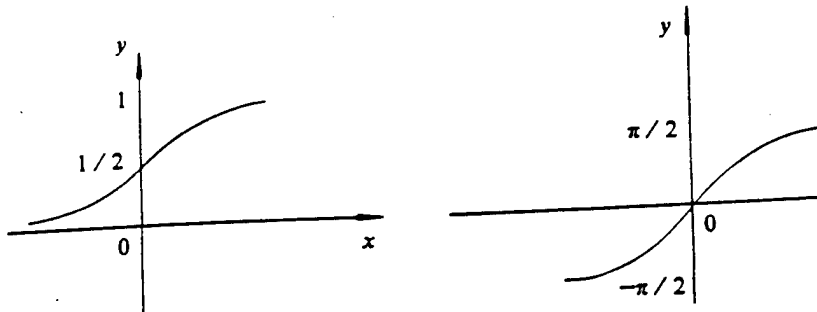


Fig.2 Neural Node Point Excitation Functions

(a) Sigmoid Function (b) Arctangent Function

2.2 Network Structures

Grade separated type forward directed networks are composed of input grades, intermediate grades (implicit layers), and output grades as shown in Fig.3. In the Fig., $x^p = [x_1, x_2, \dots, x_n]^T$ is network input. $y^p = [y_1, y_2, \dots, y_m]^T$ is network output. What are called forward directed networks are nothing else than outputs

associated with various levels of neural nodes only being able to influence the state of neural nodes below them but not being able to feed back to neural node points in levels above. Between various grades there is also no feedback.

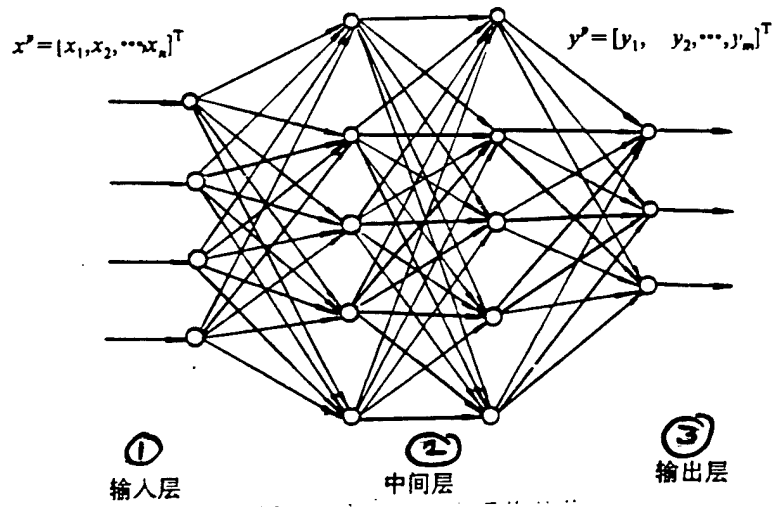


Fig.3 Grade Separated Type Forward Directed Network Structures
 (1) Input Layers (2) Intermediate Layers (3) Output Layers

2.3 BP Algorithms

BP algorithms are simple designations for error back propagation algorithms. They are a type of optimized calculation method based on gradient methods. Assuming that networks are forward directed type neural networks composed of L layers, the number of neural node points associated with each layer is n_p ($p=1, 2, \dots, L$). The input sample number is P. Use is made of X to represent input sample space. $X = \{x^{(1)}, x^{(2)}, \dots, x^{(p)}, \dots, x^{(P)}\}$. ($p=1, 2, \dots, P$). $x^{(p)}$ is each network input iteration. $x^{(p)} = [x_1^{(p)}, x_2^{(p)}, \dots, x_i^{(p)}, \dots, x_{n1}^{(p)}]^T$. ($i=1, 2, \dots, n_1$). The actual output sample space of networks is represented by the use of Y. Target space is represented by the use of

$$\dots, y_1^{(p)}, \bar{Y} = \{Y^{(1)}, Y^{(2)}, \dots, Y^{(p)}, \dots, Y^{(P)}\}, (p=1, 2, \dots, P), y_i^{(p)} = [y_1^{(p)}, y_2^{(p)}, \dots, y_i^{(p)}, \dots, y_{n2}^{(p)}]^T, Y = \{y^{(1)}, y^{(2)}, \dots, y^{(p)}, \dots, y^{(P)}\}, y_i^{(p)} = [y_1^{(p)}, y_2^{(p)}, \dots, y_i^{(p)}, \dots, y_{n2}^{(p)}]^T, /22$$

(1)

Network sample errors and system errors are defined as follows.

$$E_p = \frac{1}{2} \sum_{i=1}^{n_p} (\bar{y}_i^{(p)} - y_i^{(p)})^2 \quad (3)$$

$$E = \frac{1}{P} \sum_{p=1}^P E_p = \frac{1}{2P} \sum_{p=1}^P \sum_{i=1}^{n_p} (\bar{y}_i^{(p)} - y_i^{(p)})^2 \quad (4)$$

On the basis of gradient methods, under each sample p, the weighting value correction formula is as follows.

$$\Delta pW_j = -\eta \frac{\partial E_p}{\partial W_j} \quad (5)$$

In this, η is training increment length. When excitation functions adopt the form of Sigmoid functions, the specific iterative attitude for m u l t i s a s follows.

$$\Delta pW_j = \eta \delta_{pj} O_{pj} \quad (6)$$

With regard to output layer node points:

$$\delta_{pj} = (\bar{y}_j^{(p)} - O_{pj}) O_{pj} (1 - O_{pj}) \quad (7)$$

With regard to implicit layer nodal points:

$$\delta_{pj} = O_{pj} (1 - O_{pj}) \sum_{k=1}^{n_{p+1}} \delta_{pk} W_{kj} \quad (8)$$

In order to improve network convergence characteristics, a momentum term is introduced--that is,

$$\Delta pW_{ji}(R+1) = \eta \delta_{ji} O_{ji} + \alpha \Delta pW_{ji}(k) \quad (9)$$

In equations, α is a constant. This is designated Momentum. The size of α determines the levels of influence of changes in past weighting values on changes in present weighting values. When $\eta = 0.5-0.7$, $\alpha = 0.1-0.3$. When $\eta = 0.9-1.1$, $\alpha = 0.7-0.9$.

In this way, layer separated type forward directed neural network training processes are composed of forward propagation and back propagation. As far as forward propagation processes are concerned, input signals are processed layer by layer from input layers through implicit layer nodes. In conjunction with this, they are transmitted toward output layers. The status of each layer of neural nodes only influences the status of neural nodes in the next layer. If it is not possible to obtain the expected outputs in output layers--that is, actual network errors are greater than stipulated error limits--then, there is a shift into back propagation processes, taking error signals and returning them back along the original connection paths. Through altering various weighting values between neural nodes, it makes error signals smaller than stipulated error limits.

3 LRE FAULT DIAGNOSIS SYSTEM SCHEMATIC ASSOCIATED WITH APPLIED NEURAL NETWORKS

Fig.4 gives a type of real time system schematic suitable for use in liquid rocket motor fault diagnosis.

Various types of sensors installed at different sites on liquid rocket motors (for example, temperature, pressure, flow amount, ...) take measured parameters and transmit them to data preprocessing devices. After signals go through processing, they then go through input encoding processing and then become diagnostic neural network inputs. Network outputs are actual fault patterns. Finally, decision making structures provide fault patterns on the basis of neural networks, promoting the adoption by

implementation structures of corresponding measures with regard to
liquid rocket motors.

/23

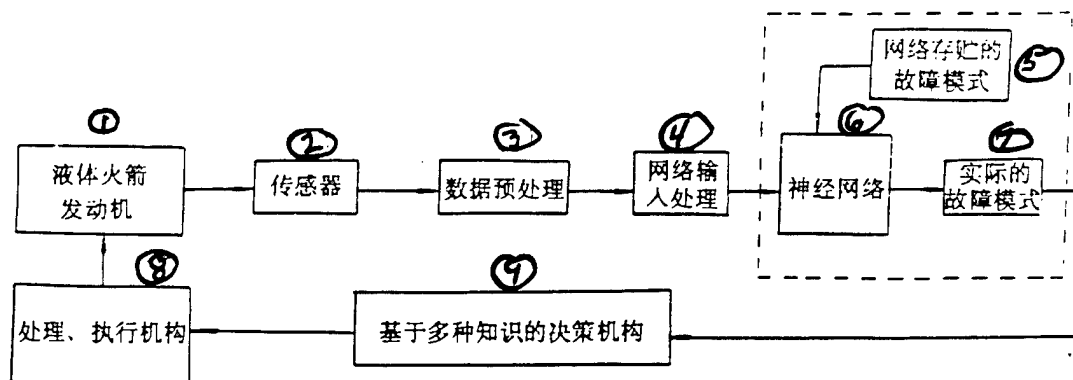


Fig.4 Liquid Rocket Motor Fault Diagnostic System Schematic

Key: (1) Liquid Rocket Motor (2) Sensor (3) Data Preprocessing Device (4) Network Input Processing (5) Fault Patterns Stored by Networks (6) Neural Network (7) Actual Fault Patterns (8) Processing, Implementing Structures (9) Decision Making Sturctures Based on Multiple Types of Knowledge Making Sturctures Based on Multiple Types of Knowledge

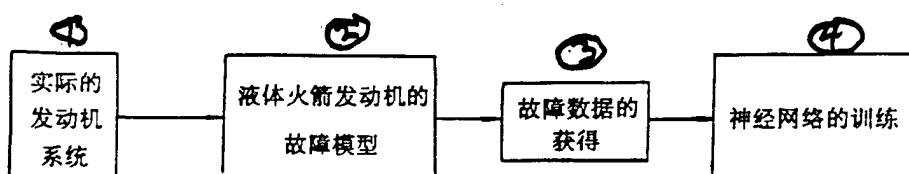


Fig.5 Algorithm Line and Block Chart to Use Fault Model Data to Train Neural Networks

Key: (1) Actual Motor Systems (2) Liquid Rocket Motor Fault Model (3) Fault Data Acquired (4) Neural Network Training

The training of neural networks here is primary. Fig.5 gives the algorithm line and block chart for the use of fault pattern data to train networks.

4 LIQUID ROCKET MOTOR FAULT MODEL DATA

Liquid rocket motor fault models are set up on the basis of fixed physical phenomena and parameter changes associated with each component. During liquid rocket motor operations, each fault will give rise to transitional processes associated with different characteristics in all cases. As a result, the motor models which are set up must not only be able to reflect the status of normal motor operations. They must also be capable of accurately reflecting motor operating characteristics in fault situations. In order to set up accurate and reliable motor fault models, it is necessary to have system diagrams for specific motor apparatuses as well as rated values associated with operating process parameters, writing out component equations with regard to the specific systems. In conjunction with this, consideration is given to all initial abnormal phenomena associated with piping, components, and control valves. When equation sets are set up, conditions associated with variable coupling should be observed as well as pressure, flow amount, and power equilibrium conditions--finally adopting the various operating parameters to act as variables.

With regard to the series connected hydrogen oxygen dual turbine motor system shown in Fig.6--on the basis of the general principles for the setting up of fault models above--large amounts of research work have already been done. Table 1 is fault data which has been acquired from fault models that have already been set up. It is also the original data associated with this article in respect to neural network training. This set of data basically reflects three types of fault situation which often occur in association with liquid rocket motors--blockages, leaks, and drops in pump efficiencies. Speaking in concrete terms, they include eight types of fault pattern.

Pattern 0 Secondary Hydrogen Venturi Blockage

Pattern 1 Secondary Oxygen Venturi Blockage

Pattern 2 Main Hydrogen Venturi Blockage

Pattern 3 Main Oxygen Venturi Blockage
 Pattern 4 Hydrogen Pump Back Leak
 Pattern 5 Oxygen Pump Back Leak
 Pattern 6 Hydrogen Pump Efficiency Drop
 Pattern 7 Oxygen Pump Efficiency Drop

/24

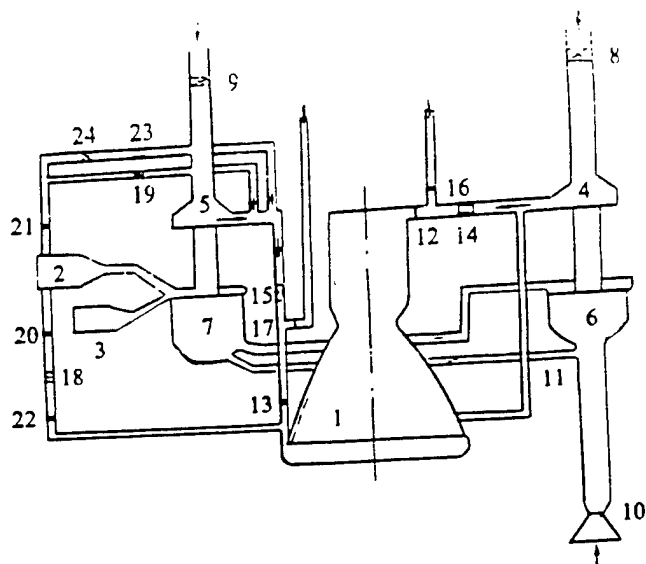


Fig.6 Liquid Rocket Motor System Diagram

Key: (1) Thrust Chamber (2) Generator (3) Starter (4) Oxygen Pump (5) Hydrogen Pump (6) Oxygen Turbine (7) Hydrogen Turbine (8) Oxygen Pump Prevalve (9) Hydrogen Pump Prevalve (10) Lawaer (Phonetic) Jet Tube (11) Sonic Nozzle (12) Main Oxygen Valve (13) Main Hydrogen Valve (14) Main Oxygen Venturi (15) Main Hydrogen Venturi (16) Oxygen Leak Valve (17) Hydrogen Leak Valve (18) Auxilliary Oxygen Venturi (19) Auxilliary Hydrogen Venturi (20) Auxilliary Oxygen Valve (21) Auxilliary Hydrogen Valve (22) Oxygen Pressure Stabilization Valve (23) Auxilliary Hydrogen By Pass Venturi (24) Auxilliary Hydrogen By Pass Valve

Table 1 Liquid Rocket Motor Model Fault Data

① 故障模式	② 氢泵转速 (n_H)	③ 氧泵转速 (n_O)	④ 氢主文氏管 压降(ΔP_{H1})	⑤ 氧主文氏管 压降(ΔP_{O1})	⑥ 氢副文氏管 压降(ΔP_{H2})	⑦ 氧副文氏管 压降(ΔP_{O2})	⑧ 燃气发生器 压力(P_g)	⑨ 推力室 压力(P_k)
0	-1.7 367 046 $\times 10^{-2}$	-9.6 386 056 $\times 10^{-3}$	-0.1 128 884 $\times 10^0$	-3.3 689 592 $\times 10^{-2}$	-0.4 084 724 $\times 10^0$	4.7 704 127 $\times 10^{-2}$	-7.0 901 193 $\times 10^{-2}$	-1.0 748 927 $\times 10^{-2}$
1	-8.3 178 259 $\times 10^{-2}$	-7.5 990 766 $\times 10^{-2}$	-0.4 680 450 $\times 10^0$	-0.2 635 711 $\times 10^0$	-6.8 501 540 $\times 10^{-2}$	3.0 025 804 $\times 10^{-2}$	-0.1 809 437 $\times 10^0$	-7.6 819 189 $\times 10^{-2}$
2	5.1 910 095 $\times 10^{-2}$	-1.4 890 323 $\times 10^{-3}$	0.9 084 549 $\times 10^0$	3.0 287 100 $\times 10^{-2}$	0.3 085 886 $\times 10^0$	-3.3 882 335 $\times 10^{-2}$	1.8 938 273 $\times 10^{-2}$	-2.257 330 $\times 10^{-2}$
3	5.8 594 346 $\times 10^{-3}$	5.6 168 798 $\times 10^{-2}$	0.4 406 040 $\times 10^0$	0.6 901 502 $\times 10^0$	4.5 468 505 $\times 10^{-3}$	0.3 476 606 $\times 10^0$	1.3 581 145 $\times 10^{-2}$	-0.1 235 252 $\times 10^0$
4	-8.9 591 295 $\times 10^{-2}$	8.2 818 035 $\times 10^{-4}$	-0.6 313 727 $\times 10^0$	3.7 470 046 $\times 10^{-2}$	-0.4 052 344 $\times 10^0$	4.6 044 078 $\times 10^{-2}$	-3.0 266 596 $\times 10^{-2}$	-1.9 537 4x6 $\times 10^{-2}$

Key: (1) Fault Pattern (2) Hydrogen Pump Rotation Speed (3) Oxygen Pump Rotation Speed (4) Main Hydrogen Venturi Pressure Drop (5) Main Oxygen Venturi Pressure Drop (6) Auxilliary Hydrogen Venturi Pressure Drop (7) Auxilliary Oxygen Venturi Pressure Drop (8) Combustion Gas Generator Pressure (9) Thrust Chamber Pressure

Table 1 (Cont'd)

故障模式	(1)	(2)	(3)	(4)	(5)	(6)	(7)	(8)
	氢泵转速 (n_H)	氧泵转速 (n_O)	氢主文氏管 压降(ΔP_{H1})	氧主文氏管 压降(ΔP_{O1})	氢副文氏管 压降(ΔP_{H2})	氧副文氏管 压降(ΔP_{O2})	燃气发生器 压力(P_x)	推力室 压力(P_A)
5	-8.1845317 $\times 10^{-3}$	-0.1008268 $\times 10^0$	-0.1944837 $\times 10^0$	-0.3724890 $\times 10^0$	-6.0937172 $\times 10^{-3}$	-0.4734075 $\times 10^0$	-1.8946232 $\times 10^{-2}$	-8.5203730 $\times 10^{-2}$
6	-5.49299990 $\times 10^{-2}$	1.0759460 $\times 10^{-4}$	-0.5652998 $\times 10^0$	-1.9883322 $\times 10^{-2}$	-0.3269944 $\times 10^0$	3.3612169 $\times 10^{-2}$	-2.3978380 $\times 10^{-2}$	-1.1366373 $\times 10^{-2}$
7	-5.7075508 $\times 10^{-3}$	-5.1148771 $\times 10^{-2}$	0.1341857 $\times 10^0$	-0.2637045 $\times 10^0$	-4.1976813 $\times 10^{-3}$	-0.3328822 $\times 10^0$	-1.3257235 $\times 10^{-2}$	-5.8982015 $\times 10^{-2}$

Key: (1) Fault Pattern (2) Hydrogen Pump Rotation Speed (3) Oxygen Pump Rotation Speed (4) Main Hydrogen Venturi Pressure Drop (5) Main Oxygen Venturi Pressure Drop (6) Auxilliary Hydrogen Venturi Pressure Drop (7) Auxilliary Oxygen Venturi Pressure Drop (8) Combustion Gas Generator Pressure (9) Thrust Chamber Pressure

5 TRAINING AND VERIFICATION OF NETWORKS

5.1 Formation of Training Samples

On the basis of the coding methods below, it is possible to obtain from Table 1 the training samples associated with Table 2.

$$x_j = \begin{cases} 1 & C_j / \bar{C}_j \geq 1.15 \\ 0 & 0.85 < C_j / \bar{C}_j < 1.15 \\ -1 & C_j / \bar{C}_j < 0.85 \end{cases} \quad (10)$$

In the equations, \bar{C}_j is the normal value of parameter C_j .

x_j is the coding result associated with C_j .

训练样本

故障模式	输入样本								输出样本(目标值)		
	节点0	节点1	节点2	节点3	节点4	节点5	节点6	节点7	节点0	节点1	节点2
0	-1	-1	-1	0	1	1	1	-1	0	0	0
1	-1	-1	-1	1	-1	1	1	1	0	0	1
2	1	-1	1	-1	1	-1	-1	0	0	1	0
3	1	1	1	-1	-1	1	-1	1	0	1	1
4	-1	-1	-1	-1	-1	1	1	0	1	0	0
5	-1	-1	-1	1	-1	-1	1	1	1	0	1
6	-1	-1	-1	1	-1	1	1	-1	1	1	0
7	0	1	-1	1	1	-1	1	1	1	1	1

-- 25 --

Fig.2 Network Training Samples

Key: (1) Fault Pattern (2) Input Sample (3) Output Sample
(Target Value) (4) Node

/26

5.2 Network Training

The number of input nodes is 8. The number of output nodes is 3. The total number of samples is 8. Selecting 3 implicit layers, there are 10 nodes on each implicit layer. The maximum training iteration number is controled at 3000. The maximum system error is fixed at 0.001. Taking training samples associated with Table 2 and adding them to networks, with the input parameters above, networks go through 532 iterations of training. System errors of 0.000999129 are finally reached--smaller than the error limit (0.001). Fig.7 gives the status of error changes associated with training processes. Network training results are as shown in Table 3.

Table 3 Network Training Results

故障模式	② 网络输出		
	节点 0 ③	节点 1 ④	节点 2 ⑤
0	0.018 552	0.022 955	0.000 094
1	0.031 957	0.000 080	0.978 128
2	0.006 123	0.995 560	0.000 816
3	0.008 136	0.997 325	0.998 550
4	0.972 591	0.026 693	0.024 155
5	0.983 059	0.013 746	0.999 932
6	0.979 505	0.964 410	0.001 695
7	0.990 922	0.985 299	0.999 995

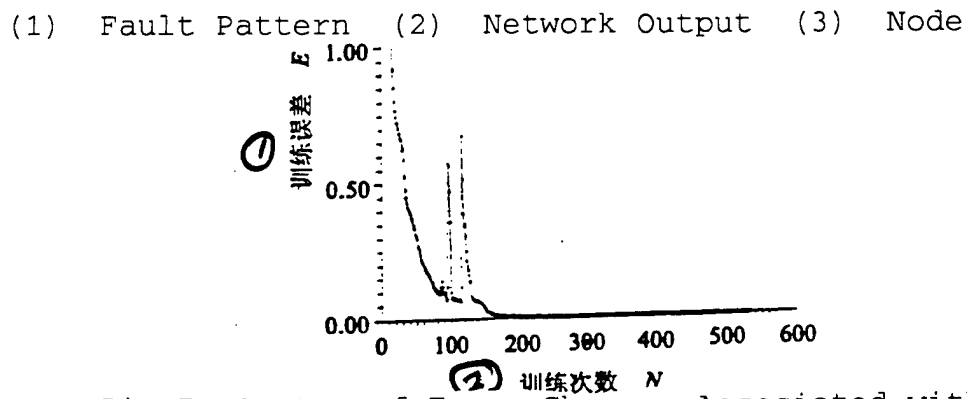


Fig.7 Status of Error Changes Associated with Training Processes

Key: (1) Training Error (2) Training Iteration Number

5.3 Network Applications

With regard to neural networks that have already been trained, use is made of Table 4 verification samples to carry out checks. Network outputs should be able to reflect anticipated fault patterns. Assuming d_{ij} stands for the degree of subordination of output pattern j with regard to target pattern i , then

$$d_{ij} = \frac{1}{\sum_{k=1}^m |y_k^{(i)} - y_k^{(j)}|} \quad (11)$$

In the equation, $y_k^{(i)}$ stands for the target value associated with output nodal point k for pattern i . $y_k^{(j)}$ stands for the actual value associated with output nodal point k for pattern j .

The size of d_{ij} reflects the degree of similarity of pattern j with respect to pattern i . The larger d_{ij} is, the more closely does it approach representing pattern i and pattern j . Table 5 gives network verification results. Table 6 is pattern subordination d_{ij} values. It is possible to see that, only when $i=j$, are d_{ij} values maximum. The explanation is that network identification is effective.

/27

Table 4 Network Verification Samples

故障模式	(2) 输入样本								(3) 输出样本(目标值)		
	节点0	节点1	节点2	节点3	节点4	节点5	节点6	节点7	节点0	节点1	节点2
0	-1.1	-0.9	-1.05	0.1	0.9	1.1	1.05	-1.1	0	0	0
1	-0.9	-1.1	-1.1	1.05	-0.9	1.1	0.9	1.1	0	0	1
2	1.1	-0.9	0.9	-1.1	1.05	-0.9	-1.1	0.15	0	1	0
3	1.05	0.95	1.05	-1.1	-0.95	1.01	-1.05	1.0	0	1	1
4	-0.9	-1.1	-0.9	-1.05	-0.9	1.05	0.9	0.1	1	0	0
5	-1.1	-0.9	-1.1	1.1	-1.05	-0.95	1.1	0.9	1	0	1
6	-0.9	-1.1	-0.95	-1.1	-0.9	1.1	0.9	-1.05	1	1	0
7	0.1	-0.9	-1.1	0.9	-1.1	-0.9	1.1	1.05	1	1	1

Key: (1) Fault Pattern (2) Input Samples (3) Output Samples
(Target Values) (4) Node

Table 5 Network Verification Results

(1) 故障模式	(2) 网络验证输出		
	(3) 节点 0	(3) 节点 1	节点 2 (3)
0	0.018 985	0.023 402	0.000 095
1	0.031 851	0.000 083	0.977 860
2	0.006 256	0.995 988	0.000 857
3	0.005 295	0.997 500	0.997 540
4	0.974 786	0.042 282	0.018 291
5	0.951 670	0.003 447	0.999 817
6	0.972 778	0.960 334	0.001 370
7	0.991 030	0.985 614	0.999 995

Key: (1) Fault Pattern (2) Network Verification Output
 (3) Node

Table 6 Pattern Subordination

(1) 实际模式 / (2) 目标模式	0	1	2	3	4	5	6	7
0	23.5 588	0.9 903	0.9 969	0.5 011	0.9 658	0.5 115	0.5 137	0.3 360
1	0.95 942	18.4 932	0.4 997	0.9 995	0.5 003	1.0 468	0.5 140	0.5 059
2	1.0 043	0.4 976	0.9 876	0.9 946	0.5 075	0.3 392	0.8 864	0.4 987

Key: (1) Actual Pattern (2) Target Pattern

Table 6 (Cont'd)

② 目标模式	① 实际模式	0	1	2	3	4	5	6	7
		3	0.5 011	0.9 488	0.9 907	96.5 717	0.3 425	0.513 240	0.3 336
4	0.9 955	0.5 156	0.5 021	0.3 345	11.6 568	0.9 509	1.0 112	0.5 014	
5	0.4 989	1.0 097	0.3 346	0.5 014	0.9 031	19.2 458	0.3 361	1.0 0.54	
6	0.5 108	0.3 395	1.0 013	0.5 013	0.9 988	0.4 891	14.6 503	0.9 772	
7	0.3 381	0.5 025	0.5 098	1.0 004	0.5 090	0.9 569	0.9 385	47.7 241	

Key: (1) Actual Pattern (2) Target Pattern

6 CONCLUSIONS

Neural networks are a type of calculation model which is suitable for the processing of large amounts of parallel information. Taking neural networks and using them in liquid rocket motor fault pattern recognition overcomes a good number of difficulties associated with traditional pattern recognition methods. Application results in this article clearly show that--with regard to given liquid rocket engine fault patterns--neural networks are capable, in all cases, of fast, accurate, and effective application of recognition--clearly showing the enormous superiority of neural networks in the areas of pattern recognition and parallel processing.

Training neural networks on the basis of fault data obtained from liquid rocket engine fault models overcomes the problem of inadequate experimental data, providing a new path for network training. In conjunction with this, there is a possibility of

discovering all possible fault patterns in liquid rocket engines during ground tests and in flight. This is advantageous to forming advanced status control and fault diagnostic systems associated with and suitable to real time processing.

REFERENCES

- 1 崔定军, 张振鹏, 刘国球. 液体火箭发动机状态监控与故障诊断现状研究. 1993.7.
- 2 White head B, Kiech E and Ali M. Rocket engine diagnostics using neural networks. AIAA 90-1892.
- 3 White head B, Ferber H and Ali M. Neural network approach to Space Shuttle Main Engine Health Monitoring. AIAA 90-2259.
- 4 左镇泉, 王煦法, 王东生编著. 神经网络与神经计算机. 科学出版社, 1992.
- 5 B A 马欣等著. 液体火箭发动机试验研制的理论基础. 王迺琦译. 国防工业出版社, 1978.

A THERMODYNAMIC VENT SYSTEM APPLIED TO CRYOGENIC
PROPELLANTS TANK UNDER MICROGRAVITY ENVIRONMENTS

Liu Chunhui Cai Ze

Translation of "Wei Zhong Li Tiao Jian Xia Yong Yu Di Wen Ran Liao Zhu Xiang De Re Dong Li Pai Qi Xi Tong"; Missiles and Space Vehicles, Overall No.213, No.1, 1995, pp 29-34

ABSTRACT A brief introduction is made of a type of cryogenic fuel storage tank zero gravity venting system which provides a possible option for use. Introduction is made of the functions and operating principles of the system in question, giving operating principles and structural diagrams for such principal system components as heat exchangers, mixer pumps, control valves, and so on. A review is made of the development of thermodynamic venting systems, critiquing the value of utilizing the system in question.

KEY WORDS Microgravity environment Cryogenic propellant Heat transfer

1 INTRODUCTION

In the late 1950's, space craft engines started a new development in advanced technology, causing venting problems in cryogenic liquid propellant storage tanks in zero gravity or microgravity environments to come to the fore. Designers hoped that, during venting, only gases would be eliminated. This is because, if any liquid propellant is expelled, in the low pressure of space, any liquid will expand rapidly. High speed effects on

space craft surfaces will produce an unbalanced force causing attitude control systems to have difficulty correcting. In severe cases, it will lead to space craft failure [1]. Besides this, the expelling of liquid or liquid gas mixtures is also not advantageous to making use to the maximum extent possible of the liquid fuel used in propulsion.

/30

In space, as far as a cryogenic propellant storage tanks are concerned, even if heating prevention and insulation systems are comparatively good, there will still be amounts of heat received constantly from various heat sources (for example, radiant heat, power heat, and so on) thus causing storage tank internal pressures to go up. In order to guarantee that storage tank pressures are maintained within a rated permissible value, it is then necessary to release gases in order to reduce tank pressures. On the surface of the earth or during the processes of powered space craft flight, just releasing gas from storage tanks is easily accomplished because gases and liquids in storage tanks always occupy positions that can be predicted. However, during the processes of microgravity or low gravity inertial flight, gas/liquid distributions in storage tanks will give rise to changes because of very small perturbations, causing their positions to be difficult to predict. The main causes producing disturbing forces are as follows.

(1) During the processes of climbing in flight, the shaking produced is one of the primary sources of disturbance associated with propellants when entering orbit.

(2) During the processes of awaiting launch on the ground and climbing, ambient heat in liquids produces convection because buoyancy forces make hot liquids rise to the tops of fluids, and, in conjunction with that, spread out along the surface of the liquid. When space craft accelerations are suddenly reduced (for example, entering orbit), fluid flow lines will then bend along the surface of the liquid, becoming perpendicular toward the front.

(3) When the process of expelling propellant from storage tanks is completed, valve closings or changes in the directions of

moments of force by fluids in the vicinity of storage tank exits will give rise to perturbations in all cases.

(4) Boost phase storage tank side walls and tank bottoms will produce elastic deformations because of liquid fuel effects. When entering orbit, structures return to original configurations and unbend. At the same time, energy will be transmitted to liquids.

(5) Despite the fact that liquids have low compression characteristics, because of the existence of static pressure heads, however, it causes the total energy stored in liquid fuel to produce important influences with respect to propellant behavior when entering orbit.

Besides the sources of disturbance described above before entering orbit, during the processes of inertial glide in orbit, a number of other forms of perturbations will also produce influences on the behavior of liquids--for example, air damping, gravity gradients, solar radiation pressure, attitude control system operation, as well as crew movements, and so on.

Making use of methods associated with propellant sunk to positions at the bottom of engines in order to complete storage tank venting associated with inertial glide processes was universally opted for as design plan in the past. However, there are a number of unanticipated drawbacks which exist in the plan in question--for example, guidance and control influencing space craft, increasing the mass associated with the entire flight process, and so on. Besides this, with regard to space craft associated with comparatively long inertial glide periods, it is also not appropriate to opt for the use of this plan.

2 SEVERAL TYPES OF PLANS WHICH CAN PROVIDE OPTIONS [2]

Following along with the development of astronavigational technology, there is a need to find storage tank venting plans suitable for utilization in long term inertial glides. A number of designs were put forward early on in the 1960's. In conjunction with that, such verifications as plan feasibility, actual operating

performance, as well as system reliability, and so on, were completed. Some had partial design, production, and testing carried out on them. In a brief review of the literature, there were four types of venting plans among them. That is

(1) Heat exchange--Released fluids are regulated into a low pressure low temperature state. In conjunction with this, fluids in the same storage tank carry out heat exchange in order to facilitate causing the vaporization of liquids which exist in released flows.

(2) Mechanical separation--Use is made of a rotating component to apply a centrifugal force to fluids in order to cause gases to separate from liquids.

(3) Dielectric pulses--Use is made of forces produced by nonuniform electric fields on fluids which do not conduct electricity to carry out gas liquid separation.

(4) Surface tension--Use is made of baffle plates or mesh sieves to utilize the surface tension of fluids in order to position liquids in storage tanks or to complete gas liquid separation in venting separation equipment.

The four types of plans discussed above had preliminary designs carried out on them with a view to the three types of space craft or mission situations which follow. a. S-IVB Class. During the process of a 4.5h inertial glide, venting was continuous. Once there was engine restart, the original settled rocket remained. b. S-IVB Class without constraining factors. c. Low Temperature Mechanical Compartment (CSM). 205h flights. Multiple iterations of restart.

/31

Carrying out comparisons with regard to preliminary designs for the four types of plans, the comparison criteria included disadvantageous consequences associated with load masses, system complexity, actual feasibility, availability of design data, performance in 100% liquid, system failure rate evaluations, and so on. Comparisons are made under the conditions set out in Table 1. The storage tank fuel is liquid hydrogen. Tank pressure is 137.9kPa.

Table 1 Comparison Conditions for Four Types of Plans

Condition	S-IVB	CSM
Maximum Venting Speed (kg/h)	571.527	0.454
Average Venting Speed (kg/h)	302.546	0.227
Design Fluid Entry Dryness	0.1	0.00138

Comparison results clearly show that mechanical separation and heat exchange systems possess greater superiority in a good number of areas. Moreover, heat exchange systems were judged as being the plan with the greatest prospects. For this reason, the S-IVB liquid hydrogen tank is used to act as a typical application example. Plan feasibility, actual operational performance verification, and primary component designs were carried out with regard to heat exchange systems. The systems which were designed required satisfying storage tank pressures of 137.9kPa, maximum venting speeds of 571.527kg/h, as well as entry fluid drynesses of zero (100% liquid). Including ducting and valves, total system mass is 51.302kg. In 4.5h inertial glide processes, requirements to maintain steady state storage tank pressures were satisfied. The mass of expeled propellant was approximately 12.712kg.

In order to give precise designs and provide needed technical information--assuring optimal operating performance of selected systems--an experimental design is presented. The experimental design in question includes a total of four parts. a. Plan feasibility verification. Using freon as the operating fluid, use is made of scaled down systems to carry out ground tests in order to verify that the selected heat exchange systems are capable of starting up and operating in a satisfactory manner under entry zone and flow conditions. b. Exploratory tests and component tests. These are used for flight system optimization and supplying data for final designs. They include hydrogen oxygen thermal transmission device tests, flow distribution uniformity tests,

expansion equipment performance and response tests, relationships between zero gravity and normal gravity results, numerical value simulation technologies, and so on, and so forth. c. Storage tank mixing tests. d. Prototype design and performance tests.

3 REVIEW OF THERMODYNAMIC VENTING SYSTEM PLANS [3]

The thermodynamic venting system which was designed and manufactured by the Sunstrand company for space shuttle/Centaur liquid hydrogen storage tanks (TVS-A Thermodynamic Vent System) is developed and formed based on an early U.S. General Dynamics Convair company foundation plan and laboratory verified. In low gravity or microgravity periods, TVS carries out control with regard to pressures in liquid hydrogen storage tanks. Moreover, it guarantees that only gas is released from low temperature propellant storage tanks.

Zero gravity thermodynamic vent systems are a type of plan put forward by the General Dynamics Convair company in 1960. The objective is to replace the original Centaur positive thrust bottom settled engine venting method which was opted for use during zero g glide periods. At that time, the TVS plan attracted a lot of interest because it is capable of avoiding expensive useful load flights. Experts believed that there was a need to carry out further developments. In 1967, tests were carried out with regard to this system on the ground in a low temperature storage tank. Test results clearly showed that the system was successful in the area of controlling liquid hydrogen storage tank pressures with venting speeds of 1.362kg/h . In 4.248m^3 liquid hydrogen storage tanks, the system in question successfully operated for over 200h. At roughly the same time in the 1960's, the Lockheed company tested a thermodynamic venting system in an 11.327m^3 liquid hydrogen storage tank. The venting speed was 0.636kg/h . The primary distinction between the TVS of the two companies was that the Convair company opted for the use of a helix tube vaporization device. The Lockheed company opted for the use of a planar thermal

dispersion plate heat exchange device. Later, in 1975, the Convair company also carried out ground tests of liquid oxygen tank thermodynamic venting systems.

The TVS which was designed and manufactured by the Sundstrand company is basically an improved form of the original version of liquid hydrogen tank design used by the Convair company in the 1960's. The system in question successfully controlled storage tank pressures in 4.248m^3 storage tank tests with venting speeds of 17.01kg/h. Ground test results proved that this TVS design concept is successful. Test results began to be published in the literature in May 1984. Ground tests of heat exchangers in this TVS were completed by the Convair company in 1983. /32

4 THERMODYNAMIC VENTING SYSTEM OPERATING PRINCIPLES [4]

The zero gravity thermodynamic venting system designed by the Sundstrand company is used to complete pressure control functions in space shuttle/Centaur liquid hydrogen storage tanks under microgravity or low gravity conditions. Through the two procedures below, objectives are reached. a. Substances inside mixed storage tanks make pressures given rise to because of local hot spots increase with limitations reaching minimums. b. Through cooling/venting processes--releasing energy from storage tanks--these processes lower storage tank pressures, causing them to be lower than independent values reached by mixing.

Fig.1 depicts the basic plan associated with thermodynamic venting systems. Under low gravity, vent piping is capable of taking in liquid, gas, or liquid gas mixtures. In order to guarantee only making superheated gases be expelled from compartments, the discharge flow is regulated to comparatively low pressures. This will lower the equilibrium temperature. After that--going through a heat exchanger--the discharge flow absorbs energy from storage tank propellant. Before leaving the TVS, it is superheated and vaporized. Fig.2 gives TVS thermodynamics diagrams.

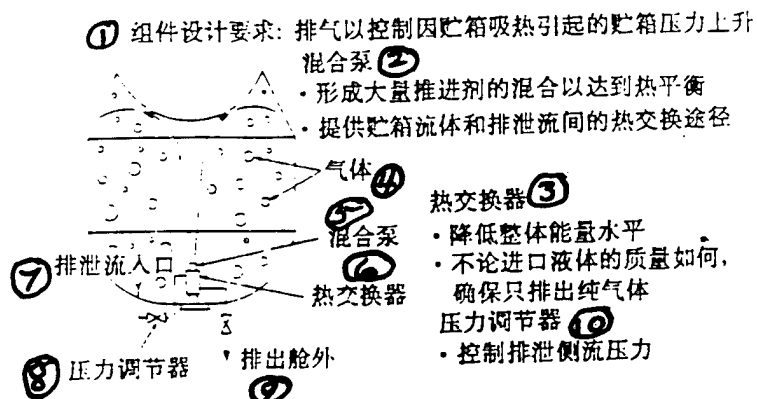


Fig.1 Zero Gravity Thermodynamic Venting System

Key: (1) Component Design Requirement: Vent to Control Storage Tank Pressure Rises Caused by Storage Tanks Absorbing Heat (2) Tank Pressure Rises Caused by Storage Tanks Absorbing Heat (3) Mixer Pump -Forms Large Amounts of Propellant Mixtures to Reach Thermal Equilibrium -Supplies Heat Exchange Path Between Storage Tank Fluids and Discharge Flows (4) Gas (5) Mixer Pump (6) Heat Exchanger (7) Discharge Flow Entry (8) Pressure Regulator (9) Discharged Outside Compartment (10) Pressure Regulator -Controls Discharge Lateral Flow Pressures

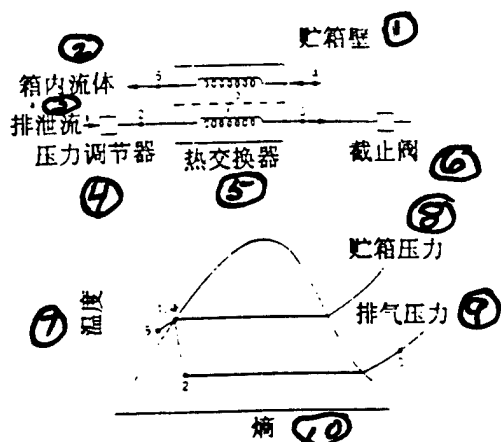


Fig.2 Venting System Thermodynamics Diagram

Key: (1) Storage Tank Wall (2) Fluid in Tank (3) Discharge Fluid (4) Pressure Regulator (5) Heat Exchanger (6) Cut Off Valve (7) Temperature (8) Storage Tank Pressure (9) Vent Pressure (10) Entropy

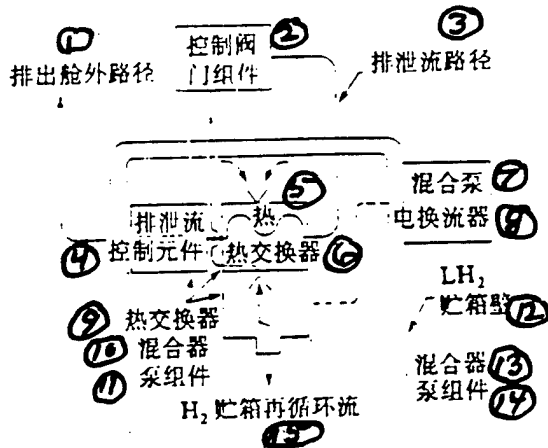


Fig.3 Zero Gravity Thermodynamic Venting System Operating Schematic

Key: (1) Path of Expulsion Outside Compartment (2) Control Valve Assembly (3) Discharge Flow Path (4) Discharge Flow Control Components (5) Heat (6) Heat Exchanger (7) Mixer Pump (8) Electrical Inverter (9) Heat Exchanger (10) Mixer (11) Pump Assembly (12) Storage Tank Wall (13) Mixer (14) Pump Assembly (15) Storage Tank Recirculation Flow

Fig.3 depicts design schematics for TVS as well as basic relationships of various components. Computer signals coming from Centaur make TVS operate, controlling LH₂ storage tank pressures in accordance with stipulated requirements. First of all, mixer pump operation forms recirculation flows. Use is made of low temperature fluids within storage tanks in order to replace warm fluids positioned on storage tank walls and break up gas clusters. Constant mixing then makes material inside storage tanks tend toward an equilibrium condition. Next, if it is necessary, start up control valve assemblies make discharge flow paths open up. In discharge flow paths, hydrogen goes through control valve assemblies after which it expands. In conjunction with this, it

then enters heat exchanger assemblies at comparatively low temperatures corresponding to pressures precisely determined by pressure regulators. At the same time as recirculating hydrogen is cooled, heat coming from flow paths associated with the hot side of storage tanks is used in vaporizing discharge flow, assuring that only gas is expeled and maintaining storage tank pressures within rated levels.

5 THERMODYNAMIC VENTING SYSTEM COMPONENTS AND THEIR FUNCTIONS

Thermodynamic venting systems are composed of three subsystems--control valve modules (CVM), heat exchanger/mixer pump modules (HEMPM), and mixing pump electric inverter modules (MPEIM).

/33

5.1 CVM Modules

CVM module functions are nothing else than regulating discharge flows, making discharge flows--in Centaur hydrogen storage tank pressure conditions--reach anticipated heat exchanger module entry location pressures. CVM are composed of two sets of parallel filters, flow regulators, and shutoff valves. The dimensions and functions of the two sets are the same. In normal operation, only one set works. When malfunctions develop, at computer command, the other set starts up and participates in the operation. What Fig.4 displays is the function diagrams associated with CVM shutoff mode and normal operating mode. Filters protect regulators and shutoff valves avoiding their being subject to micro particulate particle contamination. After going through filters, hydrogen flow goes through a regulator and cutoff valve combination. Valves are normally shut off. However, under the effects of 206.9kPa high pressure gaseous helium, valves open and complete pressure regulation functions. When arbitrary mixtures of saturated liquid hydrogen and saturated gaseous hydrogen as well as superheated gaseous hydrogen flow go through regulators, the regulators are capable, in all cases, of controling the outflow

pressures. Adjustments are carried out of regulator adjustment points through the use of thin spacers to change push rod intervals. Valves have the capability to make valve exit tubing pressures be vacuum conditions or normal operating output pressure conditions.

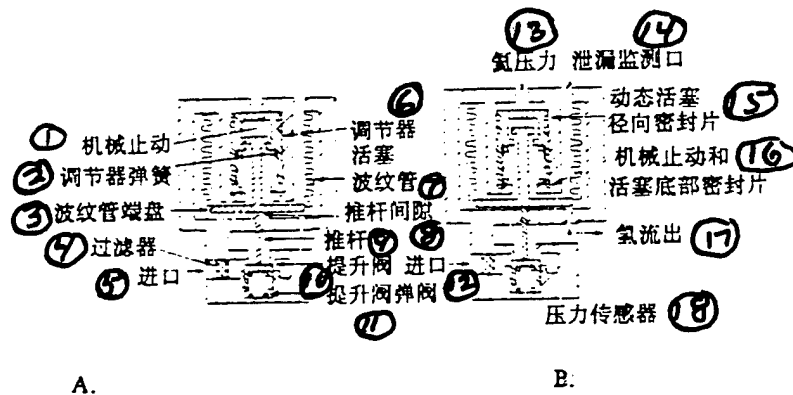


Fig.4 CVM Module Operating Principle Diagram

A. Closed Configuration

Key: (1) Mechanical Stop (2) Regulator Spring (3) Corregated Pipe End Plate (4) Filter (5) Entry (6) Regulator Piston (7) Corregated Tube (8) Push Rod Gap (9) Push Rod (10) Hoist Valve (11) Elastic Hoist Valve

B. Regulating Configuration

Key: (12) Entry (13) Helium Pressure (14) Discharge Monitoring Port (15) Dynamic Piston Radial Seal (16) Mechanical Stop and Piston Base Seal (17) Hydrogen Outflow (18) Pressure Sensor

5.2 HEMPM Modules

HEMPM modules are composed of mixer pumps, heat exchangers, venting lateral flow control elements, installation support rods, and so on.

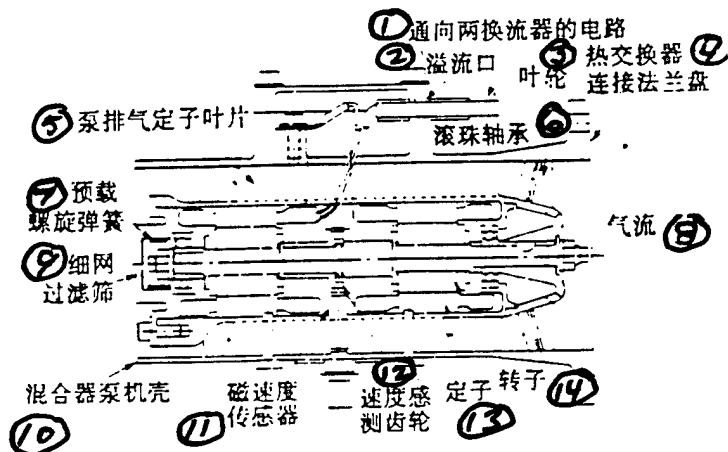


Fig.5 Mixer Pump Structural Diagram

Key: (1) Circuitry Through to Two Inverters (2) Overflow Aperture (3) Impeller (4) Heat Exchanger Connection Flange Plate (5) Pump Vent Stator Blade (6) Ball Bearings (7) Preloaded Helical Spring (8) Gas Flow (9) Fine Mesh Filter Sieve (10) Mixer Pump Casing (11) Magnetic Speed Sensor (12) Speed Sensor Gear (13) Stator (14) Rotor

/34

(1) Mixer pumps. The function of mixer pumps is nothing else than to make hydrogen go through heat exchangers to carry out circulation. Lateral heat flow is provided for discharge flows. Layered functions provide flow movements for storage tank mixing/elimination. With input powers of 15W and entry pressures of 137.9-172.3kPa, there is a requirement for mixing pump flow amounts of 227.116L/min (liquid hydrogen) and 226.535L/min (gaseous hydrogen). Fig.5 is a mixer pump structural design diagram. It is a design specially for low temperatures. In conjunction with this,

it was formed as a development of engine pumps which have already been successfully used. Mixer pumps are composed of single axis flow impellers. Two alternating current induction motor drive impellers are rotated by power provided from inverters. Impellers, two motor rotors, and a speed sensor gear are installed on the same shaft. This shaft is supported by high reliability ball bearings. High quality filters positioned at discharge terminals and associated with diameter labyrinth type noncontact seal designs protect bearings and motors from being subject to damage from exterior contaminants. Bearing preloading and thermal contraction are adjusted for by ring springs and bearing brackets. A magnetic speed sensor is used in order to indicate shaft speed. Shaft bearings, motor stators, speed sensors, discharge stator blades, and so on, are installed on pump housings. Boundary surface locations associated with pump housings and heat exchangers have flange plates.

(2) Heat exchangers. Fig.6 is a heat exchanger assembly chart. The function of heat exchangers is nothing other than to transmit heat from storage tank lateral heat flows toward lateral discharge cooling flows under all possible lateral storage tank flow conditions. Under low gravity conditions, mixing of liquid and gas groupings will severely influence the mass and volumes of flow movements passing through hot sides. However, no matter what the flow conditions are, there is a requirement in all cases that what is expeled from vaporizers is dry superheated gas. In fact, within 100 minutes of operating time, it is permissible to have not more than 0.027kg of unvaporized liquid expeled. This is equivalent to not more than 0.1% of discharged flow being permited to be unvaporized liquid remnants. Speaking in terms of conventional standards, this is a very low value. In order to design heat exchangers which are capable of satisfying stringent TVS requirements, in the early 1970's, the U.S. NASA made very great efforts [5]. The Sundstrand company completed the tests. Later, heat exchanger characteristics were improved one after the other.

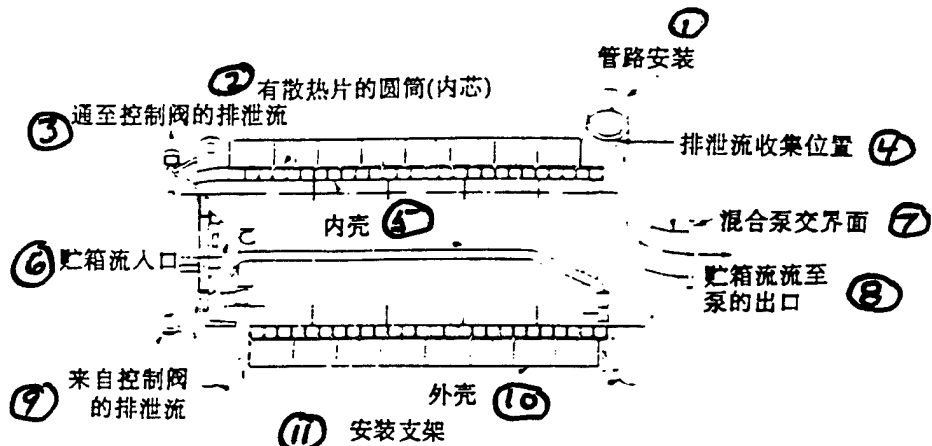


Fig. 6 Heat Exchanger

Key: (1) Tubing Installation (2) Tubes with Heat Dissipation Plates (Inner Core) (3) Discharge Flow Passes through to Control Valves (4) Discharge Flow Collection Position (5) Inner Housing (6) Storage Tank Inflow Port (7) Common Mixer Pump Boundary Surface (8) Storage Tank Flow to Pump Exit (9) Discharge Flow Coming from Control Valve (10) Outer Housing (11) Installation Frame

6 CONCLUDING REMARKS

As far as the development of a new generation of space craft is concerned, inertial glide periods will constantly lengthen. There is a need to find a new type of low temperature fuel storage tank venting system in order to replace the forward thrust motor bottom settling design. This article briefly reviewed the efforts which the U.S. has made in this area. In conjunction with that, there was a concise introduction of a type of thermodynamic venting system which can provide a utilization option.

REFERENCES

- 1 Lacovic Raymond F, et al. Management of cryogenic propellents in a full scale arbiting space vehicle. N68-25099.
- 2 Mitchell R C, et al. Study of zero-gravity vapor / liquid separators. N66-22825.
- 3 Stark J A, et al. Cryogenic zero-gravity prototype vent system. N69-10613.
- 4 Georgy L Sorensen, et al. A zero-gravity thermodynamic vent system for the Shuttle / Centaur hydrogen tank. Fourteenth Intersociety Conference on Environmental Systems. 1984.7.
- 5 Poppendiek H F, et al. Technology of Forced Flow and Once Through Boiling. NASA SP-5102. 1975.

GPS ONBOARD TRANSLATOR TRACKING SYSTEM
FOR RANGE TESTS

Yao Yu Zhang Liyu

Translation of "Yong Yu Ba Zhang Ce Shi De GPS Dan Zai Zhuan Fa Qi Xi Tong"; Missiles and Space Vehicles, Overall No. 213, No.1, 1995, pp 35-39

ABSTRACT Introduction is made of a type of GPS translator tracking system implementation plan. Use is made of ground tracking measurement stations to carry out tracking with regard to onboard (rocket) translator GPS satellite signals. In conjunction with this, vehicle (rocket) trajectory measurements are completed. It is possible to obtain more accurate results than for conventional measurement systems (for example, firing range radar range finding systems). Use is made of currently existing standard telemetry channels and ground equipment to carry out post processing with respect to translator signals, which will also save on huge and complicated external telemetry equipment.

KEY WORDS Global positioning system *Frequency translator
*Tracking system

1 INTRODUCTION

Potential applications for global positioning systems (GPS) on space flight test ranges are very broad. In various types of firing range environments, use is made of GPS to carry out external trajectory measurements to compare with conventional trajectory

measurement methods, not only raising precision, but saving on expenditures. Among these, the ones that are commonly used opt for the use of GPS translator systems. /36

Making use of ground telemetry tracking stations, it is possible to carry out tracking with regard to translated GPS satellite signals on missiles (rockets). In conjunction with this, trajectory measurements are completed. As far as GPS translation and tracking systems are concerned, discussions were had of design concepts associated with onboard GPS translators, giving methods for correcting basic translator oscillations. At the same time, ideas were put forward for using IRIG standard telemetry equipment to receive, record, and process translator signals.

2 TRANSLATED GPS SIGNAL CHARACTERISTICS

Fig.1 is a GPS translator tracking system. Translators will receive L wave band GPS C/A code signals, using the S wave band to translate them to one or multiple tracking stations on the ground. These tracking stations receive, record, and process translated signal tracking. In actuality, translators for which option is made are of two types--analog forms and digital forms. Digital translator forms are appropriate for use in situations where transmitted data requires securing. Moreover, telemetry data and translated GPS signals are able to be sent at the same time on the same link. However, due to the fact that digitized processing will also cause translated signal signal to noise ratios to experience a drop, at the same time--in situations where various performance indices are guaranteed to be the same--transmission powers needed by digital translators will be greater than analog translators.

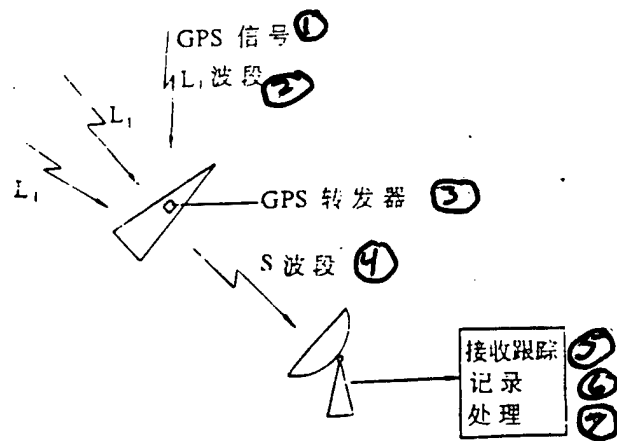


Fig.1 Translator Tracking and Reception System

Key: (1) Signal (2) Wave Band (3) Translator (4) Wave Band
 (5) Reception and Tracking (6) Recording (7) Processing

GPS satellites use the two L wave band frequencies $L_1 = 1575.42\text{MHz}$ and $L_2 = 1227.6\text{MHz}$ to continuously transmit signals. With respect to making use of L_1 frequency (C/A code) signals, the code rate is 1.023MHz . The coding associated with each satellite is unique in every case. In L_1 frequency C/A code, there is 50 bit/s code rate navigation data modulated, including navigation information.

L_1 wave band C/A code 1.5MHz band width signals are received at ground stations. Typical electrical reception level is -160dBW . After opting for the use of translators, the translation process will cause GPS signals to deteriorate. Moreover, output carrier wave side bands are capable of introducing noise into receiver input terminals. They can also produce GPS signal deterioration. Signal to noise ratios S/N associated with translator transmitted signals can be expressed as:

$$S/N_r = S/N_n \left(\frac{1}{N_1}\right) \left(\frac{1}{N_2}\right)$$

In the equation, N_1 -- is deterioration created by translation;
 N_2 -- is deterioration created due to transmitter noise.

When signal to noise ratios S/N_t in 1.5MHz band widths are lower than -30dB, it is still possible to carry out precision tracking. The reason is that, after signal spread, there is a 40dB gain.

Output frequency spectra of translators can be seen as limited band width noise. As a result, signal to noise ratios in distant terminal ground tracking systems are:

$$S/N_{tr} = S/N \cdot \frac{P_R}{P_R + P_N}$$

In the equation, P_R --is reception system input terminal translated signal power;
 P_N --is reception system noise power relative to receiver input terminal.

3 ANALOG TYPE TRANSLATORS

Opting for the use of analog type translators can be appropriate in firing range applications. In order to reduce the frequencies and power used, translators only make use of L₁ wave band C/A code operation. /37

Translators receive GPS satellite signals. In conjunction with this, they use S wave band to translate. First generation translators opt for the use of conventional heterodyne technology and A class linear power amplification in order to guarantee that nonlinearity will not produce differences with regard to satellite signals. Second generation miniaturized translators are just in

the midst of development. They are planned for use in coastal defense missile external tracking systems. It is possible to opt for the use of C class limited amplitude power amplification in order to reduce power requirements.

Fig.2 is a simplified line and block chart of a translator. Translator input includes multiple satellite signals. In reference coordinate systems fixed with regard to the earth, each satellite carrier wave has Doppler frequency shifts in all cases. Carrier wave changes are:

$$f_{ld} = L_1 \left(1 - \frac{\dot{R}_t}{c} \right) / \left(1 + \frac{\dot{R}_s}{c} \right)$$

In the equation, \dot{R}_t -- is relative motion velocity between GPS satellites and translators produced by translator motions;

\dot{R}_s -- is relative motion velocity between GPS satellites and translators produced by satellite motions;

c -- is the speed of light.

After GPS signals which are received are translated, output frequencies f_{so} are:

$$f_{so} = f_{ld} + M_1 \times (f_{lo} + f_e)$$

In the equation, M_1 -- is the multiplication factor;

f_{lo} -- is standard basic oscillation frequency;

f_e -- is basic oscillation error.

Besides this, pilot frequency f_p also comes out from the same basic oscillation.

$$f_p = M_2 (f_{lo} + f_e)$$

In the equation, M_2 -- is multiplication factor.

Pilot frequency signals can be used in telemetry, tracking, and correction of basic translator oscillation errors. Pilot frequencies can be lower than carrier waves 1-3MHz. The electrical frequencies

levels are placed so as to guarantee frequency spectra are not distorted. In conjunction with this, in situations where satellite signals are made to deteriorate at a minimum, they drop as much as possible.

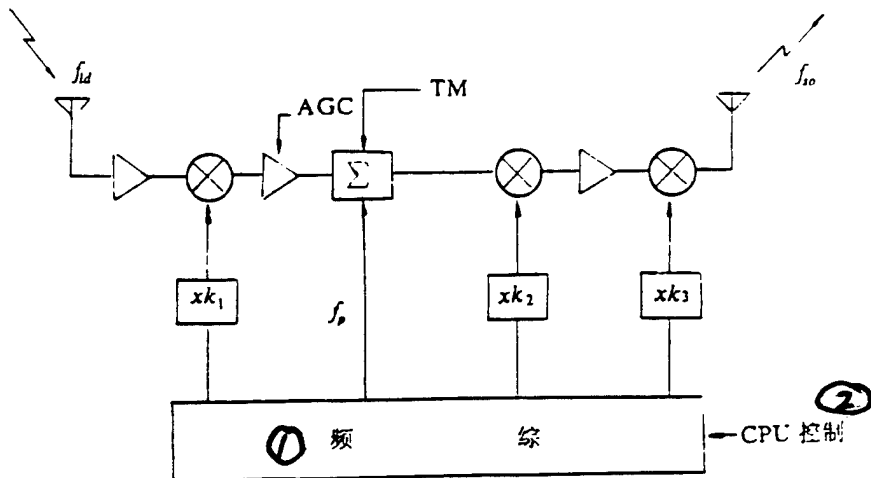


Fig.2 Analog Translator Schematic

Key: (1) Frequency Sum (2) CPU Control

4 TRANSLATOR BASIC OSCILLATION ERROR CORRECTION

With regard to analog translators, carrier wave frequencies received by tracking stations as well as pilot frequencies are, respectively,

/37

$$f_{sr} = f_{so} \cdot \left(1 + \frac{V_{tr}}{c}\right)$$

$$f_{pr} = f_p \cdot \left(1 + \frac{V_{tr}}{c}\right)$$

In equations, V_{tr} -- is relative motion velocity between translators and tracking stations.

What Fig.3 shows is one method of using pilot frequency filter signals to offset part of translator basic oscillation errors. The output results f_{ld} are input frequencies which carry translator tracking station Doppler frequency shifts. As far as the results

are concerned, when ground tracking station translator receivers require tracking signals, it is only necessary to carry out approximate calculations with regard to satellites for Doppler frequency shifts created by relative movements between translators and translator tracking stations. Tracking precisions are determined with a view to the quality of missile dynamics and receiver design (for example, acquisition band widths as well as degrees of sensitivity, and so on). When necessary, it is possible to adjust auxilliary tracking ranges.

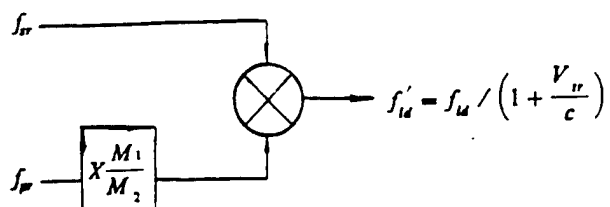


Fig.3 Translator Basic Oscillation Error Correction Principle Schematic

5 SYSTEM REALIZATION PLAN

This section introduces one type of lay out for tracking and processing ground stations as well as opting for the use of standard telemetry tracking and receiving equipment, and, in conjunction with this, methods for recording translated GPS signals.

Basic tracking station equipment is as seen in Fig.4. In the Fig., solid line sections stand for one type of basic lay out which is required to carry out signal tracking and trajectory calculations by central facilities (navigation processing). The lay out in question requires opting for the use of wide band data relays. If addition is made of GPS translator receivers (shown by

broken lines) to use in order to process translated distant terminal signals, then, it is possible to opt for the use of narrow band data channels. In the two types of lay outs, it is necessary in all cases to lower frequencies to predetermined frequency bands with regard to received translator signals, to carry out wide band recording, and, in conjunction with that, correct basic translator oscillation errors. If pilot frequency signals are eliminated, and, in conjunction with that, it is assumed that pilot frequencies are lower than carrier waves 2.0MHz--before analog translator detection--it is possible, with regard to signals, to use 1.5MHz band width wide band relay systems. If not, there is a need for 3MHz band widths. As far as data which has already been processed is concerned, it is possible to use narrow band relay systems (for example, telephone circuits) for transmission.

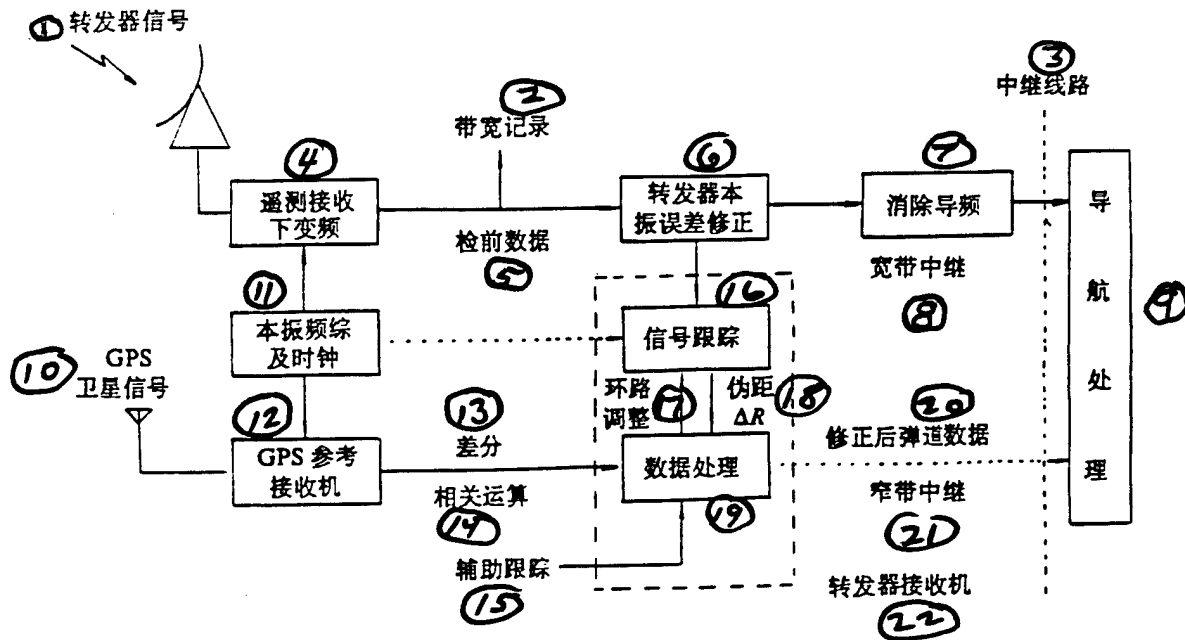


Fig.4 Basic Tracking Station

Key: (1) Translator Signal (2) Band Width Recording (3) Relay Circuitry (4) Lowered Telemetry Reception Frequency (5) Data Before Detection (6) Basic Translator Oscillation Error Correction (7) Elimination of Pilot Frequencies (8) Wide Band Relay (9) Navigation Processing (10) GPS Satellite Signal (11) Basic Oscillation Frequency Sum and Clock (12) GPS Reference Receiver (13) Difference (14) Correlation Operations (15) Auxilliary Tracking (16) Signal Tracking (17) Loop Adjustment (18) Pseudo Range (19) Data Processing (20) Trajectory Data After Correction (21) Narrow Band Relay (22) Translator Receiver

/39

This type of lay out requires at least the data associated with four GPS satellites to carry out trajectory measurements. In stations, difference corrections should also be made. Opting for the use of difference GPS, it is possible to calibrate errors created due to such things as satellite ephemeris, satellite clocks, as well as ionosphere delays, and so on--thereby improving accuracy. As far as ground tracking stations which possess capabilities for difference corrections are concerned, it is possible to use them in precision trajectory measurements. Telemetry and GPS receivers make use of common frequency and time

standards produced by low noise oscillators and frequency sums. If time delays or frequency drift can be measured or estimated calculations done using models, then, it is only necessary to use signals associated with three satellites and it is then possible to carry out trajectory measurements.

6 DATA RECEIEVED/RECORDED/AND REAMPLIFIED

With regard to using S wave bands to transmit translator signals, it is then possible to make use of standard telemetry equipment at a good number of test ranges--taking received S wave band signals and lowering their frequencies to appropriate recording frequencies and doing recordings on bands as wide as possible. After using standard time base error calibration instruments to calibrate, there is reamplification and recording. Time base error calibration equipment is capable of reducing standard recorder time base errors. In conjunction with this, it is capable of guaranteeing that the reamplification data periods associated with conventional telemetry recording instruments used by GPS receivers maintain lock in.

7 CONCLUSIONS

With respect to applications of GPS signal translators on test ranges, their roles are very clear. Analog translator signal to noise ratio deterioration is comparatively small. In situations where equipment performance is not subject to influences, required transmission powers are comparatively small. It is possible to make use of S wave band telemetry channels to transmit--saving on huge and complex external measurement equipment.

After the addition of auxilliary tracking equipment, it is possible to make GPS receivers only use overall translated signals associated with estimated calculations and tracking. As a result, speaking in terms of high dynamics applications, translator receivers only need to opt for the use of single frequency signals

for tracking, and that is all.

When data is transmitted into central facilities to carry out processing, there is a need for the most basic tracking station equipment. When tracking stations are equipped with GPS receivers to process translators, GPS reference receivers, and common frequency time standards, it is then possible to carry out trajectory calculations using data associated with only three satellites. When GPS signals are taken and transferred to S wave bands, and, in conjunction with that, option is made for the use of appropriate time base error calibration equipment, it is possible to make use of currently existing standard telemetry receiving and recording equipment.

REFERENCES

- 1 Tracking small satellite using translated GPS. AIAA 92-1684.
- 2 Tracking translated GPS signals. ION GPS-90, 345~353.
- 3 A Dual-mode kalman filter for vehicle tracking with translated GPS. ION GPS-90, 335~344.
- 4 Performance assessment in real-time for a range safty GPS translator tracking system. ION GPS-91, 609~618.
- 5 P-code versus C / A-code GPS for range tracking applications. Navigation, 1991, 38:289~293

THE REAL-TIME WEIGHTED RECURSIVE ALGORITHM OF LEAST
SQUARES ESTIMATION AND ITS INITIAL APPLICATIONS

Luo Xucheng

Translation of "Shi Shi Jia Quan Di Tui Zui Xiao Er Cheng Gu Ji Ji
Qi Chu Bu Ying Yong"; Missiles and Space Vehicles, Overall No.
213, No.1, 1995, pp 40-49

ABSTRACT Taking the weighted recursive algorithm associated with least square estimations and combining it with real time algorithms to which "forgeting factors" are added, a real time weighted recursive least square estimation method is derived. In conjunction with this, actual tracking system data processing problems are used to explain applications of this type of algorithm in multi-information source measurement data processing systems.

KEY WORDS Least square method Estimate Tracking system
Data processing

1 INTRODUCTION

Least square estimates are a type of typical engineering data processing method. They are widely used in such fields as data processing associated with measurement signals, the distinguishing of control system processes and parameters, linear statistical inference associated with mathematical statistics, and so on.

During long term development processes--in particular, since the 1950's--following along with the development of computer technology, control theory, and measurement system technology, least square algorithms appropriate to applications in various

types of engineering have been constantly developed [1-3]. Weighted algorithms permit the addition of different weights with regard to various measurement components on the basis of need. As far as recursive algorithms are concerned, after the acquisition of new data, new calculations are not used based on all the data. And, on the foundation of the original estimated amounts, it is only necessary to use information brought by the new data with regard to original estimates to do corrections and then obtain new estimates. In the recursive algorithms described above, the contributions of measurement data with regard to index functions are not related to the priority order associated with measurements obtained. They are appropriate for use in situations where estimated quantities or parameters are maintained as constant values. In order to be suitable for situations where estimated quantities are time variable signals or parameters, real time algorithms are produced. These include forgetting factor methods and limited memory methods. Forgetting factor methods are nothing else than the addition of different weights to remaining differences between new and old in index functions associated with judging estimation quality in order to lower the amount of information provided by old data. Memory limitation methods limit the length of data used in estimates, getting rid of the influences of old data on estimations in a thorough going way. Besides this, with a view to the problems associated with least square methods not being able to give consistent data without deviations in situations where there is colored noise, there are also put forward such methods as error compensation least square methods, expansion least square methods, generalized least square methods, auxilliary variable methods, as well as two step correlation methods, and so on. Each type of method corresponds to the noise associated with one type of specially designated model structure.

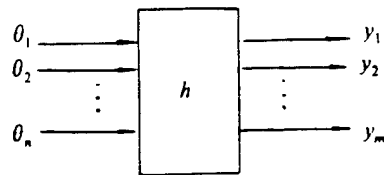


Fig.1 Multiple Variable Measurement System

In engineering, it is sometimes required to take weighted, recursive, and real time algorithms and combine them together. Referring to the multiple variable measurement system in Fig.1, input variables are $\theta_1, \theta_2, \dots, \theta_n$. Output variables are y_1, y_2, \dots, y_m . Our objective is to solve for least square estimations associated with output variables $\theta_1, \theta_2, \dots, \theta_n$ on the basis of variables y_1, y_2, \dots, y_m . The accuracies of measurement means associated with obtaining measurements y_1, y_2, \dots, y_m vary. The reliabilities differ. When it is wished to process data, different weights are then applied to different measurement components. In order to make estimation processes obey time variable inputs, it is desirable to opt for the use of real time recursive algorithms. In control system parameters and process identifications, there is also a basically similar situation. However, in the reference materials that are available, system derivations associated with the combining of weighting and real time recursive algorithms have still not been seen.

This article combines least square weighted recursive algorithms and real time algorithms with the addition of forgetting factors, deriving real time weighted recursive least square estimation algorithms. In conjunction with this, it combines unified measurement and control system tracking data processing

problems, illucidating applications of real time weighted recursive least square estimation algorithms.

2 REAL TIME WEIGHTED RECURSIVE LEAST SQUARE ESTIMATIONS

2.1 Problem Description

Refering to the n dimensional input m dimensional output measurement system in Fig.1

$$y = h\theta + \varepsilon \quad (1)$$

In this, $y \in R^{mx1}$, $\theta \in R^{nx1}$, $h \in R^{mxn}$, $\varepsilon \in R^{mx1}$, with $m > n$. We take K iterations of measurement results. In order to add weight to new measurement weightings and in order to reduce the amounts of information associated with old data, we gradually add forgetting factor $\beta < 1$ to remaining differences with old, obtaining error vectors that are

$$E_k = [\beta^{k-1} \varepsilon^T(1), \beta^{k-2} \varepsilon^T(2), \dots, \beta \varepsilon^T(K-1), \varepsilon^T(K)]^T \quad (2)$$

Paying attention to

$$\beta \varepsilon = \beta y - \beta h \theta \quad (3)$$

Considering all measurement results up to the Kth iteration, one has

$$Y_k = H_k \theta + E_k \quad (4)$$

/42

$$Y_k = \begin{bmatrix} \beta^{k-1} y(1) \\ \vdots \\ \beta y(K-1) \\ y(K) \end{bmatrix}, \quad H_k = \begin{bmatrix} \beta^{k-1} h_1(1) & \cdots & \beta^{k-1} h_n(1) \\ \vdots & \ddots & \vdots \\ \beta h_1(K-1) & \cdots & \beta h_n(K-1) \\ h_1(K) & \cdots & h_n(K) \end{bmatrix}, \quad E_k = \begin{bmatrix} \beta^{k-1} \varepsilon(1) \\ \vdots \\ \beta \varepsilon(K-1) \\ \varepsilon(K) \end{bmatrix} \quad (5)$$

Having $Y_K \in R^{mKx1}$, $H_K \in R^{mKxn}$, and $E_K \in R^{mKx1}$, the residual error index function is defined as being

$$J = \varepsilon_K^T W_K \varepsilon_K = (Y_K - H_K \theta)^T W_K (Y_K - H_K \theta) \quad (6)$$

In this, $W_K \in R^{mKxmK}$ is the hoped for weighting matrix.

$$W_K = \begin{bmatrix} w(1) & & & 0 \\ & w(2) & & \\ & & \dots & \\ 0 & & & w(K) \end{bmatrix} \quad (7)$$

$w(i) \in R^{m xm}$, ($i=1, 2, \dots, K$), is a diagonal positive definite matrix. The diagonal line elements then refer to different properties associated with various measurement components and weightings given situations.

Our objective is to derive a type of recursive algorithm. When we obtain a set of new measurements, use is made of this type of algorithm to solve corrections associated with $\hat{\theta}$ estimations with regard to θ , thereby guaranteeing that residual difference index function J is maintained at a minimum.

2.2 Problem Solution Methods

We begin to solve for inverse lemma from the matrices described below.

Lemma: If A, C, A+BCD is a nonsingular matrix, then one has

$$(A + BCD)^{-1} = A^{-1} - A^{-1}B(C^{-1} + DA^{-1}B)^{-1}DA^{-1} \quad (8)$$

In References 1 and 2, there are proofs of this lemma in both cases.

Taking the index function J in equation (6) and differentiating against θ , and, in conjunction with this, letting it be 0, one obtains

$$\frac{\partial J}{\partial \theta} = (H_k^T W_k H_k \theta - H_k^T W_k Y_k) + (H_k^T W_k H_k \theta - H_k^T W_k Y_k)^T = 0$$

getting

$$\hat{\theta}_k = P_k H_k^T W_k Y_k \quad (9)$$

In this,

$$P_k = [H_k^T W_k H_k]^{-1} \quad (10)$$

When the K+1th set of measurements is entered, the residual difference vector associated with forgetting factor β is

$$\varepsilon_{k+1} = \begin{bmatrix} \beta^k \varepsilon(1) \\ \dots \\ \beta \varepsilon(K) \\ \varepsilon(K+1) \end{bmatrix} = \begin{bmatrix} \beta \varepsilon_k \\ \varepsilon(K+1) \end{bmatrix} \quad (11)$$

Giving comprehensive consideration to all measurement results, one has

$$Y_{k+1} = H_{k+1} \theta + \varepsilon_{k+1} \quad (12)$$

In this,

$$Y_{k+1} = \begin{bmatrix} \beta^k y(1) \\ \dots \\ \beta y(K) \\ y(K+1) \end{bmatrix} = \begin{bmatrix} \beta Y_k \\ y(K+1) \end{bmatrix} \quad (13)$$

$$H_{k+1} = \begin{bmatrix} \beta^k h_1(1) & \dots & \beta^k h_n(1) \\ \dots & \dots & \dots \\ \beta h_1(K) & \dots & \beta h_n(K) \\ h_1(K+1) & \dots & h_n(K+1) \end{bmatrix} = \begin{bmatrix} \beta H_k \\ h^T(K+1) \end{bmatrix} \quad (14)$$

Using a process completely similar to that for obtaining equations (9) and (10), one has

$$\hat{\theta}_{K+1} = P_{K+1} H_{K+1}^T W_{K+1} Y_{K+1} \quad (15)$$

$$P_{K+1} = [H_{K+1}^T W_{K+1} H_{K+1}]^{-1} \quad (16)$$

In this,

$$W_{K+1} = \begin{bmatrix} w(1) & & & 0 \\ & w(2) & & \\ & & \cdots & \\ & & & w(K) \\ 0 & & & w(K+1) \end{bmatrix} = \begin{bmatrix} W_K & 0 \\ 0 & w(K+1) \end{bmatrix} \quad (17)$$

Taking equations (14) and (17) and substituting into equation (16),

$$\begin{aligned} P_{K+1}^{-1} &= \begin{bmatrix} \beta H_K \\ h^T(K+1) \end{bmatrix}^T \begin{bmatrix} W_K & 0 \\ 0 & w(K+1) \end{bmatrix} \begin{bmatrix} \beta H_K \\ h^T(K+1) \end{bmatrix} \\ &= \beta^2 H_K^T W_K H_K + h(K+1)w(K+1)h^T(K+1) \\ &= \beta^2 P_K^{-1} + h(K+1)w(K+1)h^T(K+1) \end{aligned} \quad (18)$$

Applying matrix solutions to the equations above, one obtains the inverse lemma

$$\begin{aligned} P_{K+1} &= [\beta^2 P_K^{-1} + h(K+1)w(K+1)h^T(K+1)] \\ &= \frac{1}{\beta^2} \left\{ P_K - P_K h(K+1) [\beta^2 w^{-1}(K+1) + h^T(K+1)P_K h(K+1)]^{-1} h^T(K+1)P_K \right\} \\ \hat{\theta}_{K+1} &= P_{K+1} \begin{bmatrix} \beta H_K \\ h^T(K+1) \end{bmatrix}^T \begin{bmatrix} W_K & 0 \\ 0 & w(K+1) \end{bmatrix} \begin{bmatrix} \beta Y_K \\ y(K+1) \end{bmatrix} \\ &= \left\{ \frac{1}{\beta^2} P_K - \frac{1}{\beta^2} P_K h(K+1) [\beta^2 w^{-1}(K+1) + h^T(K+1)P_K h(K+1)]^{-1} h^T(K+1)P_K \right\} \end{aligned} \quad (19)$$

$$\begin{aligned}
& \bullet [\beta^2 H_K^T W_K Y_K + h(K+1)w(K+1)y(K+1)] \\
& = P_K H_K^T W_K Y_K - P_K h(K+1) [\beta^2 w^{-1}(K+1) + h^T(K+1)P_K h(K+1)]^{-1} \\
& \quad \cdot h^T(K+1)P_K H_K W_K Y_K + \frac{1}{\beta^2} P_K h(K+1)w(K+1)y(K+1) \\
& \quad - \frac{1}{\beta^2} P_K h(K+1) [\beta^2 w^{-1}(K+1) + h^T(K+1)P_K h(K+1)]^{-1} \\
& \quad \cdot h^T(K+1)P_K h(K+1)w(K+1)y(K+1)
\end{aligned} \tag{20}$$

In the equation above, the last two terms are

$$\begin{aligned}
& \frac{1}{\beta^2} P_K h(K+1)w(K+1)y(K+1) \\
& - \frac{1}{\beta^2} P_K h(K+1) [\beta^2 w^{-1}(K+1) + h^T(K+1)P_K h(K+1)]^{-1} \\
& \cdot [h^T(K+1)P_K h(K+1) + \beta^2 w^{-1}(K+1) - \beta^2 w^{-1}(K+1)] w(K+1)y(K+1) \\
& = \frac{1}{\beta^2} P_K h(K+1)w(K+1)y(K+1) - \frac{1}{\beta^2} P_K h(K+1)w(K+1)y(K+1) \\
& + P_K h(K+1) [\beta^2 w^{-1}(K+1) + h^T(K+1)P_K h(K+1)]^{-1} y(K+1) \\
& = P_K h(K+1) [\beta^2 w^{-1}(K+1) + h^T(K+1)P_K h(K+1)]^{-1} y(K+1)
\end{aligned} \tag{21}$$

Taking equations (9) and (21) and substituting into equation (20), one obtains

$$\begin{aligned}
\hat{\theta}_{K+1} &= \hat{\theta}_K + P_K h(K+1) [\beta^2 w^{-1}(K+1) + h^T(K+1)P_K h(K+1)]^{-1} \\
&\quad \cdot [y(K+1) - h^T(K+1)\hat{\theta}(K)] \\
&= \hat{\theta}_K + K(K+1) [y(K+1) - h^T(K+1)\hat{\theta}_K]
\end{aligned} \tag{22}$$

$$K(K+1) = P_K h(K+1) \left[\beta^2 w(K+1) + h^T(K+1) P_K h(K+1) \right]^{-1} \quad (23)$$

Taking equation (23) and substituting into equation (19), one obtains

$$P_{K+1} = \frac{1}{\beta^2} [I - K(K+1)h^T(K+1)] P_K \quad (24)$$

In this, I is an nxn unit matrix. Equations (22), (23), and (24) compose a complete real time weighted recursive least square estimation algorithm. $w(K)$ applies different weighting values to the various components of new measurements obtained in association with each iteration in order to characterize the influence on estimations. Forgetting factor β^2 lowers the amount of information associated with old data, increasing the influence of new data on estimations so as to make estimates track in real time changes associated with time change data. Obviously, w and β^2 both need to be determined through testing with a view to actual systems.

Recursive operations require initial conditions. Taking the first iteration of measurement results

$$y(0) = h(0)\theta + \varepsilon(0) \quad (25)$$

/45

one has

$$\begin{cases} P_0 = (H_0^T W_0 H_0)^{-1} \\ \hat{\theta}_0 = P_0 H_0^T W_0 Y_0 \end{cases} \quad (26)$$

Here, $H_0 = h(0)$, $W_0 = w(0)$, and $Y_0 = y(0)$.

3 APPLIED RESEARCH ASSOCIATED WITH REAL TIME WEIGHTED RECURSIVE LEAST SQUARE ESTIMATIONS IN TRACKING SYSTEM DATA PROCESSING

We now discuss unified measurement and control system tracking data processing problems.

3.1 System Description

Unified measurement and control system antenna bases operate in accordance with azimuth-elevation axes. From precise determinations of missions and station sites, the systems in question primarily operate in association with low angles of elevation and negative angles of elevation. There are a number of types of ways that these systems obtain angular position information. (1) Main antennas (narrow beam) through target angular deviation information sent out by tracking receivers. (2) Main antennas through target angular deviation information sent out by range finding receivers. (3) Guidance antennas (wide beam) through target angular deviation information sent out by guidance antennas. (4) Target angular digital guidance information sent out by measurement radar associated with the same station site. (5) Antenna direction angle information sent out by antenna base angle sensor coding devices. (6) Target trajectory information sent out by firing range command centers. (7) Through target altimeter measurement data sent in by telemetry data demodulation. (8) Target radial distance and velocity data sent in by telemetry processors.

The objective of tracking system data processing is to take target data measurement output and track the areas of targets that antennas are pointed at. Servo systems only complete the tracking of targets. However, data processing systems, by contrast, eliminate or reduce such influences as dynamic lag errors, deviations, and so on, sending out accurate position data on targets. At the same time, taking digital processing technology and servo control technology and combining them--carrying out

compensation with regard to certain deviations and errors--antenna pointing accuracies and rapid target tracking capabilities are improved.

Despite the fact that it is possible to directly use measurement structures associated with the quantities described above to measure models, option is made for the use of autoadjusting Kalman filter algorithms including mobile detection to estimate target angle information [4-6]. However, doing this is certainly not very advantageous. First of all, within low elevation angle ranges, electric wave multipath reflection will cause main antennas and guidance antennas to bring in clear elevation angle tracking errors from tracking systems--becoming a primary source of errors. The error sources in question have both systemic error and arbitrary error properties--difficult to describe by the use of linear equations. This creates an impermissibility with regard to model set ups associated with corresponding measurement equations. As far as directly employing this type of measurement model is concerned, comparatively large errors will necessarily be brought into estimations. Secondly, the amount of calculations associated with Kalman filter algorithms is in direct proportion to the number of measurement equations. As far as numerous calculations are concerned, there is a possibility of making amounts of calculations associated with filter estimation devices reach levels which cannot be permitted.

One type of comparatively desirable processing method is to first of all do preprocessing on measurement data. With respect to this operational item--besides getting rid of wild values--it is primarily the adding of different weights to various measurement components on the basis of angles of depression and elevation associated with antenna pointing as well as the reliabilities of information sources. Real time weighted recursive least square estimations are solved for targets, acting as overall measurement results for target positions in order to facilitate compression of the amounts of data and reducing the influences of measurement components with severe multiple path responses on

measurement results. On this foundation and on the basis of dynamic target models, use is made of overall measurement results, filtering estimates found for target speeds, accelerations, and so on, to act as the target status output associated with system measurements. At the same time, estimation results are taken and added to antenna tracking control loops in order to improve antenna tracking precision and rapid tracking capabilities.

3.2 Data Processing Models

Referring to servo systems such as in Fig.2, one has

$$\theta_{in} = \theta_{out} + \Delta\theta \quad (27)$$

In reference to such sources of error as servo noise, mechanical deviations, responses associated with moments of force, and so on, measurement values are adopted as

$$x = \theta_{out} + \Delta\theta \quad (28)$$

/46

Moreover, measurement models are

$$x = \theta_{in} + \zeta \quad (29)$$

In this, ζ is residual measurement deviation.

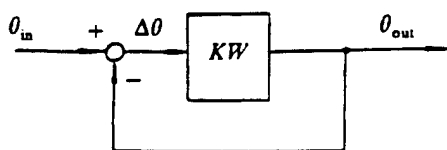


Fig.2 Servo System Schematic

Mathematical models associated with various measurement quantities obtained on the basis of the model establishment principles described above are as follows.

(1) Main antenna measurement data through telemetry tracking receivers

$$\begin{cases} x_1 = \alpha_0 + \Delta\alpha_1 \\ z_1 = \beta_0 + \Delta\beta_1 \end{cases} \quad (30)$$

In the equations, α_0 and β_0 are, respectively, antenna base azimuth and depression and elevation angle sensor coding outputs. $\Delta\alpha_1$ and $\Delta\beta_1$ are error signals associated with telemetry tracking receiver azimuth and depression and elevation angle channel outputs. x_1 and z_1 are, respectively, measurement values associated with azimuths and depression and elevation. The mathematical measurement model is

$$\begin{cases} x_1 = \alpha + \zeta_1 \\ z_1 = \beta + \eta_1 \end{cases} \quad (31)$$

In the equations, α and β are target azimuth angles and depression and elevation angles. ζ_1 and η_1 are measurement errors.

(2) Main antenna measurement data through range finding receivers

$$\begin{cases} x_2 = \alpha_0 + \Delta\alpha_2 \\ z_2 = \beta_0 + \Delta\beta_2 \end{cases} \quad (32)$$

In the equations, $\Delta\alpha_2$ and $\Delta\beta_2$ are, respectively, azimuth and depression and elevation error signals associated with range finding receiver outputs. x_2 and y_2 are, respectively, measurement values associated with azimuths and depression and elevation. The mathematical model is

$$\begin{cases} x_2 = \alpha + \zeta_2 \\ z_2 = \beta + \eta_2 \end{cases} \quad (33)$$

In the equations, ζ_2 and η_2 are residual measurement deviations.

(3) Guidance antenna measurement data through guidance receivers

$$\begin{cases} x_3 = \alpha_0 + \Delta\alpha_3 \\ z_3 = \beta_0 + \Delta\beta_3 \end{cases} \quad (34)$$

In equations, $\Delta\alpha_3$ and $\Delta\beta_3$ are, respectively, azimuth and depression and elevation error signals associated with guidance receiver outputs. x_3 and y_3 are, respectively, measurement values associated with azimuths and depressions and elevations. The corresponding mathematical model is

$$\begin{cases} x_3 = \alpha + \zeta_3 \\ z_3 = \beta + \eta_3 \end{cases} \quad (35)$$

(4) Azimuth and depression and elevation guidance angle values measured by radars associated with the same measurement and control station and sent out are x_4 and z_4 . Let ζ_4 and η_4 be, respectively, residual zig zag measurement errors associated with azimuth and depression and elevation. Then, the mathematical model is

/47

$$\begin{cases} x_4 = \alpha + \zeta_4 \\ z_4 = \beta + \eta_4 \end{cases} \quad (36)$$

(5) Target trajectory information associated with firing range command centers is real time target geocentric coordinate system data (x_o , y_o , z_o). Through carrying out coordinate transformations on antenna control device computers, they become measurement coordinate system data associated with the actual location of a measurement and control station itself (x_m , y_m , z_m). See Fig.3.

$$x_s = \begin{cases} \operatorname{tg}^{-1} \frac{y_m}{z_m} & \text{当 } y_m > 0, z_m > 0 \\ 180^\circ + \operatorname{tg}^{-1} \frac{y_m}{z_m} & \text{当 } z_m < 0 \\ 360^\circ + \operatorname{tg}^{-1} \frac{y_m}{z_m} & \text{当 } y_m < 0, z_m > 0 \end{cases} \quad (37)$$

$$z_s = \operatorname{tg}^{-1} \frac{x_m}{\sqrt{y_m^2 + z_m^2}} \quad (38)$$

The corresponding measurement model is

$$\begin{cases} x_s = \alpha + \zeta_s \\ z_s = \beta + \eta_s \end{cases} \quad (39)$$

In these equations, x_s and z_s are measurement values associated with azimuths as well as depression and elevation. ζ_s and η_s are measurement residual errors.

(6) Making use of target altitudes H measured by target altimeters as well as target radial distances R measured by range finder processors (refer to Fig.4), it is possible to obtain target elevation angle measured values z_6 .

$$z_6 = \sin^{-1} \left[\frac{H^2 - h^2 - R^2 + 2r(H-h)}{2R(r+h)} \right] \quad (40)$$

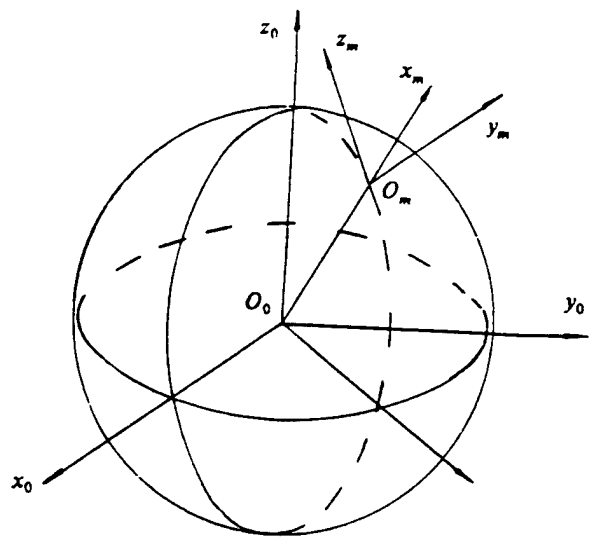


Fig.3 Center-Local Coordinate Transformation

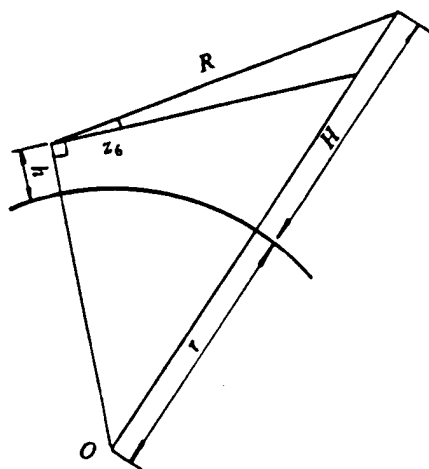


Fig.4 Target Elevation Angle Measurements

The measurement model is

$$z_6 = \beta + \eta_6 \quad (41)$$

In equations, h is station antenna phase center height. r is the radius of the earth. η_6 is measurement residual deviation.

Combining the models for the various measurement components described above, one obtains the data processing measurement model that follows.

$$y = h\theta + \varepsilon \quad (42)$$

In the equation,

$$\theta = \begin{bmatrix} \alpha \\ \beta \end{bmatrix} \quad (43)$$

$$y = \begin{bmatrix} x_1 \\ x_2 \\ x_3 \\ x_4 \\ x_5 \\ z_1 \\ z_2 \\ z_3 \\ z_4 \\ z_5 \\ z_6 \end{bmatrix}, \quad h = \begin{bmatrix} 1 & 0 \\ 1 & 0 \\ 1 & 0 \\ 1 & 0 \\ 1 & 0 \\ 0 & 1 \\ 0 & 1 \\ 0 & 1 \\ 0 & 1 \\ 0 & 1 \end{bmatrix}, \quad \varepsilon = \begin{bmatrix} \zeta_1 \\ \zeta_2 \\ \zeta_3 \\ \zeta_4 \\ \zeta_5 \\ \eta_1 \\ \eta_2 \\ \eta_3 \\ \eta_4 \\ \eta_5 \\ \eta_6 \end{bmatrix}. \quad (44)$$

As far as making use of recursive algorithms in association with equations (22) - (24). On the basis of measurements obtained in real time, it is then possible to solve for real time estimation values related to target azimuth angles and pitch angles.

3.3 Explanations of Several Points

(1) Whether or not component measurement equations are set up depends on the operating configuration of the measurement means. For instance, just as long as measurement radars are placed in auto tracking configurations, only then is radar guidance information effective. Only then is equation (36) established. So long as target altimeter operation is normal and range finder processor operation is also normal, only at that time are measurement equations (40) and (41) set up. As a result, systems must monitor as needed the operating configurations associated with various measurement means. In conjunction with this, measured values are increased and reduced in real time.

(2) As far as the weightings given by weighting matrix $w(K)$ to various measurement components are concerned, the values should consider such factors as operating configurations associated with various measurement means, reliabilities, the magnitudes of measurement errors, and so on. Perhaps it is also necessary to consider ranges of elevation angles, and there is a need to go through repeated experimental determinations. /49

(3) Due to the fact that the influences that various measurement means are subject to from multiple path effects are different--some are even completely uninfluenced--methods associated with the combination of multiple information sources are used to acquire target angle estimations. It is possible, from the entirety of them, to lower measurement angle errors formed by multiple path effect influences on antennas.

(4) From an analysis of equations (42) - (44), it can be seen that, with regard to α and β estimation devices, it is possible to decouple and dissociate them as two respective subestimation devices associated with α and β . With respect to

actual realization, estimation processes should also be taken a step further, dissociating them as recursive operations with regard to various measurement components in order to avoid matrix solutions associated with inverse operations--reducing the amount of calculations a step further.

4 CONCLUSIONS

This article derived real time weighted recursive least square estimation algorithms. They are not only capable of figuring in different properties of different contributions of measurements with regard to estimations. They are also able to process measurement data and parameters that change with time. From the cases that have been put forward, it is possible to see that the effectiveness of the application of this type of method to multiple information source measurement systems is obvious and easily observed.

REFERENCES

- 1 国家测绘总局测绘研究所. 近代最小二乘法(译文集). 测绘出版社, 1980.
- 2 夏天长, 熊光楞等译. 系统辨识——最小二乘法. 清华大学出版社, 1983.
- 3 方崇智, 萧德云. 过程辨识. 清华大学出版社, 1988.
- 4 孙仲康. 雷达数据数字处理. 国防工业出版社, 1983.
- 5 Farina A, Studer F A. Radar data processing(vol.1). Research Studies Press, 1985.
- 戴树苏等. 数字技术在雷达中的应用. 国防工业出版社, 1981.

TWO U.S. COMPANIES PUT FORWARD NEW CARRIER
ROCKET DESIGN PLANS

Translation of "Mei Guo Liang Jia Gong Si Ti Chu De Yu Zai Huo Jian Fang An"; Missiles and Space Vehicles, Overall No. 213, No.1, 1995, p 49

Two new carrier rocket design plans can be regarded as the newest put out by U.S. companies. Among them, one type is a mobile launch rocket. The other is a type of resusable carrier rocket funded by a private company.

The Veda company of Virginia has already designed a type of solid rocket named the Ulysses. This type of rocket is capable of being fired from mobile platforms at sea. It is capable of taking a 272.2kg load and sending it into near earth orbit. The launch cost is approximately 10 million U.S. dollars. The Veda company is in the midst of planning for Defense Department appropriations for development costs.

A privately run Seattle company--Kistler aviation and space flight company--is in the midst of designing a type of single stage carrier rocket capable of orbital entry and reuse. The detailed status of this type of rocket will be made public in the near term.

(Western Press Article)

FERRITE MAGNETIC HEAD
OF EXPANDING RECORDING BANDWIDTH

Zhang Peixing

Translation of "Kuo Kuan Ji Lu Dai Kuan De Tie Yang Ti Ci Tou";
Missiles and Space Vehicles, Overall No. 213, No.1, 1995, pp 50-57

ABSTRACT The ferrite magnetic head used in sets with YJ21-1 and YJ2-4 magnetic recorders breaks out of the traditional metallic models of magnetic head. Recording band width is expanded a level, reaching IRIG wide frequency band standards. Life is very, very greatly increased. This signifies that Chinese planning of magnetic head design and manufacturing technology has reached a new high. In this article, there is a description of the development background, design principles, technical characteristics, technological properties, as well as the broad applicability of the magnetic heads in question, thereby providing feasible design methods and technical manufacturing methods for ferrite magnetic heads.

KEY WORDS Magnetic recording, Broadband, Magnetic head

I INTRODUCTION

Magnetic recorders have already become an indispensable part of measurement systems associated with carrier rocket tests and satellite applications. Following along with the development of spaceflight technology, there is a requirement that magnetic recorders possess even higher recording densities--that is, at a certain predetermined tape speed, increased high frequency recording capabilities. To a very large extent, high density recording capabilities are determined by very complicated relationships between magnetic tape, magnetic heads, and head tape boundary surface properties. Magnetic heads act as the key components of magnetic recorders. The technological properties are directly related to whether or not high technology capabilities of recorders are capable of realization or not.

/51

During the initial period in the development of magnetic recorders, option was made for the use of laminated type metal magnetic heads. This type of magnetic head was developed from magnetic sound recording heads and is mature technology. However, due to the fact that specific resistances associated with the use of Fe-Ni systems of alloys are low (only $55 \times 10^{-6} \Omega\text{cm}$) and high frequency losses are large, increases in magnetic head utilization frequencies are limited. Magnetic core lamination technology also makes it difficult for magnetic heads to achieve narrow operating slits, limiting capabilities for recording short wave lengths. Moreover, because anti abrasion characteristics are bad, magnetic head life is also very low.

As far as magnetic recording devices associated with China's first generation telemetry system sets are concerned, they all pertain to low frequency band ranges (the shortest recorded wave lengths are approximately $15.2\mu\text{m}$) and are only capable of recording shunt signals after detection. They opt for the use of permalloy laminated metallic magnetic heads. At tape speeds below 1.52m/s, direct 100kHz [1] recordings are made.

In the late 1960's, the U.S. had a requirement to carry out predetection recording with regard to telemetry signals. Broad band recording devices appeared (the shortest recorded wave lengths were $2.5\text{-}2.0\mu\text{m}$). Band widths had expanded a level. Going through gradual expansion and improvement, current international standard regulation broad band recording was created. The shortest recorded wave lengths are $1.5\mu\text{m}$. At tape speeds under 3.04m/s , recording band widths reached 2MHz [2]. In this period of time, magnetic head technology provided the technological foundation and prerequisite for this progress. At the earliest stage, through opting for the use of improved Fe-Ni system alloys and photoetched chips as well as lamination technologies associated with uniform insulation layers, recorded wave lengths were made, with difficulty, to shrink to $2.5\mu\text{m}$. Recording band widths reached ultimate limit frequencies of 1.25MHz . Ferrite magnetic heads developed in the early 1970's and composite magnetic heads made up of ferrite magnetic cores and iron, silicon, and aluminum (Alfesil) pole tips finally realized capabilities associated with current broad band recording.

As far as predetection Chinese recording of telemetry data is concerned, development was promoted of broad band surface magnetic recording equipment as a main attack on technological difficulties associated with recording/reampification magnetic heads. In order to improve high frequency recording capabilities, magnetic head materials, as well as their working methods, it is necessary not only to be able to provide the magnetic properties and physical properties needed in recording/reampification but also to be able to manufacture precision narrow and shallow magnetic head operating slits. Moreover, it must still be possible to maintain permissible magnetic head life. In order for 14 channel/inch broad band magnetic heads associated with YJ21-1 and YJ2-4 magnetic recorder sets to break out of the forms of traditional installed type metallic laminated magnetic heads, option is made for the use of technologies associated with domestically produced high performance hot pressed MnZn ferrite material, magnetic head stack pole tips

and magnetic cores respectively formed as complete wholes and later glued together into structures, vacuum inlaid chromium film slits, as well as a set of simultaneously produced magnetic head pile pole tips and inlaid chromium slits. This type of new generation of magnetic heads--at tape speeds under 3.04m/s--record/reamply band widths reaching 2MHz. As far as this type of design method and manufacturing technology is concerned, successful applications have already been achieved in the development of magnetic heads associated with multiple types of recording device sets.

2 MAGNETIC HEAD DESIGN

Ferrite magnetic head designs should, on the basis of devices as a whole, carry out magnetic path design and relevant parameter calculations or estimates with regard to magnetic head requirements, selecting appropriate magnetic path materials. Going through testing, final adjustments and precise determinations are made of relevant magnetic head parameters. This section describes basic design procedures and methods. Realization problems associated with magnetic head pile performance as a whole will be described in the technological methods in the sections that follow.

2.1 Overall Requirements for Magnetic Heads

As far as broad band magnetic recorders are concerned, option is made for the use of magnetic bias recording. The magnetic biasing frequency is 8MHz. It requires that magnetic heads possess technical properties associated with the 14 channel/inch international broadband standard and the IRIG broad band II standard. The main requirements are that, under conditions where use is made of Ampex 797 or Scotch 892 magnetic tapes--when tape speed is 3.04m/s--it is possible to realize direct recording (DR) 400Hz-2MHz and frequency modulation recording (FM))-500kHz. With seven tape speed settings from 3.04m/s-0.047m/s, direct recording signal to noise ratios (S/N) > 24dB and frequency

modulation signal to noise ratios > 30dB.

2.2 Magnetic Head Requirements with Regard to Ferrite Materials

With regard to the selection of ferrite magnetic path materials, consideration should primarily be given to requirements in four areas. First, within operating frequency bands, magnetic permeabilities need to be high. Speaking in terms of reamplification, original magnetic permeabilities μ_0 must be high. This is to improve the important parameter of magnetic head sensitivity. Second, saturation magnetic flux density B_s must be adequately high. This is advantageous to the establishment of strong magnetic recording fields and high magnetic recording field gradients. Third, holding coercive forces must be small. This is advantageous to reducing magnetic head residual magnetism--guaranteeing small harmonic wave distortions. Fourth, material crystal grain sizes are uniform (average grain diameters appropriate). Gas porosity is low. Working properties are good (cut and ground grains to not fall off easily). After moving the tape, grains are not easily pulled out. Porosity is not easily expanded.

The primary properties associated with domestically produced MnZn ferrite materials are as follows. Original magnetic permeability $\mu_0 > 7000$. At frequencies under 20kHz, saturation magnetic flux density $B_s > 4000$ Gs. Constraining holding forces $H_c < 0.0550$ e. Average crystal grain diameter $d \approx 20-30\mu\text{m}$. Porosity p < 0.5%.

2.3 Magnetic Path Design

Magnetic path design should take as a principle increasing as much as possible the ratio between the overall magnetic reluctance associated with magnetic paths and the magnetic reluctance accounted for by operating slits in magnetic paths. To this end, consideration should be given to the three points below. One is that, in situations where the amount of winding and nature of the winding are convenient and permissible, the length of magnetic

paths are shortened as much as possible. Second is that, under a presupposition that requirements associated with the shortest recording wave lengths for recording and amplification are satisfied, operating slits must be wide. Under a presupposition that permissible lives will be satisfied, operating slit depths must be shallow (of course, recording heads must also prevent pole tip saturation). Third is that operating slot materials should be advantageous for raising the magnetic reluctance.

As far as the design of parameters relevant to magnetic heads is concerned, it normally gives consideration to compromises and combinations on the basis of experience. However, generally speaking, recording head parameter design is comparatively complicated. Reamplification heads are relatively easy.

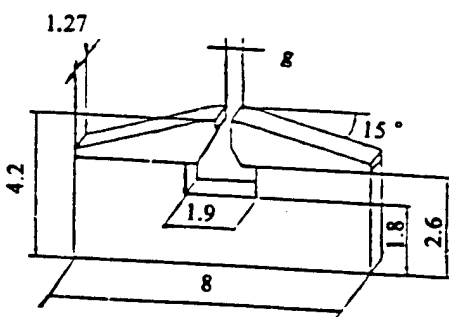


Fig.1 Magnetic Path Structure and Geometrical Dimensions

Due to the working technologies, ferrite magnetic heads are different from traditional metal magnetic heads. The magnetic path structure is then also different. Fig.1 is the magnetic path structure and geometrical dimensions associated with 14 channel/inch (double row) broad band magnetic heads. It is the result of considered compromises to design parameters relevant to magnetic heads.

As is widely known, with regard to analog recording, as far as certain signals on magnetic tape where the recording wave length is λ are concerned, the maximum point associated with reamplification

output corresponds to the reamplification head slot width $g_f = \lambda/2$. As a result, in order to effectively reamplify signals associated with minimally short recording wave lengths λ_{min} , reamplification slot widths are generally selected in accordance with $g_f/\lambda_{min} = 1/2$. Recording head slot width g_1 is generally selected as 3 to 5 times g_f .

With regard to currently effective international broad band recording standards and regulations, recording head slot widths g_1 are $(2.16 \pm 0.5)\mu m$. Minimally short recording wave lengths $\lambda_{min} = 1.5\mu m$, that is, reamplification head slot width g_f should be $0.75\mu m$. At this time, all references are to physical width. The magnetic head design in question selects $g_1 = 2\mu m$ and $g_f = 0.7\mu m$ (these are geometrical widths in both cases).

3 MAGNETIC HEAD STRUCTURE AND TECHNICAL METHODS

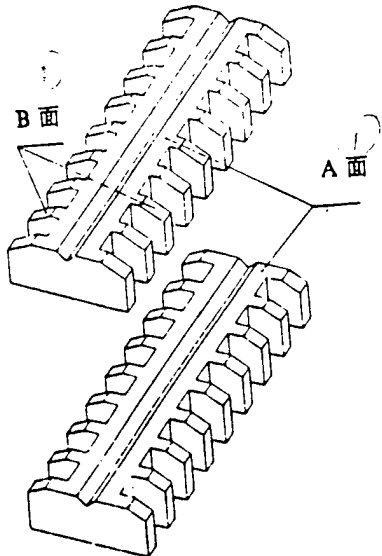
With regard to broad band magnetic heads, as far as the complete magnetic path associated with a magnetic head stack is concerned, the degree of slot dispersion must not exceed $2.54\mu m$ [3]. Magnetic head slot depth is approximately $30-50\mu m$. These points present stringent requirements associated with the uniformity of the width and depth of slots for the full magnetic path of a magnetic head stack. They also then determine the slots associated with full magnetic paths which magnetic head structures and technical methods must simultaneously form from a magnetic head stack. In conjunction with this, in terms of space, the consistency of slot width and depth is guaranteed.

The magnetic heads in question are composed of U shaped iron core parts and pole tip parts. U shaped iron core parts include U shaped iron core windings associated with complete magnetic paths. Pole tip parts include full magnetic path pole tips for which slots have already been formed.

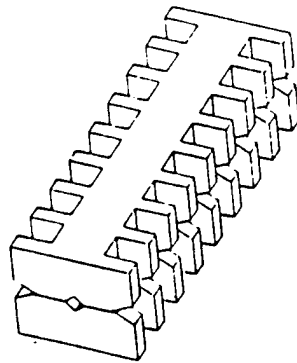
/53

3.1 Techniques Associated with the Forming of Integrated Magnetic Head Stack Pole Tips

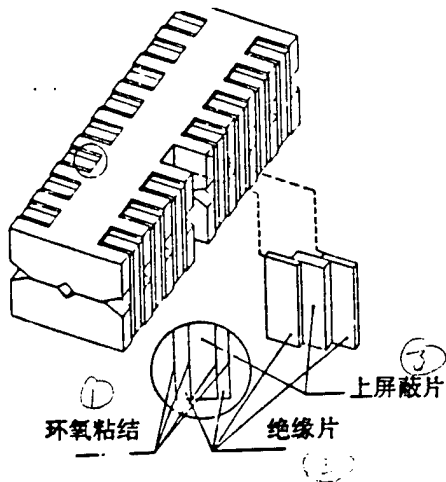
The main technical processes associated with the forming of an integrated magnetic stack of pole tips are as shown in Fig.2. They include such procedural steps as forming and slotting, grinding and polishing, vacuum plating of chromium film, gluing together to form slots, and so on. In situations where magnetic path densities are high, it is also possible to opt for the use of methods that glue chromium slits first and slot afterwards. A surface unevenness and brightness influences the uniformity of magnetic head slot widths and the clarity of the sides of slits. B surface unevenness determines the uniformity of slot depth.



(a) Forming, Slotting, Grinding, Plating Chromium Film (1)
Surface

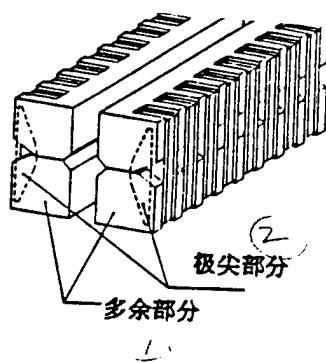


(b) Alignment of Slot Combination Surfaces



(c) Pressing, Epoxy Gluing

Key: (1) Epoxy Adhesive (2) Insulation Plates (3) Upper Shield Plate



(d) Working and Cutting Spares

Key: (1) Extra Parts (2) Pole Tip Parts

Fig. 2 Techniques for the Formation of Integrated Magnetic Head Stack Pole Tips

As far as the releasing of internal stresses associated with hot pressed MnZn ferrite and working stresses produced by cutting, grinding, and polishing are concerned, it is easy to produce deformations on combined slot surfaces, having influences on the quality of the slots. With regard to the magnetic heads in question, as far as methods breaking out of traditional domestic and foreign methods associated first with vitreous welding becoming glass or chromium slots are concerned, option is made for the use of technology associated with epoxy resin gluing to form chromium slots, making the rate of product creation associated with slot formation operational sequences very, very greatly increase. Moreover, due to reductions in stresses associated with pole tips in areas under magnetic head slots, the electromagnetic conversion properties achieve improvements. If, in certain situations, it is necessary to make slots with vitreous welding, then, particular attention should be paid to the elimination of stresses in materials as well as working stresses to prevent slot combination surfaces from deforming, leading to the scraping of slots formed in work sequences.

Upper shielding plates and insulation plates are associated with the pulling tightly together of two half pole tips, forming connected slot modules. Their heat expansion coefficients and abrasion properties must be close to those of pole tip materials. Therefore, option is made for the use in upper shielding plates of the same material as in pole tips. Insulation plates opt for the use of a type of optical glass. The optical glass in question is capable, within a very large temperature range, of maintaining a good match with hot pressed MnZn ferrite materials. Moreover, abrasion properties are close.

3.2 Vacuum Plated Chromium Film Slots

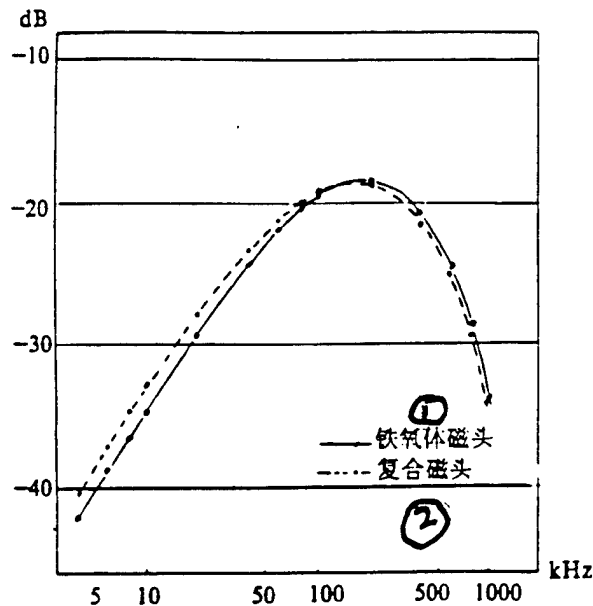
The magnetic heads in question opt for the use of slot combination surface vacuum plated chromium films (the thickness of the chromium film is determined by the width of the slot). Two pole tips glued together form a complete chromium slot, improving

slot quality and increasing magnetic head recording/reampification performance. Below, an analysis will be made of this.

4 MEASUREMENT RESULTS AND ANALYSIS

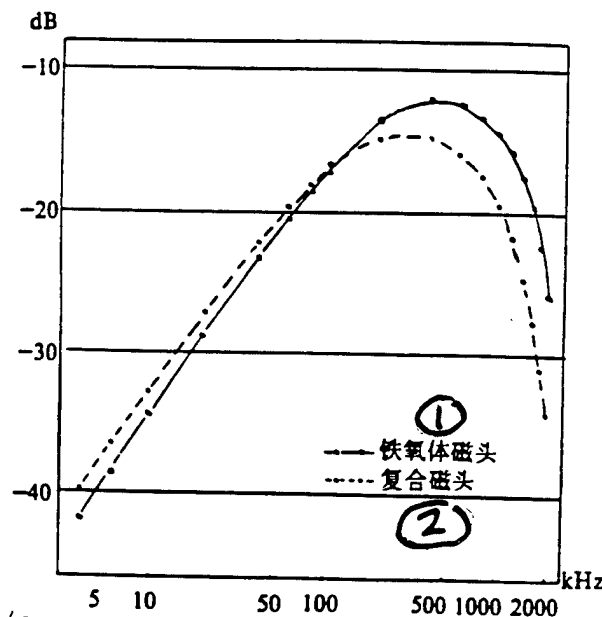
4.1 Recording/Reamplification Characteristics and Overall Signal to Noise Ratios

Fig.3 is typical recording/reampification characteristic curves. It shows that, in high frequency bands, ferrite magnetic heads possess high recording/reampification sensitivities. As far as an explanation of use is concerned, ferrite material properties have very great influences on overall signal to noise ratios. Using domestically produced magnetic recording and reampification heads made with hot pressed MnZn ferrite, it is possible to obtain comparatively high overall signal to noise ratios. At seven tape speed settings, direct recording $S/N > 24\text{dB}$. Frequency modulation recording has $S/N > 30\text{dB}$. Overall performance reaches the same type of product level as abroad. With regard to ferrite materials with comparatively bad performance, at low tape speeds, overall signal to noise ratios are relatively low.



(a) Tape Speed 1.52m/s

Key: (1) Ferrite Magnetic Heads (2) Composite Magnetic Heads



(b) Tape Speed 3.04m/s

Key: (1) Ferrite Magnetic Heads (2) Composite Magnetic Heads

Fig.3 Ferrite Magnetic Head and Composite Magnetic Head Recording/Reamplification Characteristic Curves

4.2 Saturation Problems which Do Not Appear in Recording Heads. Results of use clearly show that saturation problems do not appear with this design of recording head. When use is made of Ampex 721 magnetic tape ($H_{illegible} = 700$ Oe, $\delta = 5\mu m$), saturation still did not appear. However, during the designing of ferrite magnetic heads, the possibility of recording head saturation is a problem which must be considered.

Empirical data clearly show that media coercive holding forces H_c associated with the use of ferrite magnetic heads are, at a maximum, approximtely equal to $B_s/8$ [3]. As a result, in order to appropriately develop media with even higher coercive holding forces, development was done of composite magnetic heads composed of ferrite magnetic cores and retentive alloy in order to fully bring into play the excellent high frequency characteristics of ferrite as well as the high B_s associated with alloy materials. In conjunction with this, there is the advantage of easily forming clear slots. The recording/reampification characteristic curves in Fig.3 clearly show that, at tape speed of 1.52m/s, composite heads possess comparatively high band pass signal to noise ratios. At tape speed of 3.04m/s, composite heads in low frequency bands clearly demonstrate advantages. Ferrite heads in high frequency bands possess clear advantages. If thought is given to improving composite head high frequency band performance, it is necessary to develop laminated pole tip composite heads.

In order to coordinate media associated with $H_c = 700-1000$ Oe--following along with the development of 8mm VCR and R-DAT--from the middle of the 1980's there began to appear a type of MIG magnetic head. It is a development associated with composite magnetic heads. Normally, it is two pole plate surfaces on MnZn ferrite magnetic heads sprayed respectively with a layer of 1-2 μm iron, silicon, and aluminum (Alfesil). The B_s associated with hard

alloy materials can reach 12 500 Gs. As a result, it is possible to record on $H_c = 2$ 500 Oe media, and pole tips will not saturate [4].

4.3 Bias Current and Recording Current

The slot depth associated with practical recording heads is 45-50 μ m. Average bias current is 15mA. Average recording current is 1.5mA (1/10th of the bias current). When recording head slot depths increase, bias and recording current values follow them and increase.

4.4 Cross Talk Between Channels

Recording head static tests clearly show that, at frequencies within 2MHz, cross talk attenuations of -40dB or less satisfy overall requirements.

4.5 Chromium Slot and Glass Slot Performance Comparison

Fig.4 clearly shows that: (1) Due to glass permeability, glass slots have been expanded. That is, the physical widths associated with glass slots are somewhat larger than the physical widths of chromium slots. (2) As far as chromium slot recording heads and reamplification heads are concerned, performance in all cases is better than glass slot magnetic heads. In conjunction with this, following along with a shortening of recording wave lengths, this becomes even more clear.

Test measurement results clearly show that, after recording and reamplification curves with tape speeds of 0.0047m/s are all evaluated, chromium slot recording heads have band pass signal to noise ratios that are 5dB higher than glass slot recording heads. Chromium slot reamplification heads are 6dB higher than glass slot reamplification heads.

Analysis confirms that there are primarily two causes. One is that the slot edge clarity of chromium slots is better than glass slots. Second is that because, when glass contracts, creating stresses in slot areas, it lowers the magnetic properties of this

area. As far as these two causes are concerned--speaking in terms of recording heads--gradients associated with recording magnetic fields are lowered. Speaking in terms of reamplification, reamplification sensitivities are lowered. If option is made for the use of high strength welded glass, which is better matched to the same physical properties as ferrite material, this difference will be reduced.

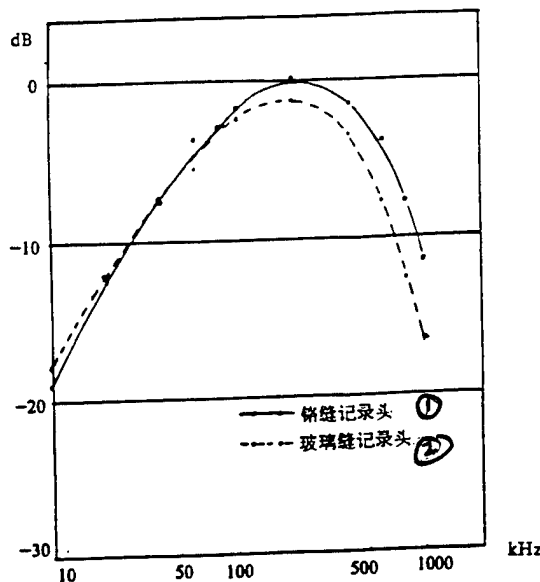
4.6 Magnetic Head Slot Stability Tests

After magnetic heads are held at a constant temperature of 60°C for 5h, slots are well maintained. Going through actual use, the stability associated with chromium slots formed by epoxy gluing techniques in the magnetic heads in question is comparable to chromium slots formed by vitreous welding techniques. No difference was seen.

5 CONCLUSIONS

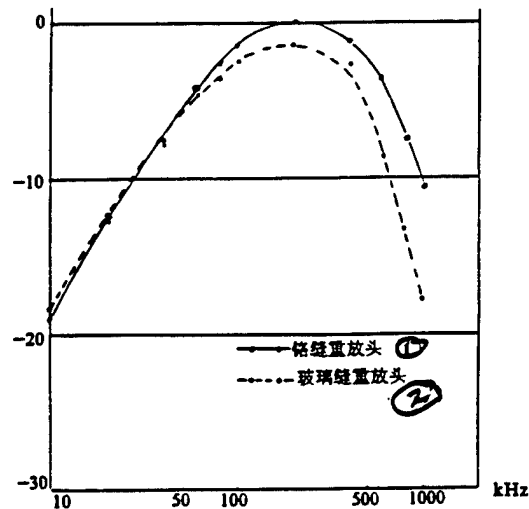
1. This article supplies design methods and manufacturing techniques associated with ferrite magnetic heads through practical realization and experience. Development of ferrite magnetic heads has been successful. High frequency, short wave length recording capabilities have been improved overall. Band widths have been expanded a level, making Chinese magnetic recording technology reach a new level.

/56



(a) Identical Chromium Slot Reamplification Head, Chromium Slot and Glass Slot Recording Heads

Key: (1) Chromium Slot Recording Head (2) Glass Slot Recording Head



(b) Identical Chromium Slot Recording Head, Chromium Slot and Glass Slot Reamplification Heads

Key: (1) Chromium Slot Reamplification Head (2) Glass Slot Reamplification Head

Fig.4 Comparison of Recording and Amplification Properties of Chromium Slot and Glass Slot Magnetic Heads With the Same Geometrical Width (Tape Speed 1.52m/s)

2. Processes associated with the development and use of the magnetic heads in question clearly show that the quality of ferrite magnetic head technology performance has very great reliability with regard to materials performance. If it is desired to think about creating high performance magnetic heads, it is necessary to have high saturation magnetic densities associated with stable performance, low coercive holding forces, high original magnetic permeability, and to possess the good physical properties of ferrite materials.

3. If it is desired to develop magnetic heads that record on media which are suited to $H_c = 700-1000$ Oe, it is necessary to make use of composite heads composed of ferrite magnetic cores and hard alloy (high B_s) pole tip combinations. With low tape speeds, composite heads composed of ferrite cores and complete pole tip modules associated with iron, silicon, and aluminum alloy (Alfesil) possess high band pass signal to noise ratios. If one wishes to improve high frequency performance associated with composite heads, it is necessary to develop composite heads associated with hard alloy laminated pole tips.

If the development of MIG magnetic heads is successful, it can be expected that they will replace ferrite magnetic heads and composite magnetic heads.

REFERENCES

- 1 IRIG 106. 1976.
- 2 IRIG 106. 1986.
- 3 Jeffers F. High-density magnetic recording heads. IEEE, 1986, 74(11).
- 4 Mallinson J C. Achievements in rotary head magnetic recording. IEEE, 1990, 78(6).

CONNECTION DEVICES USED IN SATELLITE ROCKET SEPARATION

Feng Zhenxing

Translation of "Yong Yu Xing Jian Fen Li De Lian Jie Qi"; Missiles and Space Vehicles, Overall No. 213, No.1, 1995, p 57

The U.S. Orbital Science company selected for use the G&H technological manufacturing company limited's model 876 push/pull separable connector device to act as a one time use, low cost satellite rocket separation connector component for satellites borne on Centaur and Taurus carrier rockets. The reason this type of connector device was selected for use is because it possesses reliable connection and disengagement performance during carrier rocket and missile flight stage separation. The carrier vehicle engineer of the company in question, K.Eberly, actually made this type of explanation: "The reason we made the applications we did was because after signals going through connector devices are transmitted to the aerodynamic cowlings, the connector device then separates under control, and the aerodynamic cowlings rotate and separate into two halves. Normally, the connector devices which are utilized are not like this, but during tests, they were not able to carry out separation very well. 876 model connector devices operated very well."

After the connector devices in question are inserted into locking sleeves, it is only necessary to use 53-106N, and it is then possible to pull them out of locking sleeves or release them from connector cables. This relies on plugging pin type insertion locks into bases, taking connector components and firmly meshing

them together with insertion bases and insertion pieces. It is only necessary to insert connector devices, and there is then no need to use external forces to make them mate up.

In order to eliminate unintentional separation, the designed fall away force envelope associated with the connector devices in question is very narrow. Besides that, on plug casing bodies there is an angled slot. This slot can prevent overly tight interconnection. Moreover, it is also capable of preventing falling away when subjected to lateral forces. One very key point associated with the designs is that they are capable of preventing bad match ups. They always have a colored band attached to clearly show that their match up status is normal.

The connector devices in question carried out 6.2kg impact tests, 40g vibration tests, -54 -- +71°C temperature alternation tests, endurance tests associated with 250 iterations of high speed temperature cycling and 250 iterations of normal speed high and low temperature cycling. They were also subjected to 1300V, current rms dielectric breakdown tests, as well as 500V, 100000MΩ direct current insulation resistance tests.

SIMILARITY CRITERIA OF INTERIOR BALLISTICS
IN LAUNCH CANISTER

Shao Yang

Translation of "Fa She Tong Nei Dan Dao De Xiang Si Zhun Ze";
Missiles and Space Vehicles, Overall No.213, No.1, 1995

ABSTRACT This article discusses criteria similarities associated with simulating launch canister interior ballistics parameters for two types of scale models. Similarity criteria which should be followed by these two types of models are respectively derived. In conjunction with this, comparisons are made of the various types of characteristics. Explanations are made of the reasons for the ability of test results obtained from them being able to predict full prototype interior ballistics parameters. When similarity criteria are derived, in general, option is made for the use of a conversion from four dimensions to three dimensions--that is, taking temperature units K or °C and changing them into m^2/s^2 . Derivation processes for simulation criteria are thus very, very greatly simplified.

KEY WORDS Interior trajectory calculation *Launch canister Analog simulation

I. INTRODUCTION

At the present time, as far as the resolution of a good number of large model engineering technology problems is concerned, they all have not left scientific experimental research. Experimentation is one of the most basic and most important means

for discovering objective principles. It is an important foundation for judging whether or not determinations of the regularity of things are accurate. Due to limitations associated with economic and technological conditions, use is made of actual prototypes to carry out experiments. In conjunction with this, discovering problems in them and then carrying out alterations is not acceptable. As a result, modeling research in engineering designs is then extremely important.

As far as launch canister ballistic missiles are concerned--also called cold launch technology--their development began outside China in the 1950's. Up to now, they have already become the most important type of strategic weapons launch technology. Just like artillery shells fired from guns, precise determination of interior trajectory parameters is a key problem which needs to be resolved in the design of these weapons. In the development stage of launch cannisters, in order to understand whether or not a number of interior ballistics parameters which are not capable of experimental verification using 1:1 satisfy overall design requirements--for instance, operating principles associated with propulsion systems, charge properties, maximum temperatures and pressures for combustion gases inside launch canisters, maximum overloads missiles are subjected to in movements within launch cannisters, as well as speeds at which missiles leave canisters, and so on--the use of scale model tests is, as a result, put forward in order to verify design plans. The designs of scale models are guided by similar theories. This article carries out derivations of similar criteria associated with two possible types of scale models with regard to modeling principles. In conjunction with this, comparisons of various characteristic points are made. The explanation for this is that the results of tests they are used to carry out are capable of forecasting complete interior ballistics parameters.

2 FORMULATIONS ASSOCIATED WITH LAUNCH CANISTER MISSILE INTERIOR
BALLISTICS MODELING PROBLEMS

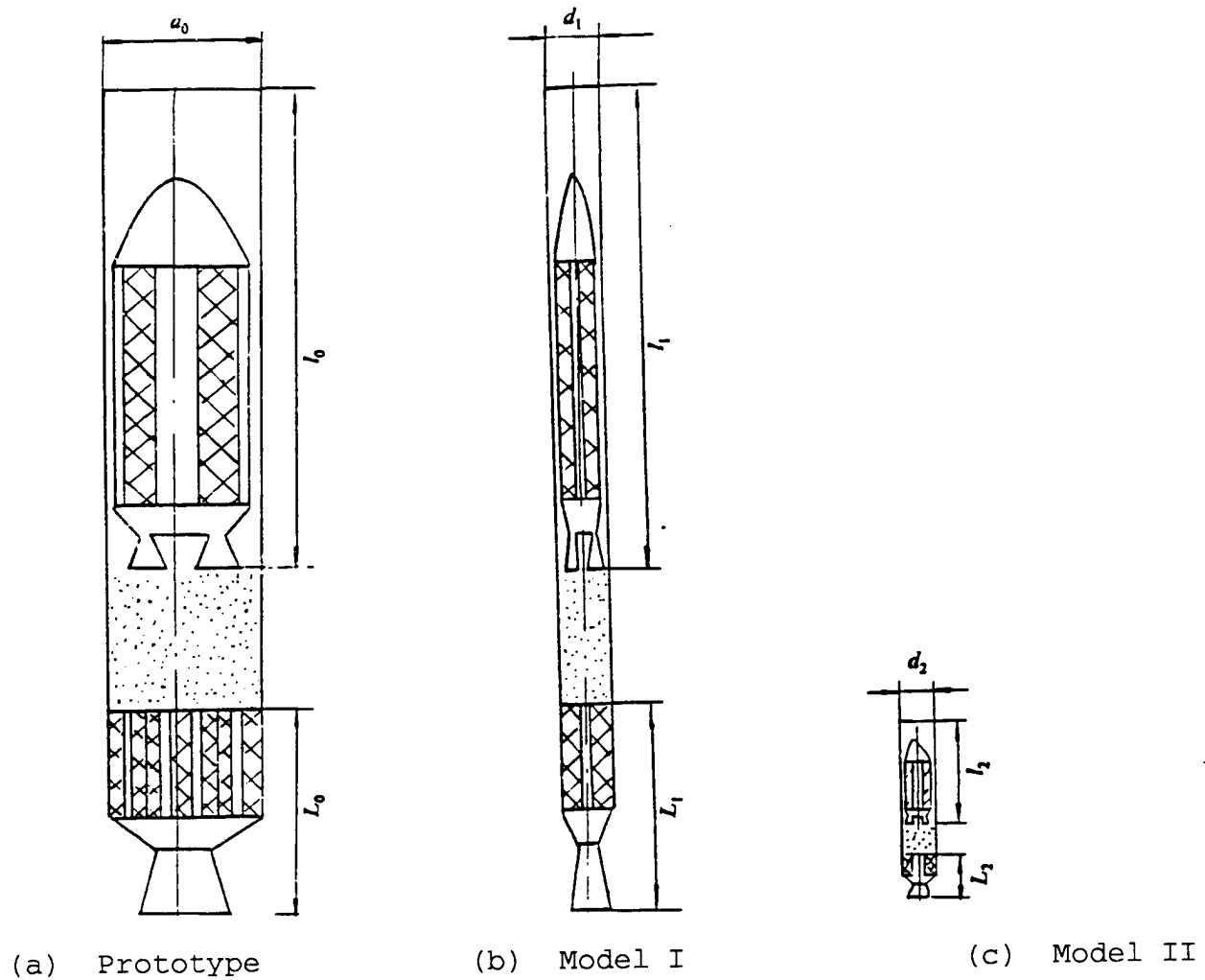


Fig.1 Launch Canister System Models

/60

Assuming that the developed launch canister system prototypes are as shown in Fig.1(a), they are composed of launch canisters, missiles, and propulsion systems. Due to the fact that prototypes are very complicated and enormous propulsion systems--in order to

assure the reliability of their interior ballistic performance parameter designs--during development processes, it is necessary to carry out scale model tests. In scale models--under the presumption that similarity criteria are obeyed--it is possible to have multiple types of physical modeling designs. The most commonly used and also the most typical designs are the two types of design plans shown in Fig.'s 1(b) and 1(c). Among these, one type is the geometrically dissimilar model (see Fig.1(b)). This is also designated Model I. The other model is a geometrically similar model (see Fig.1(c)). This is also designated Model II. Speaking in terms of theory and practice, these two types of design plans are both capable of realization. That is, it is possible to make use of Fig.1(b) or Fig.1(c) model tests to predict the internal ballistic performance parameters for the prototype shown in Fig.1(a). Moreover, both these types of models have been reported in materials outside China.

2.1 Characteristics of Model I

From Fig.1(b), one knows that, comparing Model I and Model II, the axial dimensions are equal. Only the lateral dimensions are shortened. Under conditions where models and prototypes opt for the use of the same types of charges and coolants, all interior ballistic parameters measured from Model I tests will be equal to corresponding interior ballistic parameters of the prototype--that is, the ratio of the two systems is 1:1. It is possible to see that interior ballistic parameters measured from this type of model intuitively reflect prototype performance. Charge columns used in model testing can be used in prototypes, very, very greatly simplifying the manufacturing technologies associated with charges. However, in geometrical terms, the models in question are not similar or are so called singular similarities. There are two geometrical ratio dimensions: $C_l = l_o/l_1$ and $C_d = d_o/d_1$. For this reason, model test results can give rise to a certain error. If well grasped, errors can be reduced to the greatest extent possible.

In order to guarantee Model I test results and prototypes

being completely equal, it is necessary to observe some sort of similarity criterion. This is the core of what this article will study.

2.2 Characteristics of Model II

The forms of curves associated with complete interior ballistics performance parameters measured by Model II tests are fully similar to prototypes. However, in all cases, they will form a proportional reduction, that is, the various interior ballistics parameter curves will be taken and multiplied by a proportionality coefficient after which it will only then be possible for corresponding prototype curves to overlap. Obviously, test results for the model in question are worse for direct observation characteristics than Model I. Moreover, charge columns opted for the use of in tests are not the same as prototypes. However, in geometrical terms, the model in question is similar. Proportionality coefficients associated with geometrical dimensions are common. That is,

$$K_1 = K_d = \frac{l}{l_2} = \frac{d}{d_2}$$

Relative errors are smaller than for Model I. Moreover, proportionality coefficient K_1 can be selected arbitrarily, thereby making the material consumed in models very, very greatly reduce.

3 DERIVATION OF LAUNCH CANISTER INTERIOR BALLISTICS SIMILARITY CRITERIA

3.1 The Three Theorems of Similarity

(1) As far as systems which are similar to each other are concerned, they should possess the same similarity criteria. This is called the first similarity theorem. This was first put forward by Newton.

(2) With respect to a form describing the various physical quantities associated with a phenomenon, it is possible to

transform it into an equation composed of similarity criteria. What is called the second similarity criteria theorem or π theorem was set up by Buckingham.

(3) The necessary and sufficient conditions associated with phenomena similarity are monodromatic similarity conditions for the two. Moreover, the similarity criteria composed of physical quantities associated with monodromatic conditions are equal. This is called the third similarity theorem. /61

From the similarity theorems discussed above, one knows that, if it is desired to evaluate the similarity of two phenomena, the key is nothing else than determining similarity criteria. In general, there are two methods to precisely determine similarity criteria--that is, the equation analysis method which uses similarity theory as its foundation and the dimensional analysis method which uses the π theorem as its basis.

3.2 Similarity Theory and Dimensional Analysis

Similarity theory starts out from equations associated with the description of phenomena and derives from them several nondimensional quantities. Explanations of the similarity of physical phenomena given rise to in two systems are called similarity criteria. However, in actual engineering, this type of situation is often met with. With regard to the interior of dominant physical phenomena, understanding of regularities in changes associated with various physical quantities is not clear. As a result, differential equations cannot be written, or phenomena are complicated and equations are excessively numerous. For instance, there are several tens of launch canister interior ballistics control equations. Using similarity theory equation analysis methods is too complicated. As a result, in actual engineering, option is mostly made for the use of dimensional analysis methods. In dimensional analysis methods, there is no need to write out differential equations. It is only necessary to know the phenomenon and which factors are relevant. It is then possible to derive similarity criteria. Besides this, when

similarity criteria are derived by equation analysis methods, there is a need to choose in accordance with the dynamics similarity conditions associated with the two systems. Otherwise, similarity criteria which are derived are then without any value. Moreover, only ones based on dimensional analysis need not consider the physical significance of the physical quantities related to the described phenomena when constructing similarity criteria. However, in dimensional analysis, it is necessary to select with complete accuracy all the physical quantities participating in the phenomenon. Otherwise, erroneous conclusions will be derived. Although dimensional analysis is capable of application in all phenomena, there is no need to set up equations. However, the method in question contains dangers associated with erroneous conclusions or erroneous starting points. This type of error phenomena can be often seen in the literature inside China and abroad.

The primary content of dimensional analysis is nothing else than the π theorem. It was created by Buckingham. Its meaning is that a general functional relationship associated with the description of a certain phenomenon constructed from n physical quantities can certainly be transformed into a general dimensionless functional relationship composed of $n-m$ independent dimensionless parameters. Here, m equals the basic number of dimensions involved.

3.3 Precise Determinations of Independent Physical Quantities

As was described above, when option is made for the use of dimensional analysis methods, there is a need to select with complete accuracy all physical quantities related to the phenomena being studied. If selections are incorrect, it will lead to errors. For this reason, we take the physical quantities related to phenomena produced in the air behind launch canister missiles, combustion gas generators, and water chambers and list them one by one. In all, there are the 13 types below.

- (1) The dynamic viscosity coefficient μ associated with such

gases as combustion gases, steam, and water composing the dynamic operating medium in air behind launch canister missiles, and so on;

(2) Combustion gas generator charge density ρ_p , combustion gas density ρ_r , and mixture density of combustion gas air behind missiles and steam ρ_{CM} ;

(3) Missile acceleration motions a inside launch canisters and the acceleration of a free falling body g;

(4) Charge burn speed u, combustion gas flow speed u_1 , operating medium flow speed in air behind missiles u_2 , missile motion speed inside launch canisters v;

(5) Charge combustion time t_o and missile motion time t;

(6) Propellant mass m_p , water mass m_w , and missile mass m;

(7) Charge column length l_1 , combustion chamber length l_2 , missile travel l_3 ;

(8) Propellant combustion surface area S, various levels of jet throat area S_{KP1} and S_{KP2} , as well as water chamber spray hole area S_{KP3} ;

(9) Combustion chamber volume V_r , water chamber volume V_w , and air volume behind missiles V_3 ;

(10) Ignition pressure P_{ig} , combustion gas pressure P_1 , water chamber pressure P_2 , and operating medium pressure in air behind missiles P_3 ;

(11) Constant pressure propellant combustion temperature T_o ; combustion gas temperature T_1 , water chamber temperature T_2 , and operating medium temperature in air behind missiles T_3 ;

(12) Charge column diameter d_1 , combustion chamber diameter d_r , water chamber diameter d_w , launch canister diameter d_3 , and missile diameter d;

(13) Combustion gas, steam, and air gas constants R_r , R_w , and R_k as well as K_r , K_w , and K_k .

/62

3.4 Changing Four Dimensional Factors into Three Dimensional Factors

Among all the physical quantities set out below, the

measurement units can be expressed as four types of basic units. In the SI unit system, these four basic units are mass (kg), length (m), time (s), and temperature (K or °C). Moreover, the factor associated with any one physical quantity can be expressed through use of the general factor formula below:

$$[Y] = L^a M^b t^c T^d \quad (1)$$

In the equation, L, M, t, and T, respectively, stand for the factors of length, mass, time, and temperature. a, b, c, and d are any rational numbers.

Equation (1) is then the four dimensional factor normally opted for the use of in similarity theory references. According to the opinions of the internationally renowned engineer and thermal physicist of the former Soviet Union Kutajielaze (phonetic) (

1), motion and space-time are universal forms of material existence. As a result, the physical quantities will not exceed three. That is, equation (1) can be transformed into a three dimensional one.

$$[Y] = L^a M^b t^c \quad (2)$$

In this, the unit of temperature T (K or °C) can go through relevant physical equations and be transformed into quantities expressed by the use of 3 basic units. In this article, the unit of measure for temperature is m^2/s^2 . In this way, it is possible to very, very greatly simplify similarity criteria deduction processes.

3.5 Similarity Criteria Solution Methods

As far as all of the 13 types of physical quantities selected above are concerned, each type of dimension is the same. For this reason, any one among them is selected to be the algebraic symbol for the type in question and is set out in Table 1. Among these, with regard to the gas constants R_r , R_w , R_k --because, when deducing

temperature unit T, it is defined as being a dimensionless coefficient, and the entropy indices K_r , K_w , K_k are basically dimensionless constants--their similarity constants, that is, they themselves, are, therefore, not entered into the table.

There are many types of methods for solving for the combination of dimensionless factors associated with the various physical quantities in Table 1--the values π_1 . Two types of methods are given here--power order equation methods and dimension matrix methods. In accordance with the π theorem, any three physical quantities which are adopted at random out of Table 1 with

Table 1 Physical Quantities in Phenomena and Their Dimensions

(1) 序号	(2) 现象中出现的物理量	(3) 所选代表符号	(4) 质量 M	(5) 长度 L	(6) 时间 t
1	μ	μ	1	-1	-1
2	$\rho_p, \rho_r, \rho_{CM}$	ρ	1	-3	0
3	a, g	g	0	1	-2
4	u, u_1, u_2, v	v	0	1	-1
5	t_0, t	t	0	0	1
6	m_p, m_w, m	m	1	0	0
7	l_1, l_2, l_3	l	0	1	0
8	$S, S_{KP1}, S_{KP2}, S_{KP3}$	S	0	2	0
9	V_r, V_w, V_3	V	0	3	0
10	P_{ik}, P_1, P_2, P_3	P	1	-1	-2
11	T_0, T_1, T_2, T_3	T	0	2	-2
12	d_1, d_r, d_w, d_3, d	d	0	1	0

Key: (1) Sequence No. (2) Physical Quantities Appearing in Phenomena (3) Selected Algebraic Symbol (4) Mass (5) Length (6) Time

their dimensions independent of each other are basic physical quantities. For example, choose P, T, and d in the last three lines of Table 1. In order to solve for the dimensionless product associated with the first line viscosity μ in Table 1, one writes out the power order equation below.

$$\pi_1 = (ML^{-1}t^{-2})^a(L^2t^{-1})^b(L)^c(ML^{-1}t^{-1})^d = M^0 L^0 t^0$$

Solving

$$a = -1, b = \frac{1}{2}, c = -1$$

Therefore

$$\pi_1 = \frac{\mu\sqrt{T}}{Pl} \quad \dots \quad (3a)$$

On this basis, respective solutions are made for π values corresponding to various quantities associated with the left column sequence numbers of Table 1 as follows.

$$\begin{aligned} \pi_2 &= \frac{\rho T}{P}, \quad \pi_3 = \frac{g l}{T}, \quad \pi_4 = \frac{v}{\sqrt{T}}, \quad \pi_5 = t\sqrt{T}/l, \quad \pi_6 = \frac{m l}{Pl^3}, \\ \pi_7 &= \frac{l}{d}, \quad \pi_8 = \frac{s}{d^2}, \quad \pi_9 = \frac{v}{d^3} \end{aligned} \quad (3b)$$

Now we make use of dimension matrix methods to solve for π_i . To this end, we take the various physical quantities of Table 1 and write them as the dimension matrix form below.

	1	2	3	4	5	6	7	8	9	10	11	12
	μ	ρ	g	v	t	m	l	s	V	P	T	d
M	1	1	0	0	0	1	0	0	0	1	0	0
L	-1	-3	1	1	0	0	1	2	3	-1	2	1
t	-1	0	-2	-1	1	0	0	0	0	-2	-2	0

We now come to calculate the order of the matrix in question. According to matrix theory, if the matrix in question contains an nth order determinant for which the value is not 0, its order is then equal to n. In the matrix in question, a third order

determinant is selected at random. For instance, the determinant constructed by the three lines and three columns at the right most.

$$\begin{vmatrix} 1 & 0 & 0 \\ -1 & 2 & 1 \\ -2 & -2 & 0 \end{vmatrix} = 2$$

From this, it is possible to see that the order of the dimension matrix in question is $r=3$. In systems possessing 12 physical quantities with dimensions, the dimensionless product is equal to the total number of physical quantities minus the order of the dimension matrix. That is, $12-3=9$ nondimensional combinations. In order to solve for these 9 π_i values, it is necessary to write a homogeneous linear algebraic equation set. The unknown coefficients are nothing else than corresponding numerical values in the dimension matrix lines above. The forms are as follows.

$$\begin{aligned} C_1 + C_2 + C_6 + C_{10} &= 0 \\ -C_1 - 3C_2 + C_3 + C_4 + C_7 + 2C_8 + 3C_9 - C_{10} + 2C_{11} + C_{12} &= 0 \\ -C_1 - 2C_3 - C_4 + C_5 - 2C_{10} - 2C_{11} &= 0 \end{aligned}$$

From this, one gets

$$\begin{aligned} C_{10} &= -C_1 - C_2 - C_6 \\ C_{11} &= \frac{1}{2}C_1 + C_2 - C_3 - \frac{1}{2}C_4 + \frac{1}{2}C_5 + C_6 \\ C_{12} &= -C_1 + C_3 - C_5 - 3C_6 - C_7 - 2C_8 + 3C_9 \end{aligned}$$

In turn, the right sides of the equation sets in question are respectively assigned values. /64

$$C_{1-1} = 1, \quad C_{1+1} = 0 \dots \dots C_{1+4} = 1, \quad C_{1+9} = 0$$

Because of this, one obtains the forms of π_i which were being sought as follows.

	C_1	C_2	C_3	C_4	C_5	C_6	C_7	C_8	C_9	C_{10}	C_{11}	C_{12}
	μ	ρ	g	v	t	m	l	S	V	P	T	d
π_1	1	0	0	0	0	0	0	0	0	-1	$1/2$	-1
π_2	0	1	0	0	0	0	0	0	0	-1	1	0
π_3	0	0	1	0	0	0	0	0	0	0	-1	1
π_4	0	0	0	1	0	0	0	0	0	0	$-1/2$	0
π_5	0	0	0	0	1	0	0	0	0	0	$1/2$	-1
π_6	0	0	0	0	0	1	0	0	0	-1	1	-3
π_7	0	0	0	0	0	0	1	0	0	0	0	-1
π_8	0	0	0	0	0	0	0	1	0	0	0	-2
π_9	0	0	0	0	0	0	0	0	1	0	0	-3

From this dimension matrix, one obtains 9 mutually independent similarity criteria as follows.

$$\begin{aligned} \pi_1 &= \frac{\mu\sqrt{T}}{Pd}, \quad \pi_2 = \frac{\rho T}{P}, \quad \pi_3 = \frac{gd}{T}, \quad \pi_4 = \frac{v}{\sqrt{T}}, \\ \pi_5 &= \frac{t\sqrt{T}}{d}, \quad \pi_6 = \frac{mT}{Pd^3}, \quad \pi_7 = \frac{l}{d}, \quad \pi_8 = \frac{S}{d^2}, \quad \pi_9 = \frac{V}{d^3} \end{aligned} \quad (4)$$

From equation (4) and equation (3a) and (3b), one knows that π_i which are solved for by power order equation methods and dimension matrix methods are in entire agreement.

In accordance with the π theorem, π power orders, products, and reciprocals are still π . For this reason, the 9 π_i 's in equation (4) are recombined in order to obtain π values which are appropriate for use or universal. That is,

$$\begin{aligned}
\pi_1 &= \frac{\rho v l}{\mu} = Re, \quad \pi_2 = \frac{P}{\rho v^2} = En, \quad \pi_3 = \frac{v^2}{gl} = Fr, \quad \pi_4 = \frac{v}{\sqrt{KRT}} = Ma, \\
\pi_5 &= \frac{v l}{l} = Sh, \\
\pi_6 &= \frac{m v^2}{Fl} = Ne, \quad \pi_7 = \frac{l}{d}, \quad \pi_8 = \frac{S}{d^2}, \quad \pi_9 = \frac{V}{ld^2}
\end{aligned} \tag{5}$$

Among the 9 similarity criteria above, the first 6 are criteria associated with describing processes of flow performance. They are also criteria which are often applied in aerodynamics, fluid dynamics, and thermodynamics. They are, respectively, the Reynolds criteria Re describing dynamic viscosity similarity, the Euler criteria En describing pressure similarity, Fulefa criteria Fr describing energy similarity, Mach criteria Ma describing fluid compressibility, Sitelaohaer (phonetic) criteria Sh describing nonsteady effects, and Newton criteria Ne associated with dynamic similarity. Due to the fact that launch canister missile ballistics processes are combined applications of aerodynamics, fluid dynamics, and thermodynamics, as a result, in the scale models, these criteria should be observed. During different tests, these criteria above are not able to all be satisfied. For example, Fr and Re are normally not able to be satisfied at the same time. However, in Model I, in order to guarantee that such interior ballistic parameters as model and prototype speeds leaving canisters, and so on, are equal, it is necessary to require that Fr and Re be satisfied at the same time. In Model II, however, this is not necessary.

/65

4 SIMILARITY RATIOS FOR THE TWO SCALE MODELS

4.1 Model I Similarity Ratios

We now make use of equation (5) so as to prove that--with regard to Model I--in order to guarantee that model and prototype interior ballistics parameters correspond and are equal--it is necessary to maintain Fr and Re equal at the same time, thus

leading to the reason that the axial dimensions of Model I and prototypes must be 1:1.

In order to make model and prototype simultaneously observe similarity criteria, it requires that Fr and Re must satisfy

$$\pi_3 = Fr = \frac{v^2}{gl} = \text{idem}, \quad \pi_1 = Re = \frac{\rho l v}{\mu} = \text{idem} \quad \text{or} \quad (6)$$

$$Fr = \frac{v_1^2}{g_1 l_1} = \frac{v_0^2}{g_0 l_0} \quad (7)$$

$$Re = \frac{\rho_1 l_1 v_1}{\mu_1} = \frac{\rho_0 l_0 v_0}{\mu_0}$$

Let $C_l = \frac{l_0}{l_1}$, $C_v = \frac{v_0}{v_1}$, $C_g = \frac{g_0}{g_1}$, $C_\mu = \frac{\mu_0}{\mu_1}$, $C_\rho = \frac{\rho_0}{\rho_1}$ (8)

In the equations, footnotes that are "0" represent prototypes. Footnotes that are "1" represent Model I.

Taking equation (8) and substituting into equation (6) and equation (7), and, in conjunction with that, taking the results and multiplying them by each other, one afterwards obtains:

$$C_l = \sqrt[3]{\frac{C_\mu^3}{C_g C_\rho^2}} \quad (9)$$

When models and prototypes are placed at the same latitude on the earth or at latitudes that are not very greatly different, $C_g=1$. When models and prototypes opt for the use of the same types of propellants and coolants, $C_p = C_\mu = 1$.

Because of this, equation (9) then becomes

$$C_l = 1 \quad (10)$$

This conclusion clearly shows that, in scale model tests, in order to guarantee that model and prototype interior ballistic parameters agree, through conditions where models and prototypes are simultaneously made to observe similarity criteria Fr and Re,

there is a need for the axial dimensions of models and prototypes to be equal.

Taking equation (8) and substituting into equation (6) and equation (7), and, in conjunction with that, taking the results and dividing them by each other, one afterwards obtains:

$$C_r = \sqrt[3]{\frac{C_\mu C_s}{C_p}} \quad (11)$$

$$C_\mu = C_s = C_p = 1, \text{ 故 } C_r = 1$$

$$\text{Because } C_\mu = C_s = C_p = 1, \text{ therefore, } C_v = 1 \quad (12)$$

From the Sitelaohaer (phonetic) criteria $Sh = vt/l$, it is possible to obtain

$$C_r = \sqrt[3]{\frac{C_\mu}{C_p C_s^2}} \quad (13)$$

$$C_\mu = C_s = C_p = 1, \text{ 故 } C_r = 1$$

$$\text{Due to the fact that } C_\mu = C_s = C_p = 1, \text{ therefore, } C_l = 1 \quad (14)$$

From Euler criteria $En = P/\rho v^2$, one has $C_p = C_p C_v^2$

Because $C_p = C_v = 1$, therefore

/66

$$C_p = \frac{P_0}{P_1} = 1 \quad (15)$$

From Mach criteria $Ma = \frac{v}{\sqrt{T}}$ one has $C_r^2 = \frac{T_0}{T_1}$

Therefore $C_r = \frac{T_0}{T_1} = 1 \quad (16)$

From π_8 and π_9 , one respectively obtains

$$C_d = \frac{d_0}{d_1}, \quad C_s = \frac{S_0}{S_1} = C_d^2, \quad C_r = \frac{V_0}{V_1} = C_d^2 \quad (17)$$

From Newton criteria Ne, one has

$$C_F = \frac{F_0}{F_1} = \frac{C_m C_v^2}{C_i}$$

In accordance with the reasoning described above, $C_i = 1$ and $C_v = 1$. Therefore,

$$C_F = C_m \quad (18)$$

The attention which should be paid to mass is the weight within a unit volume, that is

$$C_m = C_p C_d^2 C_i$$

(19)

Therefore,

$$C_m = C_F = C_d^2$$

Up to now, among 9 similarity criteria, there are 8 that are equal to each other. The one remaining

$$\pi_7 = \frac{l_1}{d_1} \neq \frac{l_0}{d_0} \quad (5)$$

Moreover, π_7 describes geometrical conditions associated with models and prototypes. It is precisely due to the fact that π_7 is not equal that we therefore say Model I is geometrically dissimilar. On this geometrically dissimilar surface, there are contradictions with similarity theory. However, in accordance with the reasoning described above, in order to guarantee that interior ballistic parameters associated with models and prototypes are equal, one knows from similarity theory that there is a need to require that the flow fields associated with the two systems be similar. As far as criteria maintaining the two flow processes as similar are concerned, there are six criteria (Fr, Re, En Sh, Ma, Ne). In particular, times when Re and Fr are simultaneously equal

lead to the axial dimensions of models and prototypes being equal. As a result, in order to realize flow field similarity for models and prototypes, there is a need to abandon geometrical similarity.

4.2 Model II Similarity Ratios

The Model II shown in Fig.1(c) is geometrically similar. The three dimensional scale of its geometrical configuration is reduced in accordance with the same ratio. In order to distinguish it from Model I, take the similarity ratios and opt for the use of the symbols below to express them:

$$K_l = \frac{l_0}{l_2}, \quad K_v = \frac{v_0}{v_2}, \quad K_g = \frac{g_0}{g_2}, \quad K_\mu = \frac{\mu_0}{\mu_2}, \quad K_r = \frac{\rho_0}{\rho_2}, \quad K_p = \frac{P_0}{P_2}, \quad K_T = \frac{T_0}{T_2},$$

$$K_d = \frac{d_0}{d_2}, \quad K_S = \frac{S_0}{S_2}, \quad K_V = \frac{V_0}{V_2}, \quad K_F = \frac{F_0}{F_2}, \quad K_m = \frac{m_0}{m_2} \quad (20)$$

We now take the similarity ratios above and, respectively, substitute them into π_2 through π_9 associated with similarity criteria form (5).

From Fulufa criteria $Fr = \frac{v^2}{gl} = \text{idem}$, use is made, in conjunction with this, of equation (20) to obtain $K_v^2 = K_d$. That is,

$$K_v = \sqrt{K_d} \quad (21)$$

From Euler criteria $En = \frac{\rho v^2}{P} = \text{idem}$, one obtains $K_p = K_v^2$. Making use of equation (20), one obtains

$$K_p = K_d \quad (22)$$

From Mach criteria $Ma = \frac{v}{\sqrt{T}} = \text{idem}$, one obtains $K_T = K_d$ (23)

From Sitelaohaer (phonetic) criteria $Sh = \frac{vt}{l} = \text{idem}$

one has $K_v = \frac{K_d}{K_v}$, . Taking equation (20) and

substituting in, one obtains

$$K_i = \sqrt{Kd} \quad (24)$$

From Newton criteria $Ne = \frac{mv^2}{Fl} = \text{idem}$, one has

$$K_m = \frac{K_F K_d}{K_i^2}, \quad \text{Making use of equation (20), one}$$

obtains $K_m = K_F$.

However, $K_m = K_F K_d^3$, therefore $K_m = K_F K_d^3$, 所以 $K_m = K_F = K_d^3$ (25)

From π⁷, π⁸, and π⁹, one obtains $K_i = K_d$, $K_s = K_d^2$, $K_v = K_d^3$ (26)

Up to now, similarity ratios of the two models have already been completely solved for. Use is now made of equation (10), equation (12), and equations (14)-(26). They are all taken and combined in the list in Table 2.

Table 2 Similarity Ratios Associated with the Two Models

模型 I ①	模型 II ②
$C_l = l_0 / l_1 = 1$	$K_l = l_0 / l_2 = K_d$
$C_d = d_0 / d_1$	$K_d = d_0 / d_2$
$C_p = \rho_0 / \rho_1 = 1$	$K_p = \rho_0 / \rho_2 = 1$
$C_g = g_0 / g_1 = 1$	$K_g = g_0 / g_2 = 1$
$C_\mu = \mu_0 / \mu_1 = 1$	$K_\mu = \mu_0 / \mu_2 = 1$
$C_v = v_0 / v_1 = 1$	$K_v = v_0 / v_2 = \sqrt{K_d}$
$C_t = t_0 / t_1 = 1$	$K_t = t_0 / t_2 = \sqrt{K_d}$
$C_P = P_0 / P_1 = 1$	$K_P = P_0 / P_2 = K_d$
$C_T = T_0 / T_1 = 1$	$K_T = T_0 / T_2 = K_d$
$C_V = V_0 / V_1 = C_d^2$	$K_V = V_0 / V_2 = K_d^3$
$C_S = S_0 / S_1 = C_d^2$	$K_S = S_0 / S_2 = K_d^2$
$C_m = m_0 / m_1 = C_d^2$	$K_m = m_0 / m_2 = K_d^3$
$C_F = C_m$	$K_F = K_m$

Key: (1) Model I (2) Model II

/68

5 CONCLUDING REMARKS

As far as model tests using similarity theory are concerned, they are an important means right along in the resolution of new types of or complicated tasks. This article carried out detailed derivations of similarity criteria with regard to two types of scale models simulating launch canister missile interior ballistics (Model I and Model II). In conjunction with this, they underwent verification in actual testing, that is, the interior ballistics performance parameters which were measured for Model I or Model II as built under the direction of similarity criteria described agreed very well with data measured in 1:1 prototype tests.

Because option was made for use of the "convert four dimensional factors into three dimensional factors" method, it made

the similarity criteria which were derived both succinct and conceptually clear. This has very important significance in similar practical engineering applications.

REFERENCES

- 1 邱绪光. 实用相似理论. 北京航空学院出版社, 1988.
- 2 Седов Л И. Методы подобия и размерности в механике. Москва : Наука, 1987.
- 3 Кутателадзе С С. Анализ подобия в теплофизике. Издательство Науки, 1982.
- 4 Гухман А А. Введение в теорию подобия. Москва, 1973.

LECTURE BULLETIN

Chun Hui

Translation of "Jiang Xue Duan Xun"; Missiles and Space Vehicles, Overall No. 213, No.1, 1995, p 68

Responding to an invitation by the Beijing Intensity Environmental Research Institute, the Chinese American scholar Dr. Hung Ru Jen--Professor at the U.S. University of Alabama in Huntsville--lectured on 7-8 December 1994 in Beijing's Long March Guest Hall. The main content of the lectures was three dimensional calculation studies associated with the kinetic behavior of gas bubbles on liquid gas boundary surfaces in low temperature fuel storage tanks under microgravity conditions. Scientific and technical personnel from a good number of units such as three permanent committee members of the Chinese Carrier Rocket Technology Research Institute science and technology committee--Fan Shihe, Liu Erxun, and Li Bangfu, Chairman Shi Weiying of the science and technology committee of the Beijing Long March Science and Technology Information Research Institute, Institute Chief Li Zhiji of the Beijing Intensity Environmental Research Institute, as well as the Beijing Astronavigational Systems Engineering Design Department, the Liquid Rocket Engine Research Institute, and so on, listened to the lectures, and, in conjunction with that, participated in informal discussions. The Beijing Intensity Environmental Research Institute's General Engineer, Huang Huaide, hosted the conference.

Chairman Wang Xinqing of the Beijing Astronavigational Systems Engineering Department science and technology committee led discussions which were carried out by relevant scientific and technical personnel and Professor Hung with regard to related technical questions.

The entire lecture activity was the responsibility of and

arranged by the Beijing Intensity Environmental Research Institute science and technology office. These lectures achieved good results, and there were hopes among the conference participants that, hereafter, bilateral Sino-U.S. exchange activities would be strengthened in the field of microgravity research.

NEW USES ASSOCIATED WITH COMBINED
ENVIRONMENTAL TEST MODULE

Feng Zhenxing

Translation of "Zu He Huan Jing Shi Yan Cang De Xin Yong Tu";
Missiles and Space Vehicles, Overall No. 213, No.1, 1995, p 68

Wright Laboratory's dynamics testing section has recently opened up to the public that section's combined environmental acoustics experimentation module. This test module is specialized simulation equipment constructed for supersonic flight tests as well as the U.S. national space plane (NASP) and other materials for astronavigational use. This installation is capable of testing the space plane's large dimension advanced composite material structures. The combined environmental testing module, with a price of 7 million U.S. dollars, is capable of producing high acoustic intensities and thermal environments reaching as high as 1650°C. On the basis of test module project management, the chief engineer T. Gerardi said: "This equipment is capable of carrying out tests on 0.5mx0.5m - 1.2mx1.2m materials as well as structural members." The acoustic pressure levels it produces are extremely high. Thermal flow rates are also extremely high. Thermal flow rates are produced by the use of a set of five quartz lamps. The peak powers are capable of reaching 2.5MW. As far as this test module is concerned, despite the fact that it primarily serves the U.S. national space plane, it also provides services to other government agencies and private enterprises when research testing is carried out.

-INFORMAL DISCUSSION OF HOT TOPIC- EDITOR'S NOTE At the beginning of 1994 and at the end of the year, the Arian carrier rocket failed at launch in two instances. This then drew the attention of the ordinary people of the world. "Malfunctions" also became the problem grabbing peoples' attention. For this reason, in the "Informal Discussion of Hot Topics" column, we have carried an article introducing the status of the propulsion system malfunctions leading to rocket launch failures, hoping to be able to give the readers some lessons to draw from.

ENGINE MALFUNCTIONS EXPOSED BY
SPACE FLIGHT LAUNCHES

Sun Guoqing

Translation of "Hang Tian Fa She Bao Lu De Fa Dong Ji Gu Zhang"; Missiles and Space Vehicles, Overall No. 213, No.1, 1995, pp 69-74

1 INTRODUCTION

Carrier rocket propulsion systems are sites which are susceptible to many occurrences among the malfunctions in the rockets as a whole. Outside China, statistical figures clearly show that propulsion system malfunctions account for 60%-70% of the failure rates in rocket launches over all. In the last few years (1990-1994), among world space flight launches, in 15 instances of major carrier rocket launch failures, 14 of the instances were accounted for by propulsion system malfunctions leading to rocket launch failure (the appended tables set out 11 instances among these)--accounting for 93% of the entire launch failure rate. It is possible to see how important a place engine reliability has in

rockets as whole. As a result, there is a need to pay serious attention to improving engine reliability and safety--paying particular attention to preventing the often seen engine malfunctions below.

2 SEVERAL TYPES OF MALFUNCTIONS WHICH OCCUR OFTEN

2.1 Turbopump System Malfunctions

Turbopumps are the most key subassemblies in engines. Their primary malfunction modes and causes are: hyposynchronous vibration, impeller vibration, fatigue cracks, turbine blade stress concentrations, bearing wear, burning loss, embrittlement, cavitation, overheating and overload, bad quality welding, materials defects, and so on.

As far as the U.S. space plane is concerned, up to now, it has not been able to satisfy design requirements for reuse. The main thing is nothing else than turbopump problems. For example, on 6 April 1992, the space plane Endeavor carried out prelaunch ignition tests on the launch pad at the Kennedy space center. It was discovered that the No.2 engine had bearing wear and the No.1 engine oxygen pump was bringing in hydrogen. There was nothing to do but to take the three main engines and completely switch them out. During the development of Japan's H-2 rocket LE-7 engine, problems came primarily from turbopumps--for example, turbine blade damage, low hydrogen pump revolution speeds, turbopump piping leaks, catching fire and exploding, even to the point of producing casualties.

On 10 September 1982, due to a three sublevel turbopump bearing and gear malfunction, it led to a failure of the first commercial launch of the Arian 1. On 28 May 1985, because of a core level turbopump malfunction in one motor of an Atlas 34D, there was fuel leakage, causing the launch to fail. On 24 January 1994, during the 63d Arian launch of an Arian 44L, a third stage engine turbopump overheated. A liquid oxygen lateral bearing malfunction caused the launch to fail, damaging two satellites.

2.2 Engine Ignition Malfunction

There have been engine combustion chamber and ignition system malfunctions in the past. When the former Soviet Union's Proton rocket was launched on 30 January and 27 April 1987, due to upper stage liquid rocket motors not igniting, satellites were not able to enter orbit. As far as the Ariane rockets are concerned, early in their engine ground development testing phase, they had many instances of the appearance of ignition problems. However, they were not taken seriously with the result that, on the 15th and 18th iterations of Ariane flights, the third stage did not ignite normally, creating launch failure. In order to correct igniter malfunctions, launches were suspended for a year. Ignition systems were redesigned and tested. Only then was an end put to this type of malfunction.

On 16 October 1992, the U.S. also had a rocket cause launch failure because of a second stage not igniting.

Causes giving rise to ignition system malfunctions include control malfunctions, flaws in the designs of igniters themselves, combustion chamber pressure abnormalities, ignition system transport valve and jet valve malfunctions as well as contamination, and so on. These will create ignition malfunctions or ignition delays. If it is desired to prevent these malfunctions, there is a need to strengthen quality control, improve ignition performance, and, in conjunction with that, there is a need, under limit conditions, to carry out ground tests and high altitude simulation tests.

/70

① 附表 1990~1994 年各国运载火箭发射失败记录

② 序号	③ 运载火箭名称	④ 试验/飞行	⑤ 发射日期	⑥ 故障模式	⑦ 故障简述	⑧ 故障原因	⑨ 纠正措施
L.01	欧洲局阿里安 2 星发射 ⑩	V36 次 商业卫星	1990. 2.22	一级推进发动机故障 ⑪	阿里安第 36 次发射中，飞行 6s 后，一级发动机水阀堵塞，注入燃气发生器的水流减少，导致推力不足发射失败	在打捞的水管阀门残骸检查中，发现故障原因是由于一块碎布堵住了冷却水管。纯系因人为造成外来物而失败的 ⑫	加强质量管理和责任心 ⑬
L.02	欧洲局阿里安 42PL 星发射 ⑯	V63 次 商业卫星	1994. 1.24	三级 HM7 发动机故障 ⑭	当火箭升空飞行到 6min47s 时，涡轮泵过热，7min7s 关机，箭星双保险入大西洋 ⑮	涡轮泵过热，液氧侧轴承故障 ⑯	在轴窝内增加一轴气管散热，并对轴承涂润滑油 ⑰
L.03	欧洲局阿里安 4 星发射 ⑯	V70 次 商业卫星	1994. 12.2	三级 HM7 发动机故障 ⑯	三级发动机燃气发生器压力不足，其功率只有 70%，飞行 15min，星箭坠入大西洋 ⑯	燃气发生器压力不足，具体原因待查 ⑱	待定 ⑲
L.04	日本 H-1 星发射 ⑲	商业卫星	1990. 3.12	一级 MB3 发动机故障 ⑳	H-1 于种子岛准备发射卫星时，一级主发动机起火，烧毁了发动机。 ⑳	由于液氧涡轮泵叶轮密封圈混进水，水迁低温推进剂结冰，致使密封圈失效，又使氮气漏进波压系统中 ⑳	加强密封圈设计，采用堵头，防止射前进入水蒸汽 ⑳
L.05	俄罗斯质子号 ⑳	通讯卫星	1993. 5.27	二级 PO7 发动机故障 ㉑	此次发射，二级发动机起火，三级发动机过早关机，飞行 572s 时，火箭失控引爆，卫星坠入海中 ㉒	推进剂混入杂质，污染燃料引起火灾 ㉓	防止有机物混入推进剂 ㉔
L.06	俄罗斯天顶号 ㉕	卫星发射	1990. 10.4	一级 RD170 发动机故障 ㉖	天顶号在拜克努尔发射卫星时，火箭起飞爆炸，炸毁了发射台 ㉗	一级发动机故障，情况不详 ㉘	一级发动机故障，情况不详 ㉙

(KEY TO APPENDED TABLE ON NEXT PAGE)

Key: (1) Appended Table A Record of Carrier Rocket Launch Failures by Various Nations 1990-1994 (2) Sequence No. (3) Launch Vehicle Nomenclature (4) Test/Flight (5) Launch Date (6) Malfunction Mode (7) Brief Description of Malfunction (8) Malfunction Cause (9) Corrective Measures (10) European Space Agency Arian 2 (11) V36 Commercial Satellite Launch (12) First Stage Vicalloy Engine Malfunction (13) During the 36th Arian Launch, After 6s of Flight, the First Stage Motor Water Valve Blocked Up. Water Flow Infused into Combustion Gas Generators Was Reduced, Leading to Inadequate Thrust and Launch Failure. (14) During Inspection of the Remnants Salvaged from Water Tubing Valves, It Was Discovered that the Cause of the Malfunction Was a Piece of Cloth Blocking Up Cooling Water Tubes. The Failure Was Purely Due to Man Made Foreign Objects. (15) Strengthened Quality Control and Sense of Responsibility. (16) European Space Agency Arian 42PL (17) V63 Commercial Satellite Launch (18) Third Stage HM7 Motor Malfunction (19) When the Rocket Rose in Flight for 6min47s, There Was Turbopump Overheat. At 7min7s, There Was Shut Down. The Rocket and Satellite Both Fell Into the Atlantic. (20) Turbopump Overheat. Liquid Oxygen Lateral Bearing Malfunction. (21) In Shaft Pit, Added a Shaft Air Pipe to Diffuse Heat. In Conjunction With This, Lubricated Bearings. (22) European Space Agency Arian 4 (23) V70 Commercial Satellite Launch (24) Third Stage HM7 Engine Malfunction (25) Third Stage Engine Combustion Gas Pressures Inadequate. The Power Was Only 70%. After a 15min Flight, Satellite and Rocket Fell Into the Atlantic. (26) Combustion Gas Generator Pressures Inadequate. Actual Cause Awaits Investigation. (27) Awaits Determination. (28) Japan's H-1 (29) Commercial Satellite Launch (30) First Stage MB-3 Engine Malfunction (31) When H-1 Was Preparing to Launch a Satellite on Zhongzi Island, There Was First Stage Main Engine Ignition. The Engine Burned Up. (32) Due to Liquid Oxygen Turbopump Impeller Seal Ring Mixing in Water, the Water Went Around the Low Temperature Propellant and Froze, Leading to Loss of Seal Ring Effectiveness. Leakage of Nitrogen Gas Into Liquid Oxygen System Was Also Caused. (33) Strengthened Seal Ring Designs. Opted for the Use of Stoppers to Prevent Water Vapor from Entering Before Launch. (34) Russian Proton (35) Communications Satellite Launch (36) Second Stage P07 Engine Malfunction (37) At This Launch, Second Stage Engine Ignited. Third Stage Engine Shut Down Too Early. After 572s of Flight, the Rocket Went Out of Control and Exploded. The Satellite Fell in the Sea. (38) Propellants Were Mixed With Impurities. Contaminated Fuel Gave Rise to the Fire. (39) Prevent Organic Materials Mixing Into Propellants. (40) Russian Zenith (41) Satellite Launch (42) First Stage RD170 Engine Malfunction (43) When the Zenith Was Launching a Satellite at Baikenuer (phonetic), the Rocket Caught Fire and Exploded, Blowing Up the Launching Pad. (44) First Stage Engine Malfunction. Status Unknown.

① 续表

② 序号	运载火箭名称	试验/飞行	发射日期	故障模式	⑦ 故障简述	⑧ 故障原因	⑨ 纠正措施
1.07	俄罗斯天顶号	卫星发射	1991.8.30	二级 RD120 发动机故障	天顶号在发射卫星过程中,火箭发生爆炸,发射设施遭破坏,总计损失1亿多美元	二级煤油导管中,混入有机物(油)污染燃料引起爆炸	⑯
1.08	俄罗斯天顶号	卫星发射	1992.2.24	二级 RD120 发动机故障	发射过程中二级发动机出故障	乌克兰火箭发动机生产厂工人质量控制欠佳	⑰
1.09	美国宇宙神1	商业卫星发射	1991.4	上面级 RL10 发动机故障	火箭发射升空275s失控,导致发射失败	调查开始时,曾认为一碎布堵塞涡轮泵,但一年后,宇宙神1发生故障时,经重新调研,确认为是RL10的一个单向阀在起飞时没关闭,使空气进入液氢涡轮泵,氮被冷凝,涡轮泵无法旋转,导致飞行失败	⑳
1.10	美国宇宙神1	商业卫星发射	1992.8.22	上面级 RL10 发动机故障	火箭升空后289s失控,发射失败	故障原因同上,这两次故障的真正原因是在这次飞行失败后才找出的	㉑
1.11	美国宇宙神1	海军讯卫星发射	1993.3.25	MAS 发动机故障	宇宙神 AC74,发射卫星后未被送入预定轨道	助推发动机燃气发生器液氧流量控制器杆式调节螺钉松动,使出口压力降低,推力下降 66%,上面级人马座虽工作,但卫星被送入低于要求轨道	㉒

Key: (1) Table Continued (2) Sequence No. (3) Launch Vehicle Nomenclature (4) Test/Flight (5) Launch Date (6) Malfunction Mode (7) Brief Description of Malfunction (8) Malfunction Cause (9) Corrective Measures (10) Russian Zenith (11) Satellite Launch (12) Second Stage RD120 Engine Malfunction (13) In the Process of Satellite Launch, the Zenith Rocket Exploded. The Launch Facility Was Destroyed. The Total Damage Was Over 1 Hundred Million U.S. Dollars. (14) In Second Stage Kerosene Guide Tubes, Organic Matter Was Mixed in (Oil/Grease). The Contaminated Fuel Gave Rise to the Explosion. (15) Russian Zenith (16) Satellite Launch (17) Second Stage RD120 Engine Malfunction (18) During the Launch Process, There Was the Appearance of Second Stage Engine Malfunction. (19) Worker Quality Control at the Ukrainian Rocket Engine Production Plant Was Not Good Enough. (20) U.S. Cosmic Spirit 1 (21) Commercial Satellite Launch (22) Upper Stage RL10 Engine Malfunction (23) The Rocket Launched and Ascended for 275s, Losing Control. This Led to Launch Failure. (24) When Investigations Began, It Was Confirmed that a Piece of Cloth Had Blocked Up a Turbopump. However, a Year Later, When the Cosmic Spirit 1 Developed Malfunctions, Investigations and Studies Were Gone Through Again. It was Confirmed that a One Way Valve Had Not Closed During Take Off, Causing Air to Enter Into Liquid Hydrogen Turbopumps. Nitrogen Had Been Condensed. Turbopumps Had No Way to Revolve, Causing the Flight to Fail. (25) U.S. Cosmic Spirit 1 (26) Commercial Satellite Launch (27) Upper Stage RL10 Engine Malfunction (28) After the Rocket Ascended for 289s, There Was Control Loss. The Launch Failed. (29) Analysis of the Causes of the Malfunction Was the Same as Above. The Real Cause of These Two Instances of Malfunction Was Only Found After This Flight Failure. (30) Redesign Was Done on the Cosmic Spirit 1 RL10 Engine One Way Valve. Option Was Made for the Use of the Installation of Electromagnetically Opened and Closed Redundant Valves, to Effect Seal Redundancy. (31) U.S. Cosmic Spirit 1 (32) Navy Communications Satellite Launch (33) MA5 Engine Malfunction (34) The Cosmic Spirit AC74--After Satellite Launch--Was Not Put Into Predetermined Orbit. (35) Booster Engine Combustion Gas Generator Liquid Oxygen Flow Amount Control Device Rod Type Adjustment Bolt Was Loose, Causing Exit Pressures to Drop. Thrust Dropped 66%. Although There Was Upper Stage Sagittarius Operation, Satellite Insertion, However, Was Below Required Orbit.

2.3 Upper Stage Engine Malfunctions

The majority of carrier rocket launch failures are caused by engine malfunctions. Moreover, among engine malfunctions, it is clearly upper stage engine malfunctions which are in the majority. For instance, the U.S. Cosmic Spirit Centaurus rocket has been fired over 20 times from May 1981 until now. All four failures were engine malfunctions. Among these, one instance was a booster engine (MA-5) malfunction. Besides this, three instances of malfunction were all given rise to in the Centaurus stage RL10 hydrogen oxygen rocket engine. Another instance is the Arian carrier rocket with a total of seven launch failures up to now. These seven instances were all engine malfunctions. Among them, four cases were third stage hydrogen oxygen engine malfunctions. The former Soviet Union's Zenith launch vehicle went into service in 1985. 13 launches in a row were successful. However, from 1990 until now, three successive launch failures have occurred. Among these, two were upper stage RD-120 engine malfunctions. The Proton launch vehicle had a firing failure on 27 May 1993. This was also the occurrence of a second stage engine problem.

Upper stage engines operate under high altitude conditions. The influences of space environments on engine operating configurations are difficult to anticipate. As a result, space engine malfunction modality analyses should be carried out fully, strengthening ground simulation tests. Testing proves that the majority of upper stage engine malfunctions can all be reproduced under ground simulation conditions. For example, on 30 August 1991, a Zenith second stage engine liquid oxygen guide tube was penetrated by contaminants (oil/grease), producing an explosion. Later, on the foundation of expert malfunction analysis, this malfunction was reproduced in ground tests. In conjunction with this, option was made for the use of corrective measures.

2.4 Special Attention Should Be Paid to the Prevention of Engine Low Temperature System Icing Problems

In low temperature engine systems--particularly, liquid hydrogen liquid oxygen rocket engines--special attention must be paid to the prevention of the penetration of the water content in dampness into liquid oxygen liquid hydrogen systems. Among carrier rocket launches, cases of flight failures due to channel blockages associated with water vapor icing appear commonly. For instance, on 12 March 1990, when Japan's H-1 rocket was launched at the Zhongzi Island space flight center, the first stage main MB-3 engine gave rise to a fire, damaging the engine. The cause was oxydyzer turbopump impeller seal rings mixing in water. The water that was mixed in froze because it met with low temperature oxygen, causing seal rings to lose their effectiveness, thereby causing large amounts of liquid oxygen to leak into nitrogen gas, leading to a fire. The water was mixed in from the nitrogen gas exhaust tube because of a storm at the time of the launch. Water also mixed in at the site of the turbopump connection heads.

On 18 April 1991 and 22 August 1992, the Cosmic Spirit I rocket launched two commercial satellites. After the rockets went aloft, they lost control after 275s and 289s, respectively, leading to launch failure. Going through in depth analysis, it was confirmed that the two instances of malfunction were completely the same. Both were RL-10 engine one way valves not closing before rocket launch, leading to dampness entering liquid hydrogen turbopumps, and, in conjunction with that, icing. Nitrogen in the air was also condensed, thereby causing turbopumps to have no way to revolve, leading to flight failure and creating serious damage. As far as the Cosmic Spirit RL-10 engine is concerned, option was made for the use of redesigned one way valves, installing electromagnetic redundant seal valves. In conjunction with this, before launch, monitoring is done of the opening and closing of the valves in question. Temperature controls were added, thus preventing air and nitrogen gas from entering into the engines.

2.5 Booster Malfunctions

Solid boosters used by launch vehicles easily produce

explosions, adding to unsafe factors. Solid rocket boosters and solid missiles alike must pay special attention to safety during production, testing, transport, and launch. /73

On 7 September 1990, a solid booster of an Atlas 4 carrier rocket--while being tested on a test bed at the Air Force space flight laboratory at Edwards Air Force Base in the U.S. state of California--lost equilibrium when a crane hung the solid motor on an erect position test bed. The suspension arm and the engine fell over on the ground. This gave rise to an explosion and fire, causing one dead and eight injured.

On 1 April 1991, a new model Atlas 4 solid rocket engine--on a test bed--produced excessively high pressures within the engine due to solid propellant formation flaws. An explosion occurred.

3 SEVERAL PROBLEMS WHICH SHOULD BE PAID ATTENTION TO

3.1 Pay Attention to Preventing the Randomly Occuring Nature of Malfunctions and Reproducability

Going through investigations with regard to carrier rocket launch mishaps in the last few years, one discovers among them suddenly occurring characteristics and reproducible characteristics.

Since the Union carrier rocket of the former Soviet Union went into service in November 1963, it has already carried out 996 successful launches. There have been a total of 16 failures. With two failures from September 1983 to 27 April 1993, the launches in the last ten years were all successful. From April 1985 to 4 October 1990, the first 13 launches of the Zenith rocket were a string of successes. However, after 4 October 1990 to 1992, in these three years, each year saw the appearance of one launch failure. The explanation of this is that malfunctions sometimes carry with them very great random occurrence characteristics.

On the other hand, there are a number of malfunctions which still continue to appear several times. For example, as far as 18 April 1991 and 22 August 1991 are concerned, the Cosmic Spirit 1 rockets AC/71 and AC/70 showed the appearance of the same

malfunction when launching commercial satellites. The opening and closing of one way valves before launch caused air and nitrogen gas to enter into engine low temperature systems, icing and creating failures. Another case would be the failures of the two satellite launch flights of Arian V15 and V18. They were both caused by ignition system malfunctions.

With regard to the reoccurring malfunctions discussed above, they are all determination errors in analysis of the causes of a previous malfunction. With respect to Cosmic Spirit 1, the first instance was wrongly adjudged to be extraneous matter blockage. As far as the Arian rocket is concerned, in the first instance, the malfunction analysis determined that liquid hydrogen jet valves in the three sublevel of the engine gave rise to leakage, creating combustion chamber internal pressures, temperatures on the low side, and ignition failure. These were only possible causes for ignition failure. There was no doubt that igniter design was flawed. In these two cases of recurring malfunction incidents, both were ones where the basic causes were not found in analyses of the previous malfunction. As a result, there was also no way to correspondingly alter designs to get rid of recurrences of the same type of malfunctions.

3.2 Prevent Extraneous Materials and Strictly Forbid Human Errors

On 22 February 1990, the Arian 44L launch vehicle--while carrying out a 36th commercial firing--acted oddly in flight 6s after launch. At 101s, the rocket exploded. This failure was not a problem with the rocket itself but was produced by extraneous matter entering into the engine and human errors. When investigation and analysis was done of wreckage associated with the engine, it was discovered that a 30mmx30mm piece of cloth was blocking the inside of prepump tubing associated with water supply pumps. This was left inside the tube by operators who did not clean out the tube carefully during the period of engine monitoring and debugging.

On 14 March 1990, when the commercial Atlas 3 made a second

launching of the international communications satellite 6F3, the second stage rocket and the satellite did not separate. The two went into the wrong orbit together. This instance of rocket and satellite separation failure was purely human error, created by hardware and software personnel not communicating with each other or coordinating consistently. Software personnel believed that separation signal lead line circuitry should be arranged in front of the satellite. In conjunction with this, on this basis, separation signal software was designed. However, hardware personnel believed that, when a single satellite is launched, the best arrangement is at the back of the satellite. In conjunction with this, at this point, they altered the circuit design plans. Hardware personnel took the amended designs in question and orally notified the software personnel on the same work period. However, notification was not made in accordance with alteration procedure regulations to software personnel. In the end, the computer programming sent separation signals by the forward lead lines. However, the satellite was actually still connected to the rear lead line. As a result, during rocket separation, computers had no way to send out separation commands, leading to the failure of satellite and rocket separation. Later, a 20 item detection measure to prevent human errors was drawn up. These measures are able to guarantee that it will then be possible to discover potential malfunctions during rocket and useful load preparation. On 27 May 1993, 205s after a Proton rocket was launched at Baikenuer (phonetic) and went aloft, there was a second stage engine explosion. This was also due to fuel contaminated with extraneous material, leading to launch failure.

/74

3.3 Prevent Fueling and Storage Tank Malfunctions

The adding of fuel carries with it extremely great risks. Once a certain link shows the appearance of problems, explosions occur. The aftermath is extremely grave.

On 23 June 1973, as far as the former Soviet Union's Cosmos rocket is concerned, during fueling at the Puliexiecike (phonetic)

space flight firing range, a rocket gave rise to an explosion, creating casualties. On 18 March 1990, during the adding of fuel at a firing range, the Dongfanghong rocket also gave rise to an explosion, killing or wounding 55 people. On 25 August 1991, with respect to the Cosmic Spirit 2 rocket--during the carrying out of fueling tests for its first launch of the international communications satellite 3 in September at the Cape Canaveral launch pad--during the fueling of low temperature liquid hydrogen and liquid oxygen into Centaurus, the common bottoms of storage tanks cracked under thermal stresses, creating a severe accident. With regard to the early U.S. Atlas 2 and Delta rockets, they have both shown the appearance of malfunctions or accidents given rise to by the adding of fuel. On 1 August 1991, when Japan's H-1 rocket was practicing together with the BS-3B direct broadcast satellite which it was about to launch from Zhongzi Island, the first stage oxydyzer tank liquid oxygen leaked, causing the launch to be postponed. On 9 August 1991, when Japan's Mitsubishi Heavy Industry Co. carried out H-2 rocket propulsion system tests, there was the occurrence of an explosion when fuel tubing was pressurized full of nitrogen gas. One person died.

APCATS '94 CONVENED IN HANGZHOU

Chun Hui

Translation of "APCATS '94 Zai Hang Zhou Zhao Kai"; Missiles and Space Vehicles, Overall No. 213, No.1, 1995, p 74

On 10-13 October 1994, Zhejiang University convened the first session of the Asian Pacific Conference on Aerospace Technology and Science in Hangzhou. Over 200 representatives attended the conference, coming respectively from Japan, South Korea, Australia, India, Israel, the U.S., Germany, France, China, as well as China (Province of Taiwan), and so on. The main objective of the conference was to exchange new results associated with aviation and space flight technology as well as scientific research in order to promote the development of this academic field, strengthening friendship and cooperation between scientific and technical personnel of the Asia Pacific region.

Over 170 papers were read to the conference. The fields involved included materials and structures; fluid mechanics and thermodynamics; the mechanics of flight; guidance, navigation, and control; propulsion systems; space shuttle systems; delivery systems; satellite communications and broadcasting; remote sensing and image processing; microgravity, and so on. The collected papers associated with the conference, "Proceedings of the Asian-Pacific Conference on Aerospace Technology and Science 1994.10", is printed and published by the Wanguo Academic Press.

The Asia Pacific region aviation and space flight field faces a good number of challenges. Relevant experts were enabled by APCATS '94, which was hosted by the Beijing Aviation and Space Flight University, to discuss together problems of concern. No

doubt, it will have promoting effects on the development of high science and technology in the 21st century Asia Pacific region.

CHINESE SPACE FLIGHT SCHOLARS WITHIN CHINA
AND ABROAD GET TOGETHER IN BEIJING

Chun Hui

Translation of "Hai Nei Wai Hua Ren Hang Tian Xue Zhe Jyu Hui Bei Jing"; Missiles and Space Vehicles, Overall No. 213, No.1, 1995, p74

The second session of the academic symposium of Chinese space flight scholars from inside and outside China was held on 1-4 December 1994 at the Beijing Debao Restaurant. Over 100 people attended the conference--Chinese space flight scholars residing abroad as well as Chinese space flight scholars associated with the Taiwan, Hong Kong and Macao areas, and the mainland. Leaders and experts associated with such units as the General Aviation Company, the China Astronavigational Association, the Chinese Academy of Launch Vehicle Technology, the Chinese Space Technology Research Institute, and so on, as well as U.S. overseas Chinese scholars Hong Ruzhen, etc., made reports at the opening of the general meeting. The conference divided up into teams associated with carrying out academic exchanges in specialized fields such as overview, engines, control, manned space flight, microgravity science, and so forth. The collected papers of the conference, which have already been published, included the papers that were read at the conference.

This meeting was hosted by the Chinese Astronavigational Association. It continues as another academic gathering following the first conference which was convened in Hong Kong in 1992. The purpose of the conferences is to promote technical exchange and cooperation between Chinese space flight scholars inside China and

abroad. This distinguished gathering--in mutual learning, joint improvement of areas, as well as promoting the bringing into play of their own technical strengths by space flight scholars inside and outside China--play an active role in areas of interest to the Chinese space flight industry.

NEWS IN BRIEF

CZ-3A RISES SMOOTHLY ALOFT
ARIAN FALLS IN THE OCEAN

Yu Tian

Translation of "CZ-3A Shun Li Sheng Kong A Li An Zhui Ru Da Hai";
Missiles and Space Vehicles, Overall No. 213, No.1, 1995, p 75

On 30 November 1994, China's CZ-3A launch vehicle was successfully fired, taking China's newly developed Dongfanghong-3 communications satellite and sending it into a geosynchronous transfer orbit. CZ-3A is, at the present time, China's high orbit carrier rocket with the greatest carrying capability. The rocket is composed of three stages. The first and second stages opt for the use of conventional propellants. The third stage propellants are liquid hydrogen and liquid oxygen. The rocket's lift off weight is 240t. Lift off thrust is 300t. Geosynchronous transfer orbit carrying capability is 2.6t. This launch is CZ-3A's second successful firing. On 8 February 1994, it carried out its first launch at the Xichang satellite launch center, successfully taking simulated satellites of the Shijian No.4 experimental satellite and the Dongfanghong No.3 and sending them into predetermined orbits.

On 1 December 1994, Europe's Arian rocket carried out its 70th launching in French Guiana. After the rocket rose aloft for 15min--at 218km--there was a high altitude accident. It fell into the Atlantic. The U.S. PAS-3 model communications satellite, which the rocket carried, was destroyed. On the 2d, at the Kulu (phonetic) space flight center, the Arian space flight company's director, Xiaer Bige (phonetic), announced that the cause for the failure of

this iteration of Arian rocket launch was gas generator pressure abnormalities associated with the third stage engine, leading to third stage thrust only reaching 70% of normal values. This is the seventh launch failure associated with Arian rockets since their first launch on 24 December 1979. It is also the second failure in 1994. On 24 January 1994, during the 63d launch iteration of the Arian, the rocket launch failed because of third stage hydrogen oxygen engine liquid oxygen bearing overheating.

INDIA'S POLAR ORBIT SATELLITE CARRIER
ROCKET LAUNCH SUCCESSFUL

Yu Tian

Translation of "Yin Du Ji Gui Wei Xing Yun Zai Huo Jian Fa She Cheng Gong"; Missiles and Space Vehicles, Overall No. 213, No.1, 1995, pp 75-76

On 15 October 1994, India's second launch of a polar orbit satellite carrier rocket was successful in taking a remote sensing satellite IRS P2 and sending it into orbit. This is the first successful launch for this type of rocket. On 20 September 1993, when this type of rocket was launched for the first time, because of the appearance of software problems, it was not able to send a useful load into orbit. According to the person in charge of the India space flight research organization, this launch iteration achieved total success. The rocket accurately took an 802.8kg satellite and sent it into an 825km high solar synchronous orbit. The satellite angle of orbital inclination is 98.6°. Indian and Western experts believe that, because the Siliheligeda (phonetic) firing range for this rocket launch is located on India's southeast coast, the launch azimuth limit is 140°. Therefore, if it is desired to achieve ideal orbital entry precisions--speaking in terms of this type of rocket--there is an even higher requirement to control precisions. In order to take satellites and send them into polar orbits of 98.6°, 100s after rocket lift off--before first stage separation--there is a need to carry out a yaw flight maneuver of 55°, thereby losing 272kg of potential useful load capability.

The polar orbit carrier rocket associated with this launch is similar to the U.S. Delta-2. However, the polar orbit useful load

capability is equivalent to the U.S. Cosmic Spirit E rocket.

The overall length of the Indian polar orbit satellite carrier rocket is 44.2m. Lift off weight is 282.5t. It is composed of four stages. The first stage PS-1 core stage mounts a five section type solid rocket motor. The diameter of the motor in question is 2.8m. The length is 20m. Propellant weight is 129t. Thrust is 458.1t. According to Indian officials, this motor is the third largest solid rocket motor used on unmanned rockets in the world--only second to the U.S. Atlas and the Japanese H-2 rocket engine. Onto the core stage are strapped six solid rocket boosters. The thrust associated with each unit is 67.3t. Operating time is 74s. During rocket lift off, the core stage and two booster units ignite. 30.5s after lift off, the other four booster units begin to operate. 111s after rocket launch, the first stage shuts down. The second stage begins to operate. The second stage mounts a liquid rocket engine unit. The thrust is 73.4t. The propellant is dinitrogen tetroxide/metadimethylhydrazine. Propellant weight is 37t. The operating time for the second stage is 150s--that is, 261s after lift off, the second stage shuts down. The third stage begins to operate. The third stage opts for the use of solid rocket engines. Propellant weight is 7.2t. Thrust is 34.7t. Operating time is 76s. After third stage shut down, and, in conjunction with that, separation, the rocket glides 3.5min. After that, the fourth stage ignites. The fourth stage opts for the use of two liquid rocket engine units producing a total of 1.5t of thrust. Propellant weight is 2t. Operating time is 405s.

The Indian space research organization asserts that India's polar orbit satellite carrier rocket will go onto the commercial launch market from now on. Each launch of the rocket in question costs 25 million U.S. dollars. It is capable of taking a 1000kg useful load and sending it into a 900km circular solar synchronous polar orbit. India plans--before 1999--to use polar orbit satellite carrier rockets to launch another 3 Indian remote sensing satellites.

On the foundation of polar orbit satellite carrier rockets,

India is just in the midst of developing geosynchronous satellite launch vehicles (GSLV). The first stage core stage of this type of rocket as well as the second stage are the same as the polar orbit satellite carrier rocket. In conjunction with this, four autocombustive liquid propellant rocket booster units are strapped on. The rocket's third stage plans to opt for the use of a Russian low temperature engine. In accordance with a 9 million U.S. dollar contract, Russia is just in the midst of supplying to India three engine units. This type of rocket--opting for the use of Russian engines to act as the third stage--can anticipate a first launch in 1997. India is still independently developing low temperature engines for use in the third stage. A synchronous satellite launch vehicle using independently developed third stages will not be able to launch until 1998. This type of new model rocket can take a 2500kg communications satellite and send it into synchronous transfer orbit.

A U.S. COMPANY PUTS FORWARD DESIGN PLANS FOR REUSABLE
SINGLE STAGE ORBITAL ENTRY ROCKETS

Yu Tian

Translation of "Mei Yi Gong Si Ti Chu Dan Ji Ru Gui Ke Chong Fu Shi Yong Huo Jian Xin Fang An"; Missiles and Space Vehicles, Overall No. 213, No.1, 1995, p 76

In October 1993, a newly established U.S. small model spacecraft company--Kistler Aviation and Space Flight Co.--has recently put forward design plans for a type of reusable single stage orbital entry rocket. Kistler, the director of the company in question, asserts that his company will opt for the use of currently existing technology and private funds to carry out the development of this type of rocket. Development costs will only require 250 million U.S. dollars. In 1993, the U.S. Defense Department carried out a study clearly showing that developing a type of practical model of single stage orbital entry rockets would require funds exceeding 20 billion U.S. dollars.

The 77 year old physicist, Kistler, believes that the expenses which are required by astronavigational transport are unacceptable to people. Reusable single stage orbital entry rockets are the only possible way of very, very greatly lowering the costs. Kistler's plan is first to develop a type designated K-0 of scale model suborbital test rockets. After that, on the foundation of the experimental rockets, a practical model K-1 rocket is developed. The K-1 rocket is capable of taking a 907kg useful load and sending it into near earth orbit. Later, two types of comparatively large model Kistler rockets will be developed. Their near earth orbit carrying capabilities will be, respectively, 2721kg and 9071kg. It is said that the K-0 test rocket will use

hydrogen peroxide as fuel. Option is made for the use of catalysts for start up. Production of the hardware has already begun. According to plans, tests will begin to be carried out in the spring of 1995. K-1 rocket suborbital flight tests will be carried out early in 1998. Launch tests will be carried out at the Pacific Rocket Association Testing Ground located in California's Mojave Desert. Kistler helped to design and build the testing ground in question. Kistler is also consulting with officials, planning to conduct rocket tests at the Kennedy space flight center. Kistler has not revealed the cost of the K-0 experimental rocket. However, it is said that the K-1 rocket would only require 500 U.S. dollars for each pound of useful load sent into near earth orbit. Other rockets, by contrast, require 5000-10000 U.S. dollars.

The K-1 rocket is composed of a platform and a space flight vessel that is placed on the platform. The platform uses Pratt and Whitney Company RL-10 engines as power. At speeds of 643.7km/hr, in approximately 5min, the space flight vessel is sent to a height of 24.4km. After the space flight vessel is released, the platform returns to the launch site. When the space flight vessel returns, use is first made of reverse thrust rockets to reduce speed. After that, it falls onto a spring bed made from steel cable netting.

EUROPEAN SPACE AGENCY SELECTS REUSABLE
ROCKET DEMONSTRATOR DESIGN

Translation of "Ou Kong Jyu Xuan Ding Chong Fu Shi Yong Huo Jian Yan Xhi Ji Fang An"; Missiles and Space Vehicles, Overall No. 213, No.1, 1995, p 76

The European Space Agency and the German Space Flight Bureau have already decided that the reusable rocket demonstrator (RRLD) associated with satellites and freight delivery vehicles in the future of Europe is opting for the use of a winged vertical take off and horizontal landing design plan. The purpose of this project is to develop a type of low cost, simple and easy demonstrator to supply suborbital test flight uses. The length of the demonstrator in question is 15.8m. The propulsion system is a set of Arian 4 rocket third stage variable HM-7B liquid hydrogen liquid oxygen engines. The demonstrator's propellant tanks opt for the use of enlarged model Arian 5 propellant tanks. As far as heat elimination systems are concerned, option is made for the use of Europe's Messenger God space shuttle technology, which has already been canceled.

U.S. AIR FORCE LAUNCHES MINUTEMAN 3 MISSILE

Translation of "Mei Guo Kong Jun Fa She Min Bing 3 Missile"; Missiles and Space Vehicles, Overall No. 213, No.1, 1995, p 76

On 5 October 1994, the U.S. Air Force successfully launched a Minuteman 3 intercontinental ballistic missile from Vandenburg Air Force Base. This launch was the first time option was made for the use of the rapid execution and combat aiming (React) system. This system is designed to be used in order to shorten test measurement times before missile launches. The missile that was launched in this instance came from Minot Air Force Base in North Dakota. In accordance with the requirements of the strategic weapons reduction treaties, missiles must carry only one warhead. The missile was lauched from pad No.4 on the north side of the base at 01:00 Pacific Summer Time. The missile drop zone was in the Kwajalein missile target range. This launch was a part of the U.S. Air Force's testing and evaluation plan.

UKRAINIAN ASTRONAVIGATIONAL ACTIVITIES

Ukrainian Astronavigation Bureau

Deputy Bureau Chief

Walieyi Gaolejiaoweiqi Kemaluofu (Phonetic)

Translation of "Wu Ke Lan De Yu Hang Shi Ye"; Missiles and Space Vehicles, Overall No. 213, No.1, 1995, pp 77-78

After the break up of the Soviet Union, Ukraine became--with the exception of Russia--the No.2 space great power among the independent federated entities. In 1992, Ukraine set up a national space structure--the Ukrainian National Astronavigational Bureau. The primary mission of the bureau in question is to preserve relevant technologies. In conjunction with this, corresponding plans were drawn up. This is a central organization composed of cabinet members as well as other members (65 people). It has two scientific research centers. One is set up in Kharkov. It primarily handles instrument manufacture. One is set up in Dniepropetrovsk and is primarily engaged in theoretical research as well as rocket manufacture and space flight research. The set up of this bureau organizational structure is seen in Fig.1.

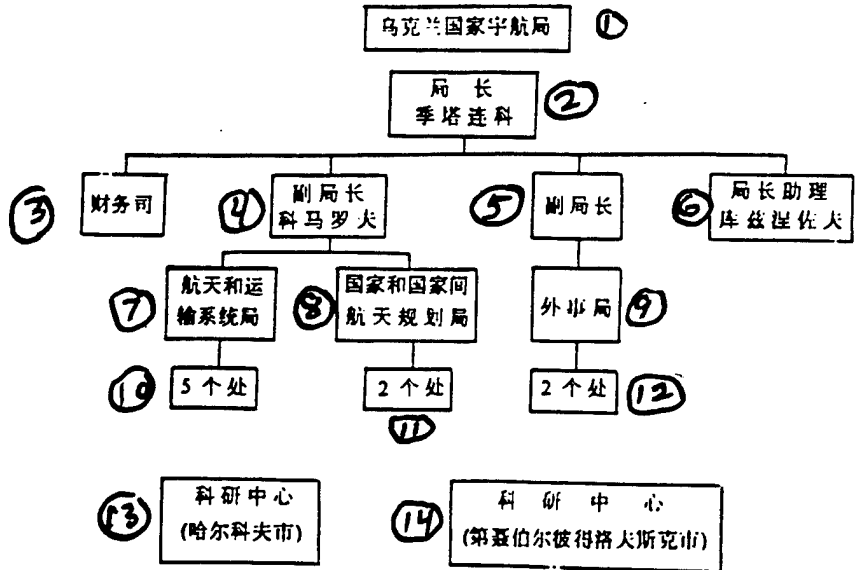


Fig.1 Ukrainian National Astronavigation Bureau Organizational Structure Diagram

Key: (1) Ukrainian National Astronavigation Bureau (2) Bureau Chief Jitalianke (Phonetic) (3) Financial Affairs Directorate (4) Deputy Bureau Chief Kemaluofu (Phonetic) (5) Deputy Bureau Chief (6) Bureau Chief Assistant Kuciniezuofu (Phonetic) (7) Space Flight and Transport Systems Bureau (8) National and International Space Program Bureau (9) External Affairs Bureau (10) 5 Offices (11) 2 Offices (12) 2 Offices (13) Scientific Research Center (Kharkov) (14) Scientific Research Center (Dniepropetrovsk)

In 1993, the Ukrainian government approved a space technology development five year plan. Its resolution of the question of military transfers in the space flight departments was one of the most significant moves. The realization of the plan in question is not only capable of preserving national defense departments' scientific research organizations as well as scientific research production capabilities of enterprises, it is also a new starting point for Ukraine and provides a possibility to continue to participate in the relevant space flight development work of independent federated nations. Moreover, cooperation with independent federated nations is beneficial for the Ukrainian nation. As a young and independent state, Ukraine will realize this plan through the effects of newly specified military industrial departments on the national economy.

The plan in question specifies a series of priority development projects.

- 1) Constructing this nation's geostationary orbit communications satellites;
- 2) Developing earth remote sensing and ecogeologic satellites;

3) Setting up surface information systems (the systems in question include flight control centers, spacecraft information reception and processing centers, information recording and processing centers, as well as information processing centers needed by users);

4) Zenith and Whirlwind rocket production and upgrades;/78

5) On the foundation of conventional aircraft-space flight delivery vehicles as well as specialty rockets launched from aircraft, develop aviation-space flight rocket systems.

Ukrainian enterprises and scientific research units participating in this plan exceed 100. The primary units associated with completing this plan include:

- Southern Design Bureau (located in Dniepropetrovsk);
- Southern Machinery Manufacturing Plant (located in Dniepropetrovsk, Plant Chief Aliekseyefu [phonetic]);

--Scientific research production consortium XAPTPOH [original text unclear, possibly wrong] (located in Kharkov, General Engineer Aisenbeige);

--Technical Machinery Academy (located in Dniepropetrovsk, Academy Chief Pilipianke [phonetic]).

Ukraine supports the development and permissible inherent expenses for these. It is also possible to obtain projects associated with the results of science--for example, such programs as "Mars", "Initiation", "Early Warning", "Forecast", and so on, as well as such projects as the automated multipurpose space station (AYOC), and the Peace space station.

Ukraine possesses its own carrier rocket technology. The Southern Design Bureau and the Southern Machinery Manufacturing Plant, respectively, are its design unit and manufacturing unit. At the present time, the two large Ukrainian models with the best development prospects are the Zenith and the Whirlwind. They are two stage rockets using liquid oxygen and kerosene as fuel. In the Ukrainian space development five year plan, preparations have already been made to carry out upgrades of them, making them into four stage rockets. In this way, it is then possible to take 6t or more of useful load and send it into geosynchronous orbit.

Ukraine possesses the largest missile factory in the world. It is located in Dniepropetrovsk. Ukraine also has the capability to produce satellites. As far as a total of over 1000 of the former Soviet Union's famous Cosmos satellites is concerned, 40% of them were produced in Ukraine. At present, the Southern Design Bureau is in the midst of designing and producing earth remote sensing satellites. According to plans, in 1997, the Southern Design Bureau will launch synchronous communications satellites. Ukraine is also prepared to locate a flight control center 120km from Kiev. This center makes use of a former military facility to receive space information. A satellite surface station will be set up 150km from Kiev at Qielenituofu (phonetic), and so on.

At the present time, Ukraine pays very serious attention to developing relations with surrounding countries. Ukraine has a

great many research organizations which are just in the midst of carrying out explorations in the area of space. Among these, 76 units participated in the independent federated entities space plan. Within independent federated entities, it is stipulated that there will be cooperative projects between countries using a specialized committee of Russia and Ukraine, as the major member states, set up in Moscow. Ukraine pays serious attention to solidifying and developing relations with Russia. In the international space research plan of independent federated entities, Russia and Ukraine take charge of the main operational missions as well as development expenses. For example, 35% of the expenses required to guarantee the flight of the Peace are paid by Ukraine. On the Peace, the overall movement systems and control systems as well as the Proton control system were also developed by Ukraine. Besides this, Ukraine also uses 29 billion Kubangs (phonetic) (Ukrainian monetary unit) to support the Baikenuer (phonetic) space flight center.

At the same time as this, Ukraine is also actively developing relations with the European Space Agency and such countries as the U.S., Canada, India, Poland, Germany, Austria, and so on. At the present time, cooperation between Ukraine and China primarily includes the areas below.

- 1) Exchange of experts and annual organizational technical meetings;
- 2) Holding periodic meetings of the space flight administration departments of the two countries, resolving in a coordinated manner problems existing in the cooperation as well as opening up new cooperative projects and enlarging fields of cooperation;
- 3) Drawing up cooperative accords with regard to observation of the earth;
- 4) Enlarging the cooperation of the two countries in such fields as space flight biology, and so on.

In this visit of a Ukrainian delegation to China (referring to the participation in the September 1994 third session of the China-Ukraine International Astronavigational Science and Technology

General Meeting convened in Xian), along with talks of experts on the Chinese astronavigational field, subsequently, the Ukrainian side will take further steps to supplement suggestions associated with relevant areas of Ukrainian-Chinese cooperation in astronavigational science and technology.

SIMPLE RULES FOR THE SOLICITATION OF CONTRIBUTIONS TO
"MISSILES AND SPACE VEHICLES"

Translation of "<<Dao Dan Yu Hang Tian Yun Zai Ji Shu>> Zheng Gao Jian Ze"; Missiles and Space Vehicles, Overall No. 213, No.1, 1995, p 79

"Missiles and Space Vehicles" is a scholarly and technical publication sponsored by the China Academy of Launch Vehicle Technology. It is openly published inside and outside China and is a bimonthly.

This publication is a venue for China's space flight technology personnel to carry out scholarly exchanges. It primarily carries research papers associated with Chinese missiles and space vehicles and subsystems in such areas as research, design, test manufacture, production, testing, and launch--also, technical reports and such articles as empirical summaries. In conjunction with this, appropriate reports are made of a number of research results from various nations of the world in this area. At the same time, introduction is also made of articles associated with space flight technology results in the area of national economic services. This publication has such columns as summaries, expert forums, missile and space vehicle systems, propulsion technology, guidance, navigation, and control, warhead technology, strength and environmental engineering, materials and manufacturing processes, telemetry technology, ground equipment, experiments and test measurements, computer applications, military personnel transfers, systems engineering management, systems effectiveness and safety, discussions of hot topics, high science and technology windows, news in brief, information windows, advertisements, and so on. Target readers are relevant specialized engineering and

technical personnel, science and technology management personnel, relevant specialized teachers and students associated with institutions of higher learning, as well as other readers with an interest in space vehicle technology.

Requirements for Incoming Contributions

1. As far as contributions are concerned, content must be substantiated, arguments clear, data reliable, succinct, clear and coherent. Number of characters 7000 or less.

2. Incoming drafts must be in neat handwriting. The draft pages must be clean and punctuation marks used correctly. Do not write with erroneous characters, miswritten characters, or self-created simplified characters. Drafts are uniformly written with fountain pen or marker horizontally on one side of 400 character grid lined manuscript paper or use floppy disk to do the draft, and, in conjunction with that, append a print out.

3. Article structure is generally: main text title, author's name, author's unit external designation, abstract, theme statement, main body of text, references and appendices.

4. Please append an English language abstract with drafts on a separate sheet. The structure is: English title, author's translated English name, English translation of author's unit external designation, abstract, and statement of theme. English abstracts should be around 1000 words (it is best to type them on a typewriter).

5. Mathematical symbols, chemical molecular formulae, foreign language letters in upper and lower case, and subscripts and superscripts must be annotated clearly. Please use pencil notes on easily confused words (for example, English upper and lower case or English rarities, and so on).

6. As far as inserted Fig.'s are concerned, please use drawing paper to draw them in accordance with the requirements. Composition must be rational. With respect to photographs, always use black and white photos. On Fig.'s, write text, numbers, symbols, and so on clearly in pencil. All Fig.'s should be shown using blocks at corresponding positions in the text. Inserted

Fig.'s in each article draft generally do not exceed 6.

7. Measurement units should make use of national legally set units of measure. Moreover, always use symbols to represent them.

8. Only record the most important references. Set them out at the back in accordance with the sequence in which they are quoted in the text. Always refrain from quoting material which has not been made public. The form for writing references is:

Author, article name or book name, publication name or publishing house name, publication no., publication time, page no.'s

9. Incoming drafts must be sure to have no involvement with classified content. In conjunction with this, append security check certificates (affix an unclassified stamp). Any content which involves classifications must go through declassification processing.

10. With regard to the content of articles--in particular, their veracity, accuracy, conclusions, as well as consequences are covered in all cases by the application of the principle of the author's sole responsibility for his or her views.

11. In respect to drafts, please give a clear indication of authors' real full names (upon publication, it is possible to use pen names in accordance with the authors requests), unit, communications address, postal no., and telephone in order to facilitate contact.

12. Please do not submit a manuscript more than once. If there is no sign of an editorial department notification of the processing of the draft within 4 months, it is permissible to initiate procedures oneself. Any papers or reports which have already been published in open publications will not be reissued by this magazine. Please give clear indications of papers which have already been in|mznillyx}kli{hmlor read at scholarly conferences. Authors are requested to keep manuscripts. Contributions are never returned.

13. As far as manuscripts (illegible) published are concerned, two copies of the issue in question will be presented as

a gift. In conjunction with this, remuneration will be paid in accordance with regulations.

14. Please send manuscripts to Beijing postal box 9200 subbox 21, attention "Missiles and Space Vehicles" Editorial Section. Postal code: 100076.

MISSILES AND SPACE VEHICLES

Established in 1972 February 1995 No.213

Sponsor: China Academy of Launch Vehicle Technology

Chief Editor: Shi Weiyang

Editor & Publisher: Editorial Office of Missiles and
Space Vehicles

Address: P.O.Box 9200-21, Beijing 100076, China

Distributor: China International Book Trading Corpora-
tion(P.O.Box 399,Beijing 100044,China)